國立中山大學機械與機電工程學系研究所

博士論文

Department of Mechanical and Electro-Mechanical Engineering

National Sun Yat-sen University

Doctoral Dissertation

微流體液相分離晶片及其於金奈米粒子
合成與多巴胺檢測之應用

Microfluidic Chip for Immiscible Liquids Separation and Its
Applications on AuNPs Synthesis and Dopamine Detection

研究生：李和政 撰

Ho-Cheng Lee

指導教授：林哲信 博士

Prof. Che-Hsin Lin

中華民國 103 年 7 月

July 2014

論文審定書

國立中山大學研究生學位論文審定書

本校機械與機電工程學系博士班

研究生李和政（學號：D973020020）所提論文

微流體液相分離晶片及其於金奈米粒子合成與多巴胺檢測之應用
Microfluidic Chip for Immiscible Liquids Separation and Its
Applications on AuNPs Synthesis and Dopamine Detection

於中華民國 103 年 7 月 31 日經本委員會審查並舉行口試，符合博士學位論文標準。

學位考試委員簽章：

召集人 黃志青　＿＿＿＿＿　委　員　林哲信　＿＿＿＿＿

委　員　莊漢聲　＿＿＿＿＿　委　員　朱訓鵬　＿＿＿＿＿

委　員　潘正堂　＿＿＿＿＿　委　員　傅龍明　＿＿＿＿＿

委　員　莊承鑫　＿＿＿＿＿　委　員　曾韋龍　＿＿＿＿＿

委　員　＿＿＿＿＿＿　　委　員　＿＿＿＿＿＿

指導教授（林哲信）　＿＿＿＿＿＿（簽名）

Acknowledgements

　　「十年寒窗無人問，一舉成名天下知。」相信這句話是每位研究生最刻骨銘心的台詞，而在博士生涯的漫漫長夜裡，又曾流下多少的膽汁和淚水才能換來今日的仰天咆哮。成功並非一朝一夕但也不是只有靠努力，每個成功者的背後一定都有位偉大的女人，而我卻幸福的擁有世上最棒的兩個人。母親扮演著重要的推手和給予最大的鼓勵與支持，父親則是開啟我智慧及遠見的新好男人，今天能有這小小的成就都要歸功於無私奉獻的他們。然而，良師則以振興國家，在浩翰的學海中若沒有引領的掌舵者，我們這些漂洋的博士船便永遠無法成功到達彼岸。在此，很感謝林哲信 教授在這條航道上給予我許多的指導與栽培，讓我在追求學識及面對人生的態度上都能保有樂觀進取之心，更要感謝許多口委教授不吝給予論文豐富的指導，才能使這研究成果賦予更高的價值與肯定。

　　此外，更要感謝一直陪伴在身邊的好友們，謝謝你們時時警惕著我的歲數不該再這樣虛度下去，讓我更有大步向前的動力。感謝楊小安總是提供大家許多天馬行空的鬼點子，讓實驗室充滿著聒噪和歡樂的氣氛，還幫地下室養了許多的花草及昆蟲(小虎哥和阿螂哥)；陳阿波總是擔任實驗室夜間的管理員，保衛著那震耳欲聾的質譜儀；陳必軒是個很愛斯巴特的碩班學弟，總是讓新生敬畏三分。另外還要謝謝一群天真的小學弟妹們，幫我在口試上打點許多事，蘇小妹總是開心的被大家抨擊且毫無怨言的處理許多行政業務；殷寬教導大家如何保持完美曲線外，更是認真執行計畫的好學生；爽哥對於情人和實驗成果上的自信心，是值得去好好學習的榜樣；尚璟是個凡事追求完美且認真負責的棒球小子；高毅總是努力的重復別人所講過的話語，且常常對著空氣在交談的好老闆。在博士求學生涯中，謝謝你們這些獨具特色的小鬼，讓我在這段孤獨的研究生活中增添許多美好的回憶。往後的新進學弟們，也希望你們在這實驗室能培養出堅強的實力，當踏出校門之日便是一起為 BEMS Lab 爭取榮耀並提升台灣競爭力的時刻。

　　成功只是一時，努力卻是一輩子，夢想並非遙遠，做人必定踏實!!

中文摘要

本研究發展了一創新的液相分離微流體晶片，利用設計不同深度的管道結構創造足夠的毛細管作用力與液體表面張力之間差異，將兩不互溶且低表面張力液體達到近 90%的分離效率，如：甲苯和水。此外，液滴式微流體系統擁有較多的雙液相界面，且藉由液滴內部持續循環的流場，有助於提供化學反應穩定且擴散均勻的液相混合，對於奈米粒子的合成有較佳的應用。因此，本研究開發之微流體晶片有效提升金奈米粒子(AuNPs)於雙液相合成，在 T 字型的管道中穩定控制還原劑(連續相)與金鹽甲苯溶液(分散相)的流速，便由連續片段的流體(Segmented flow)中合成出粒徑分布均勻的金奈米粒子，其粒徑尺寸相較於一般容器中所還原的粒徑小。利用液相分離微流體晶片，成功獲得簡易且高效率的方式收集金奈米粒子於甲苯溶液，減少粒子與過多還原劑反應而使粒徑持續成長。

本研究亦提出一種高靈敏度的多巴胺(DA)比色法檢測方式，由 4-二甲氨基吡啶(DMAP)分子將甲苯中還原的金奈米粒子轉移到水相環境，再作為檢測樣品中多巴胺濃度的探針。實驗結果得知，經由相轉移的水相金奈米膠體加入多巴胺溶液後，金奈米粒子溶液會由原本珠紅色轉變為墨綠色，從吸收光譜亦可觀察到特徵吸收波峰發生藍位移(Blue shift)的情形。此外，由穿透式電子顯微鏡(TEM)更發現，原本溶液中存在粒徑 13 nm 的金奈米粒子被多巴鞍分子將核心蝕刻至粒徑約為 2~5 nm，藉由粒徑的顯著變化來作為多巴胺生物樣品之檢測。本研究發展之 DMAP-AuNPs 探針對於多巴胺的檢測更擁有高靈敏度偵測極限(5 nM)，在常見的量測干擾物如：抗壞血酸(AA)、高香草酸(HVA)和鄰苯二酚(CA)等物質存在下，仍擁有良好的選擇性而不會對量測造成干擾。

然而，為了使金奈米粒子應用於生物檢測時，可獲得快速樣品反應且能夠即時的作量測，本研究最終整合其生醫檢測技術於微流體晶片之開發，以玻璃光纖作為樣品吸光度量測的訊號傳輸。本研究發展的光學量測感測器是將蝕刻後的多模光纖(Multimode optical fiber)導入晶片設計的管道中，待測樣品先由液滴式微

流體系統達到均勻的混合，再注入晶片中的光學檢測微管道作即時吸收光譜量測。然而，利用光學量測感測器作為吸收光譜量測時，其消耗的樣品體積只需 50 nL，相較於一般光譜檢測儀擁有相對微量的耗費。由實驗結果得知，液滴式微流體系統對於化學反應動力學擁有較快的反應速率，利用本研究發展的光學檢測微流體晶片，更可提供快速且連續動態的化學反應研究。

由以上結果指出，本研究發展之液相分離微流體晶片，提供多樣性應用的潛力，有利於金奈米粒子的合成或作為液相樣品的萃取。此外，藉由整合簡易的光學量測系統，便可在微流體晶片中進行快速且連續的樣品檢測。因此，本研究發展之光學檢測微流體晶片與金奈米粒子生醫檢測技術，有助於未來開發高靈敏度且快速檢測的生醫感測器，以實際應用於生物、醫藥和病理等方面的分析與檢測，更有效的縮檢樣品之銷耗及檢測時間。

關鍵字： 微流體晶片、液相分離、金奈米粒子、多巴胺、光纖、吸收光譜

Abstract

In the conventional sample extraction approach, to achieve efficient liquid-liquid phase separation for the sample analysis is an important issue. However, it is challenging to separate the immiscible liquid of low surface tension from water by using microfluidic device. Therefore, this study developed a microfluidic chip that composed of T-junction, reaction channel and a novel liquid-liquid phase separator for continuously synthesizing fine gold nanoparticles (AuNPs) in the organic solvent (toluene). The design of glass chip is capable for separating water (surface tension = 72.75 mN/m) and toluene (surface tension = 30.9 mN/m) with 92% separation efficiency, owing to design different depths of microchannel that creates large difference between liquid surface tension and capillary force. Furthermore, AuNPs that synthesized in the microdevice exhibits narrower size distribution and better dispersion in comparing to the typical vessel synthesis process.

Besides, this study successfully developed a novel and high performance colorimetric probe for dopamine (DA) detection. Aqueous-phase AuNPs extracted via 4-(dimethylamino) pyridine (DMAP) from toluene were used as the reaction probes. Interestingly finding that the original diameter of AuNPs around 13 nm which separated into 2-5 nm size after adding DA. This exhibits change in the color of AuNPs colloid from red to blackish green. Transmission electron microscopy (TEM) and dynamic light scattering (DLS) showed the AuNPs break into the smaller sizes right after addition of DA. The DA concentration is quantitatively monitored by using UV-Vis spectrometer with a limit of detection (LOD) as low as 5 nM. In addition, the developed DA detection approach appears no significant problems in detecting DA with present common interferents such as ascorbic acid (AA), homovanillic acid (HVA) and catechol (CA).

However, many study reported that using microfluidic chip is capable to provide fast chemical reaction and rapid detection approach for biochemical analysis. This study developed a novel optical detection sensor by using the etched multi-mode optical fibers assembling in a droplet-based microfluidic system to achieve on-site absorbance measurement. Hence, the reaction of AuNPs detecting DA biosample was also capable to achieve rapid and continuously detection by using the microdevice. The proposed optical detection sensor composed by initially forming AuNPs droplet in segmented flow and measuring for sample absorbance in a 10 mm long of optical detection channel. Note that using the microdevice for absorbance measurement only required sample volume for 50 nL, which exhibits lower sample consumption in comparing to detect in the conventional cuvette system. Results indicated the developed microdevice capable for steady measuring sample absorbance with operating flow rate in the range from 5-25 μL/min. In addition, the detection approach shows faster reaction response for kinetic measurement of DA core etching AuNPs.

Therefore, this study successfully developed microfluidic chip to provide efficient liquid-liquid phase separation, which benefit to use for the sample extraction and synthesizing AuNPs of uniform size distribution in toluene. In addition, assembling optical fibers on the microfluidic chip that have offers simple and high performance optical detection to the bioanalysis. In this regard, the proposed microdevice with using AuNPs probes shows great potential to achieve high sensitivity detection for the future applying to such as biology, medical and clinic diagnostic applications.

Table of Contents

List of Figures

xiv

List of Tables

Nomenclature

A: absorbance

A: channel cross sectional area

AgCl: chlorination of silver

Au: gold

Ca: capillary number

c: analytes concentration

$C_{12}H_{25}SH$: dodecanethiol

D: diffusion coefficient

$HAuCl_4$: chloroauric acid

l: optical path length

M: molarity

mM: minmolar

$Na_3C_6H_5O_7$: sodium citrate

$NaBH_4$: sodium borohydride

NaCl: sodium chloride

nL: nanoliter

nM: nanomolar

P: liquid pressure

PPh_3: triphenylphosphine

Pt: platinum

Q: flow volume

Re: Reynolds number

S/V: surface to volume ratio

-SR: alkane thiol

stl: initial striation length

t_{diff}: time for diffusion

v: flow velocity

W: channel width

η: fluid viscosity

μm: micrometer

α: numerical factor

γ: interfacial tension

ε: extinction coefficient

ΔP: pressure drop

(ξ): thiol to gold ratio

Abbreviations

AA: ascorbic acid

ARI: absorption ratio index

AuNPs: gold nanoparticles

CA: catechol

CV: cyclic voltammetry

DA: dopamine

DI: deionized

DLS: dynamic light scattering

DMAP: 4-dimethyl-aminopyridine

EC: electrochemical

GC: gas chromatography

GSH: glutathione

HPLC: high performance liquid chromatography

HMDS: hexamethyldisilazane

HVA: homovanillic acid

LEDs: light emitting diodes

LOD: lowest limit of detection

LSPR: localized surface plasmon resonance

MEMS: micro electro mechanical system

NIR: near infrared

PBS: phosphate buffered saline

PDMS: polydimethylsiloxane

PR: photoresist

PVP: poly (N-viny-2-pyrrolidone)

QCs: quantum clusters

RTD: residence time distribution

SAMs: self-assembled monolayers

SERS: surface-enhanced Raman scattering

SPR: surface plasmon resonance

TEM: transmission electron microscopy

THPC: tetrakis (hydropxymethyl) phosphonium chloride

TOAB: tetraoctylammonium bromide

UV: ultra violet

UV-Vis: ultra violet visible

μTAS: micro total analysis

Chapter 1 Introduction

In recent years, microfluidic system has been widely developed for such medical diagnostics, drug screening, environmental and food analysis applications. Microfluidic chips were considered to provide many advantages for reducing the sample consumption, achieving faster detection and system miniaturization, which exhibits great potential for integrating experimental process (e.g. sample preparation, reaction, separation and detection) on the microdevice. Furthermore, the development of micro total analysis system (μTAS) has enhanced the analysis capability for using in the chemical and biological research field. Many analyzing methods have been widely developed for assembling onto the microchip such as mass spectrometry, optical and electrochemical detection. However, they all have some drawbacks with the detection process usually needs for a complex integration procedure and exhibits the smaller signal when compared to detect by using the conventional system. Therefore, developing high performance detection method by using the microfluidic system is an important issue for the study of biosensing applications.

Further, optical detection methods have been widely using for chemical analysis in the microfluidic system due to its noninvasive nature, easy coupling, rapid response and exhibits high sensitivity for the detection. Most of the optical detection approach is based on measuring for the absorbance or fluorescence signal of the analytes. However, they may suffer from relative low sensitivity of the detection signals due to measuring by using the small optical path length and insufficient analytes. Thus, many researchers interested on improving optical detection sensitivity by extending optical path length in the axial-direction, using waveguide or integrating optical fibers on the microfluidic chip. In addition, droplet-based microfluidic system exhibits many advantages such as using smaller sample consumption, have faster mass transfer and

1

high-throughput fabrication that is benefit using for the microreactor, chemical reaction and biological analysis. Therefore, the development of optical detection sensor by using droplet-based microfluidic system shows great potential to achieve high sensitivity bioanalysis.

Furthermore, noble metal nanoparticles exists unique electrical and optical properties, in which the solution color is highly correlated to the shape and size of particles, and the dielectric constant of surrounding medium. Hence, many studies have widely investigated for the nanoparticles synthesis approach and the biosensing applications in recent years. As well, due to the gold nanoparticles (AuNPs) exhibits great biocompatible of surface and the tunable particle shape and size. It is attractive for using such as chemical and biosensing, drug delivery, optical detection enhancer and surface-enhanced Raman scattering (SERS) applications. Except for the typical AuNPs synthesis approach in the aqueous, the alternative method for preparing AuNPs in the water has reported by phase transferred from the organic phase. In this approach, different kinds of biofunctional groups can be used for surface modify AuNPs and achieve a promising platform for biosensing applications.

In order to achieve rapid and high performance biosensing by using the microfluidic system, optical fibers is benefit to be assembled on the microdevice for on-site absorbance measurement. In addition, utilizing the colorimetric detection method of AuNPs is benefit to prove high sensitivity biosensing and chemical analysis. Therefore, this study successfully developed a microdevice applied for liquid-liquid phase separation and synthesizing fine AuNPs in the organic solvent. Moreover, novel and high performance DA detection approach was demonstrated to achieve in an off-chip system and measured by using the proposed optical detection microdevice. In this reagads, the developed microfluidic system shows great potential to provide a fine analysis for the biosensing applications.

1.1 Motivation and objectives

The main purpose of this research was developing a high performance optical detection sensor with using AuNPs for biosample detection in the microfluidic system. However, typical AuNPs synthesis approaches by using a two-phase solution that the reduction reaction is carried at the adjoining phases between water and toluene. When using a vessel for AuNPs synthesis is not easy to control the concentration gradient of chemical reaction, which usually causes AuNPs exhibits large size distribution. In contrast, multiphase microfluidic system provides large interfacial area, fast mixing and mass transfer which exhibits great potential for synthesizing uniform size of AuNPs relative to the typical large scale systems. Therefore, this study is developing a novel liquid-liquid phase separation microdevice for efficiently separates AuNPs from reducing agent which reduce unnecessary reduction reaction. Using this design microfluidic chip is benefit for synthesizing AuNPs in the organic solvent (toluene) with uniform size distribution.

Besides, AuNPs have been widely developed using for colorimetric detection which exhibits great ability to achieve high sensitive biosensing. In the conventional approach using AuNPs for bioanalysis, many studies reported the detection method was based on observing from the cross-linking of particle aggregation. Thus, the preparation for surface modify of AuNPs to enhance the affinity with sample molecules is an important issue. However, developing a sensitive measurement of dopamine detection is essential for the analysis of Parkinson's disease. The conventional detection approach requires for sophisticated equipment which is not benefit to the DA analysis. Hence, this work is developing an alternative colorimetric detection method for DA analysis, which by using a novel core-etching of DMAP-AuNPs. The proposed technique considered to provide sensitive DA detection

which based on DMAP molecules separating Au atom form the outermost surface. AuNPs colloids observing for color changes by adding into different DA concentration. This novel core-etching technique was analyzing for DA detection performance in the off-chip system.

Furthermore, optical detection methods have well developed for analytical chemistry by using the microfluidic system. Most of the analyzing approach is based on measuring for absorbance or fluorescence signal of the analytes. However, these optical sensors may suffer from relative low sensitivity of signal due to microchip provides small optical path length and insufficient analytes. This study developed a droplet-based microfluidic optical detection system for on-site absorbance measurement that is benefit using for AuNPs analysis. Therefore, the development of optical detection sensor with AuNPs colorimetric probes by using microfluidic chip is capable providing rapid and accurate bioanalysis. This approach shows great potential for providing high performance detection in the future biosensing applications.

Following summarizes the main purpose in this study for developing simple method to achieve these goals:

(1) Developing stable segmented microfluidic system for synthesizing uniform size distribution and better dispersity of AuNPs in the solution.

(2) Developing efficient liquid-liquid phase separation microdevice for collecting the synthesized AuNPs in organic solvent (toluene).

(3) Developing high sensitivity and good selectivity approach for DA detection based on using AuNPs as the detection probes.

(4) Developing high performance optical detection sensor for providing rapid AuNPs bioanalysis by using the droplet-based microfluidic system.

1.2 Thesis organization

The dissertation is simply organized into six chapters to describe the research and development efforts as shown in **Figure 1.1**.

I. **Chapter 1.** Introduction

This chapter simply introduces the development of detection approaches in microfluidic system and the applications of using AuNPs for biosensing. Due to the conventional detection methods exhibit some drawbacks when using for the bioanalysis. This study describes the motivation and purpose for developing novel microdevice to enhance the detection performance and solve the problems in typical analyzing methods.

II. **Chapter 2.** Background and literature review

This chapter briefly introduces recent developments and applications of using segmented microfluidic system, which integrated optical detection approach to provide rapid and sensitive biosensing. Many studies reported the advantages of using segmented flow to achieve fast and uniform sample mixing. Using the chemical synthesis approach in microfluidic system was capable to prepare uniform size distribution of AuNPs in the solution. Furthermore, AuNPs exhibits specific optical and electrical properties which capable for providing better platform in the biosensing. Review showed the recent development of optical detection by using microdevice and the AuNPs colorimetric probes to provide high sensitive bioanalysis in the wide range applications.

III. **Chapter 3**. Working principle and theory

The chapter describes the working principle and the optical detection theory in

this study. The developed microdevice was design to achieve liquid-liquid phase separation and synthesizing uniform size distribution AuNPs in the toluene. Besides, by coating with DMAP molecules on the synthesized AuNPs in organic-phase was used for phase transferring to the aqueous. This developed DMAP-AuNPs using as the reaction probes to provide high performance DA detection. At last, the study developing a simple optical detection microdevice that is for getting rapid AuNPs absorbance measurement by using multiphase microfluidic system.

IV. **Chapter 4. Materials and methods**

This chapter illustrates details of developing microfluidic chip with AuNPs colorimetric detection in the research, including reagent preparation, apparatus detection, chip fabrication process and experimental setup. The sequence experiment showed the developed microfluidic chip used for separating immiscible liquid and achieved high separation efficiency. The ability of using microfluidic chip for AuNPs synthesis have in comparing to typical approach, which evaluate by the particle size distribution. DMAP-AuNPs was prepared by extracting from toluene solvent and used for providing high performance DA detection. The optical detection sensor was design by assembling optical fibers on the microfluidic chip, which capable measuring for sample absorbance by using a segmented flow system.

V. **Chapter 5**. Results and discussion

Results indicate the developed microfluidic chip capable for achieving high separation efficiency for separating toluene from water via controlled appropriate flow pressure. AuNPs synthesis by using the microfluidic chip exhibits uniform size distribution in comparing to synthesize in the conventional vessel. In addition, the developed AuNP etching protocol for DA detection provides a novel and versatile

approach for rapid biosensing applications. Finally, the developed optical detection sensor successfully provides lower sample consumption, faster chemical reaction and rapid absorbance measurement which in comparing to analyze by using the conventional cuvette system.

VI. **Chapter 6.** Conclusions and Future works

The achievements and contribution of the dissertation are summarized in this section. This study successfully developed a microdevice that is capable to achieve high separation efficiency for separating immiscible liquid of low surface tension (toluene/water). When using microdevice for AuNPs synthesis, it is benefit to produce uniform size distribution and better dispersity. Besides, core-etching technique for detecting DA neurotransmitter by using the synthesized DMAP-AuNPs is a novel and versatile approach for further rapid biosensing. Finally, the proposed optical detection sensor provides low sample consumption and fast chemical reaction to achieve on-site absorbance detection by using microdevice. Ultimately, this research works successfully developed a high performance microfluidic device for AuNPs synthesis and biosensing applications.

In the future work, the ability for precisely controlled of the generate AuNPs size and shape is considered to achieve by synthesizing in the droplet-based microfluidic system under well control of several parameters (e.g. droplet size, sample mixing rate, reagent concentration). Besides, due to high performance optical detection was achieved by using the microfluidic chip which has been accurately assembled optical fiber on the chip. Thus, the future tends to develop simple device for optical fiber assembling, and design for the multi-detection channels that benefits to achieve faster biosensing and multi-samples detection.
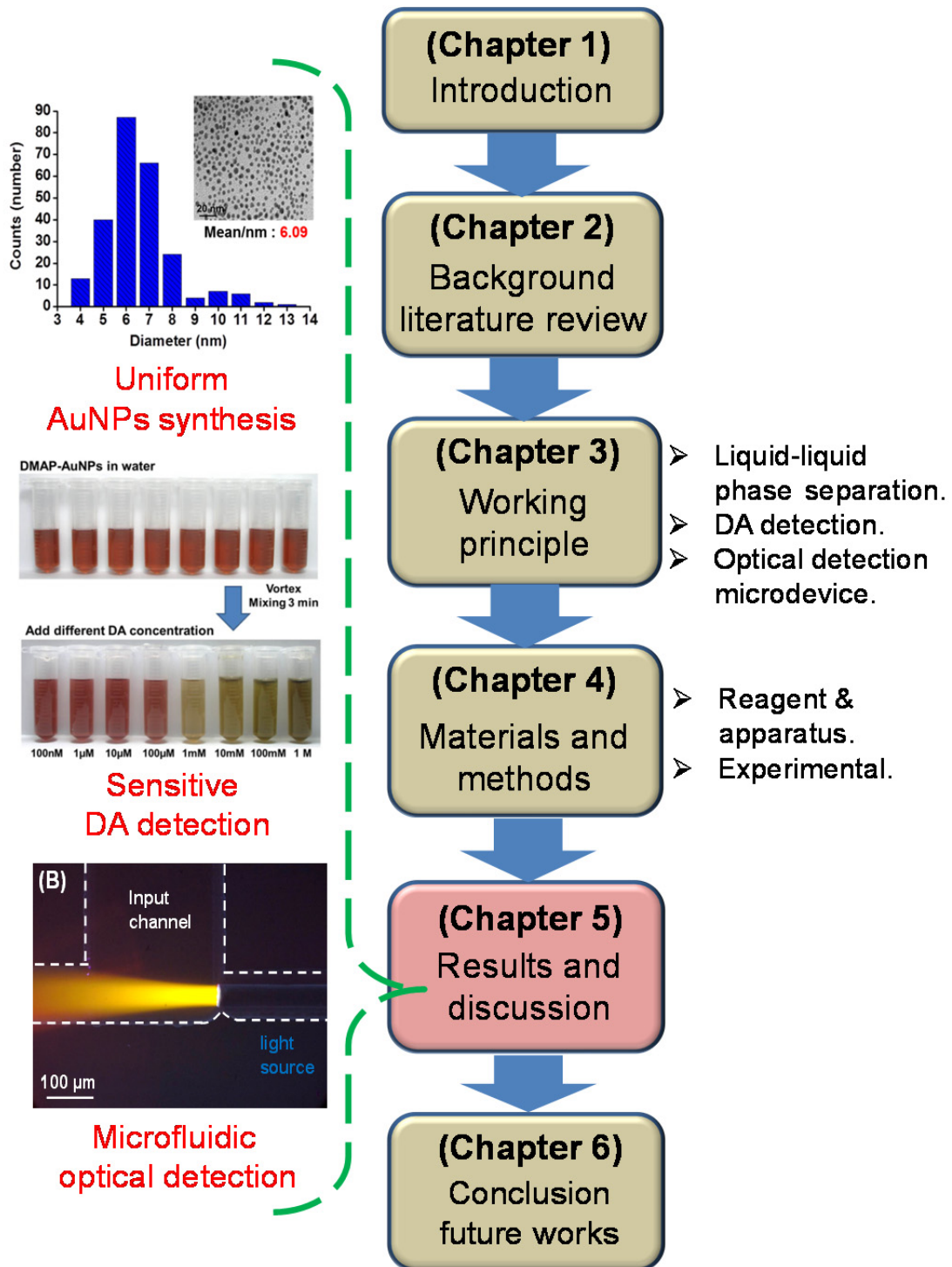
Figure 1.1 Chapter overviews.

Chapter 2 Background and literature reviews

2.1 Multiphase microfluidic systems

2.1.1 Microfluidic systems

Microfluidic system has been well developed for wide range of applications in recent years, due to the system exhibits many advantages including small sample consumption, fast analysis time and high throughput production [1]. This technology exhibits great potential to provide high performance assay within the microscale fluidic system, which holds the typical laboratory experiment by using the reagents volume from milliliters to microliters or femtoliters. Moreover, using the microfluidic systems for chemical analysis also provides rapid reaction time which in the few second or less. Therefore, it is benefit to develop scaling down of analytical platform by using lab-on-a-chip microdevice, which brings many advantages for the clinical diagnostic applications [2].

However, using the microfluidic system for samples mixing in many applications may suffer from the problems of that exist with nonuniform mixing and slow diffusion process. Due to the low values Reynolds number *Re* causing for laminar flow in the microfluidic system, which sample mass transfer between the liquid phases only based on the diffusion approach. Hence, the initial striation length *stl* (0) plays the key role for enhancing diffusion ability and the time for diffusion t_{diff}(s) that can be described by eq. (1), where D (m^2/s) is the diffusion coefficient [3].

$$t_{\text{diff}} = stl(0)^2/2\text{D} \tag{1}$$

Furthermore, several researches have reported simple methods for enhance the sample mixing ability in microfluidic system by reducing mixing length or create the chaotic advection in the flow [4], develop for active and passive micro-mixers by using the microfluidic chips.

2.1.2 Droplet-based microfluidic systems

Unlike the continuous flow in microfluidic system, droplet-based microfluidic system provides many advantages for such sample extraction [5, 6], micro-reactor [7] and micro-mixer which offer a new technology to manipulate such small volume of reaction system [8]. Due to the droplet microfluidic system exhibits high surface to volume ratios (S/V) that has a shorter diffusion distance to provide heat and mass transfer, which is benefit for achieve faster reaction process [9]. Most of all, droplet microfluidic system offers great potential of producing higher throughput rate (200000/s) [10, 11] and stable analysis than the continuous flow system. They even reduce the biosamples have sensitive to the channel surface properties, due to the droplets are isolated from the channel walls by the carrier liquid. Therefore, this approach has been widely developed for wide range of applications such as kinetics measurement [12, 13], chemical and biological analysis [14, 15], protein crystallization [16, 17] and nanoparticle synthesis [18, 19]. Furthermore, based on using the droplet microfluidic system is considered to provide rapid and uniform sample mixing that can be accurately control with the reaction time.

2.1.3 Multiphase droplet formation in microfluidic systems

Many studies reported the microfluidic devices have been widely fabricated by using polydimethylsiloxane (PDMS), which is cheap and easily molding of the elastic polymer. However, PDMS usually suffer to the problem of leading material occur swelling and deformation while present in the organic solvents. Thus, several materials with good solvent resistance such as glass and silicon [20] have been well developed for the alternative option. In addition, the wetting properties of microchannel walls are important for stably generating uniform droplets in the

microfluidic system. Thus, having the hydrophilic channel wall is benefit to generate the stable oil droplets by surrounding of aqueous phase. To improve the capability of controlling generated droplets of exhibit monodispersity, surfactant is usually added to the continuous phase for providing better fluidic manipulation.

The condition to form droplets in the multiphase microfluidic system based on the competition force between liquid interfacial tension and viscosity in the small scales of microchannnel. Therefore, the liquid surface tension should be approaching to capillary number *Ca,* which leading the fluid attempt to be formation as plugs flow. The Capillary number can be described by the eq. (2) [21].

$$Ca = \eta v / \gamma \tag{2}$$

Where η (kg/m·s) presents the viscosity of fluid, v (m/s) is the flow velocity and γ (N/m) symbol for the interfacial tension between aqueous phase and the carrier fluid. Therefore, low value of *Ca* simply indicates that interfacial tension is larger than the viscous stress, which the disperse phase liquid would attend to form as spherical to minimize the surface area.

In the typical droplets formation approaches based on using two-phase microfluidic system usually divided by two kinds of methods: T-junction [22, 23] and flow focusing [24, 25] in the multiphase microfluidic system (**Figure 2.1**). The key point to stably generating uniform droplets in the microdevice, have reported by well control the external flow pressure between viscous shear stresses. Most of all, such capillary number usually operating in the range between 10^{-3} to 10^{1} for the wide range applications based on droplet formation in the microfluidic devices [26]. Therefore, to steadily generating uniform droplets in the microfluidic system is benefit for providing efficient and rapid chemical reaction inside each formed droplets.
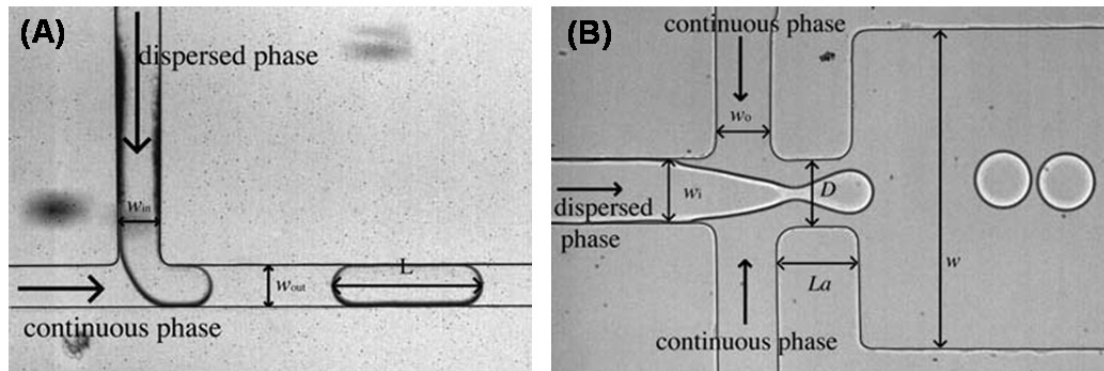
Figure 2.1 The experimental of droplet formation by using (A) T-junction and (B) flow focusing device in the multiphase microfluidic systems. [26]

2.1.4 Segmented flow in microfluidic systems

Recently, multiphase microfluidic systems have been widely developed for those heat exchangers, miniature fuel cells and micro-reactors. Due to the segmented flow exhibits the circulation motion within the flow and the gas bubbles are usually separated from the channel wall with thickness smaller than 1 μm [27], which greatly provide rapid mixing and efficient mass transfer in the discrete droplets. Therefore, this approach significant increase the capability of providing efficient chemical reaction in many applications such as micro-separations [28], protein crystallizations [29] and chemical computing [30]. The main advantages of using segment flow that compared to the continuous flow is that having the ability to improve flow uniformity, exhibit the superior analytic control in the small sample volumes and reduce the susceptibility to fouling. In this regards, segment flow has proven to be the significant platform using for chemical and biological applications with using ultra-small of sample volumes (nanoliter to femtoliter).

In general, segmented flows are composed by at least two immiscible fluidic which using for liquid-gas and liquid-liquid mixtures. It is usually divided into two types of segmented flows, which is depends on the phase where the sample reaction

taking place. The first approach shows liquid droplets have been encapsulated by the carrier fluid that is wetting the microchannel (**Figure 2.2 (A)).** These droplets also called as "plugs" to using as the sample reaction chamber in the microfluidic system, which the rapid and uniform mixing is achieved by the circulation flow inside the droplets. Note the reagents reacting in the plugs flow are not contacting to the microchannel wall and without occurring sample dispersion during the liquid transportation. However, the other method of segmented flow shows liquid "slugs" are divided by discrete gas bubbles (**Figure 2.2 (B)**). Based on using this approach for the sample mixing, which chemical reaction happening in the slugs usually formed as the continuous phase [31]. Therefore, it is considered the circulation flow in the slugs have leading to low diffusion process for achieve uniform sample mixing.
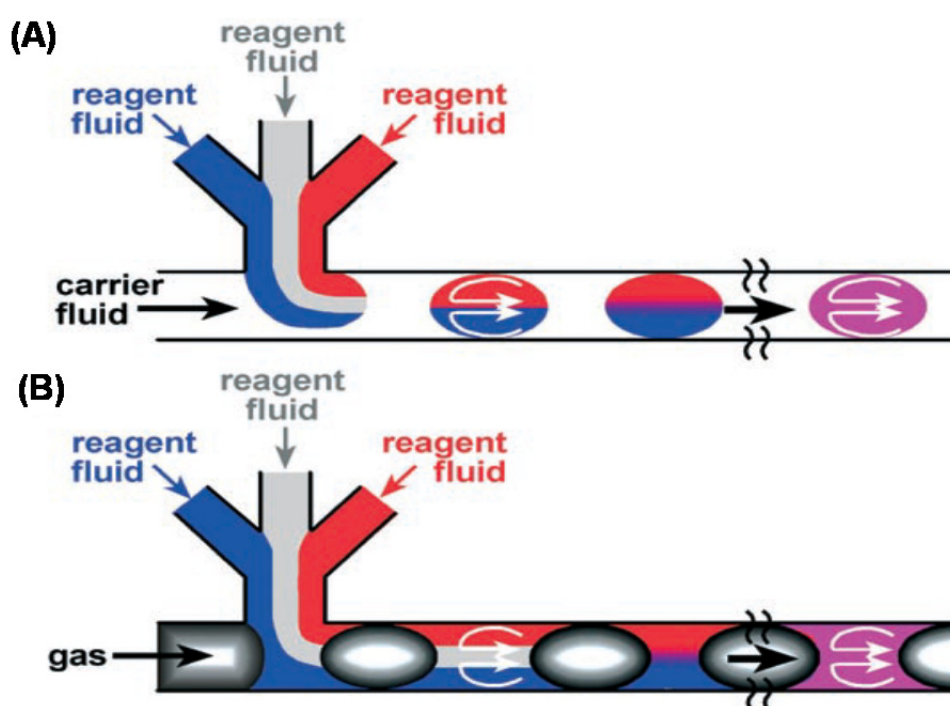
Figure 2.2 The comparison of different reaction by using two types of segmented flows in the microfluidic channels. (A) The liquid plugs are encapsulated by the carrier of immiscible continuous phase. (B) The aqueous slugs are divided by another liquid phase, which the reaction is occurring in the continuous phase. [31]

2.1.5 Taylor circulation of the segmented flow

Moreover, segmented flow and laminar flow are the most common used method for liquid extraction in micro-reactors applications. Due to slugs moving through the small capillary rely on channel physical properties and flow operating conditions, which causing for the internal circulations within the slugs (**Figure 2.3 (A)**). However, these circulation phenomenon can be described as two regions in the slugs: a recirculation zone at the center and a stagnant zone where shows zero of the liquid velocity [32]. Therefore, it is considered to provide the rapid sample mixing and efficient interphase mass transfer by using the segmented flow in the capillary. In addition, the thin aqueous wall film that caused by the surrounding solution have also increasing the recirculation ability in the slugs flow (**Figure 2.3 (B)).**

Due to the capillary segmented flow has generating of Taylor vortices inside the slugs, which is induced from the shear force between channel wall surface and the flow pressure. This multiphase flow pattern successfully reducing the thickness of boundary layer at the interface, which is capable for greatly enhance the diffusive penetration in the applications of chemical reaction. Most of all, for generating the stable and uniform slug flow pattern that several important parameters is essential to be considered such as the specific interfacial area, the mass transfer coefficients and energy demand (shown in **Table 2.1**). Therefore, well controlling for the interfacial force between flow pressure and the channel surface energy that is benefit achieve fast and uniform micromixing in the segmented microfluidic system.
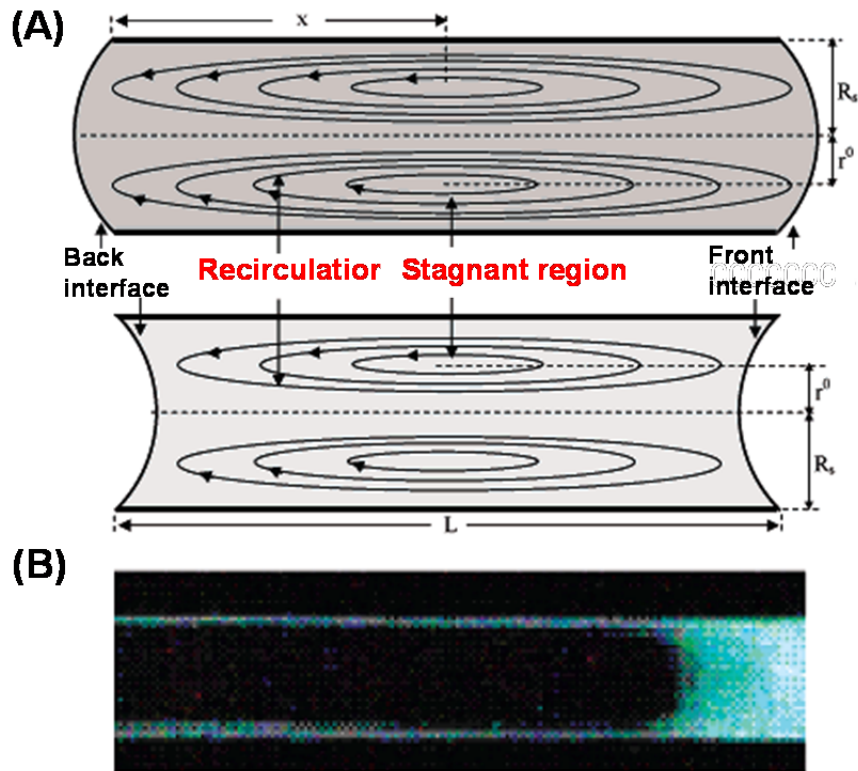
Figure 2.3 (A) Schematic illustrates of internal circulations inside the aqueous and organic slugs, respectively. (B) The photo shows typical two-phase segmented flow pattern of water (with fluorescence) encapsulated oil slugs in the capillary, which clearly observing there exhibit a thin layer between the slugs and wall surface. [32]

Table 2.1 Operating parameters of the comparison between using capillary slug flow and the stirred tank system. [33]

Contactor	Slug flow capillary	Stirred tank
Mass transfer coefficient [s^{-1}]	0.02-1.5	$2 \cdot 10^{-5}$ - $2 \cdot 10^{-3}$
Interfacial area [m^{2}m^{-3}]	~ 3200	~ 500
Energy requirement [KJ m^{-3}]	0.2-20	150-250
Contacting time	well-defined	statistically distributed
Stochastic phenomena	absent	dispersion & coalescence
Temperature profiling	facile	infeasible

2.1.6 Different patterns of the segmented flow

However, based on producing the segmented flow in the capillary there usually exhibits with three kinds of flow patterns. In the typical approach for generating stable segmented flow presents the uniform flow pattern (**Figure 2.4 (A)**), which by setting in the wide range of operating flow rates and controlling with slugs length in 2 mm or less [34]. Note the smaller of the capillary diameters is benefit for stabilizing the slug flow to the formation degree [35]. In the smaller slugs of dispersed phase (**Figure 2.4 (B)**), which the suspended droplet shows no Taylor vortices insides due to the weakness wall shear forces can be transmitting to the droplet surface. Based on using this approach, mass transfer is difficult to achieve within such hard sphere droplet. The mixing process happen in the droplet was dominated by the nature diffusion ability. Furthermore, due to exist of multiple vortices along the longer slugs have leads to the complex interference for the mass transfer within the droplet (**Figure 2.4 (C)**). Therefore, controlling with optimal slug length is benefit to achieve faster mass transfer rate for chemical reaction by using the segmented flow system.
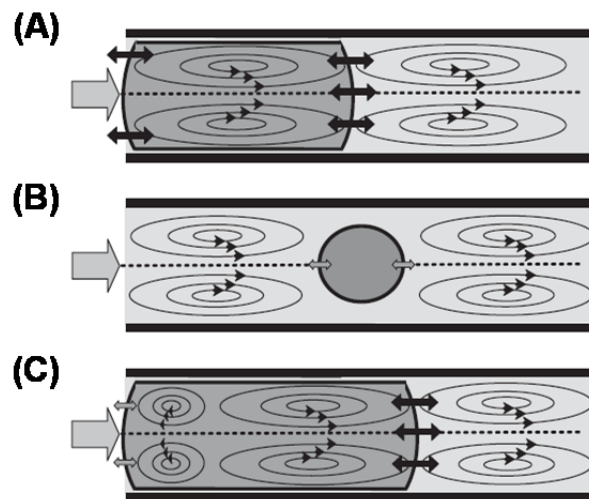
Figure 2.4 Schematic illustrates the different slug length for mass transfer. (A) The typical Taylor vortex structure, (B) suspended droplet without internal circulation, (C) multiple vortices and the additional stagnant zones in the longer slugs flow. [33]

2.2 Liquid-liquid phase separation

2.2.1 Liquid phase separation in microfluidic systems

Many studies reported that micro-reactors and micro-mixer operating with the multiphase flow have provided larger interfacial area, faster mixing and mass transfer process, which achieved the better performance relative to the typical batch scale systems. Furthermore, diverse of separation process and sample extraction has proven to be achieved in the micro devices [36]. Since the typical operation process for sample extraction can be divided into contacting and separation of the immiscible liquid phase. There are still many off-chip analyses, such as gas chromatography (GC) and spectroscopy measurements required for detecting the sample products such that separating different phase of fluids become desirable.

However, the conventional liquid-liquid phase separation is difficult to achieve in the micro scale due to the surface tension has dominate over the body forces under the length scales. Thus, based on using the gravity force of the liquid is not capable for phase separation within the microsystem [37]. **Figure 2.5** shows the different approaches for liquid-liquid phase separation by using the laminar flow and segmented flow. Comparing to achieve the efficient phase separation in the parallel flow, it is much more difficult to be separated from the segmented flow. Due to both liquid phases stay within the same channel. Therefore, several researches reported efficient methods for separating gas-liquid and liquid-liquid phase samples by using the microdevice of treated different region in the channel with hydrophilic or hydrophobic surface modification [38, 39], or by using the hydrophobic membrane [40, 41]. In this regard, these approaches successfully achieved liquid phase separation by using the microfluidic system, which based on creating large difference between the surface tension and channel surface energy.

(A) Stratified flow:

(B) Segmented flow:

■ Toluene   ■ Water
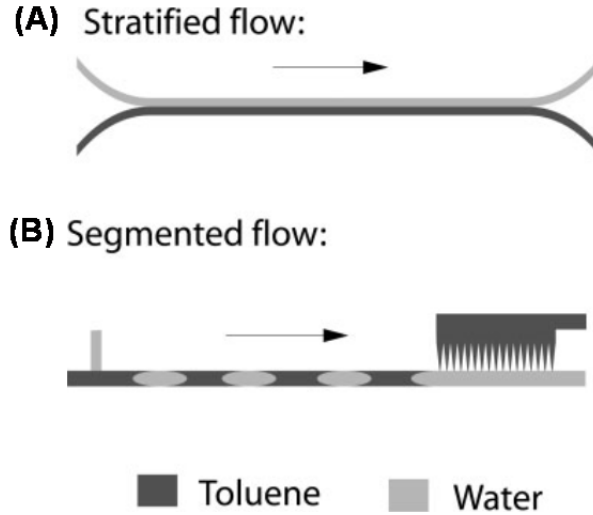
Figure 2.5 Schematic illustrates typical two types of liquid-liquid phase separation methods. (A) Design of Y shape output channel for phase separation in the laminar flow and (B) using capillary force for phase separation in the segmented flow. [42]

2.2.2 Capillary force for liquid-liquid separation

In addition, surface tension and capillary force of the microchannel are the most useful technique for dominant the phase separation in the segmented flow system [43-45]. It is considered to have great potential for continuously separating the immiscible liquid of different interfacial tensions. The main working principle of the gas bubble or droplet filter by using the capillary force is based on, that the surface energy of the droplet getting increases while forced to move into the narrower channel (**Figure 2.6**). When considering the droplet geometry as two-dimensional shape, surface energy difference should be control with equal to the work required of states A and B. The operating pressure difference can be described as eq. (3).

$$P_1 - P_2 = 2\gamma \left(\frac{1}{w} - \frac{1}{W}\right) \tag{3}$$

Where P (Pa) is liquid pressure, γ (N/m) the interfacial tension between liquid-liquid phases, w is the width of narrower channel and W is the width of wider channel [46]. Therefore, due to the size of droplets or bubbles are larger than the channel diameter

18

and difficult to pass through the capillary. The droplet was able to flow into the fine liquid output channel not inter the smaller channel. In this regards, it is easily to separate the immiscible of two liquid phases in the segment flow by controlling with the proper threshold pressure.
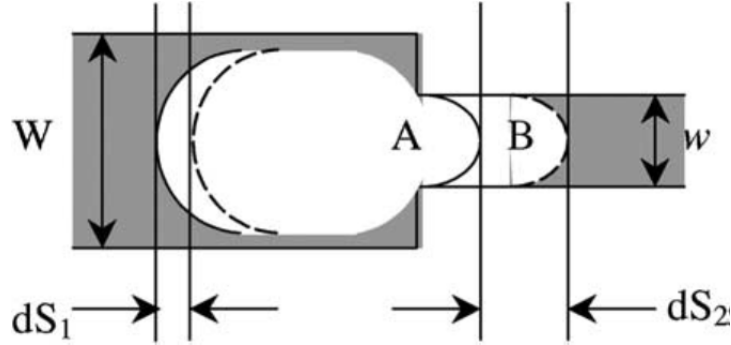
Figure 2.6 Schematic illustrates gas bubble deformation process into a narrower channel, which the surface energy have increases between the variation of state A and B. [46]

However, using the capillary force is the most powerful methods for efficiently separating two immiscible liquids in the segmented flow. Based on well control the flow breakthrough pressure is benefit for phase separation by using different diameter branch microchannels (**Figure 2.7**). Most of all, design for optimize combination of narrow separation channel and well controlled the flow pressure drop is considered to achieve higher phase separation efficiency. Hagen Poiseuille's law enable for the calculation of pressure drop, which based on the laminar Newtonian flow along the channel with the known geometry. The pressure drop can be described as eq. (4) [47].

$$\Delta P = \frac{\alpha \eta Q L}{A^2} \tag{4}$$

Where ΔP (Pa) is the pressure drop of presenting fluid flow, α the numerical factor related to the geometry of channel cross-section, η (Pa·s) the fluid viscosity, Q (m³/s) the flow rate of fluid, L (m) the design channel length and A (m²) the cross sectional area of the channel.
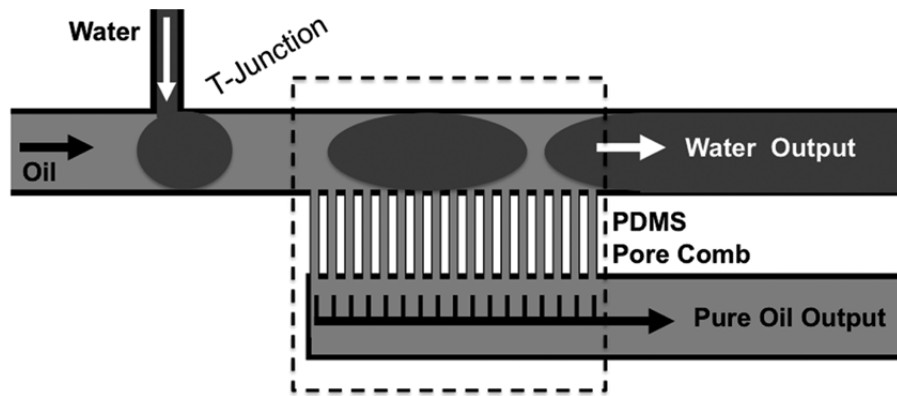
Figure 2.7 Schematic illustrates the conventional pore comb microchannel for achieving liquid-liquid phase separation by using the segmented flow system. [48]

2.3 Gold nanoparticles

2.3.1 Applications of gold nanoparticles

Nanoparticles usually defined as the material with the average diameter less than 100 nm. Since the noble metal nanoparticles exists the specific physical properties of surface plasmon resonance (SPR) that makes the particles have the strong scattering and absorption of the visible light wavelengths. Hence, the color showing from the nanoparticles colloids is found highly related to its shape, size and the local environment [49]. The development based on using these specific physical properties of the nanoparticles is considered to provide new generation for the sensing and bioanalysis applications. Most of all, due to the nanoparticles exhibit large specific surface area which provides great capability for signal enhancement while utilizing the nanoparticles as the amplification labels. Furthermore, based on self-assembling specific biomolecular on the nanoparticles surface has also been widely developed for increasing the detection signals of such optical sensing [50, 51], electrochemical tags [52, 53] and micro-gravimetric transduction of different biomolecular recognition [54, 55]. In this regards, the development of this nanotechnology has provided high performance detection for many applications.

However, gold nanoparticles (AuNPs) in the solution which also called the gold colloids have been early reported by Faraday in 1857, that the deep red solution of AuNPs was reduction from chloroaurate ($AuCl_4^-$) by using the phosphorus as the reducing reagent. He investigated the optical properties of thin films that was dried from the AuNPs colloids and observed with the reversible color changes (bluish-purple to green) during compressing with this AuNPs film [56]. Since the discovered of AuNP have unique optical properties in the early century, the intensive of development and research for AuNPs fundamental knowledge and the sensing applications have been widely reported in recent years. In addition, AuNPs have many advantages for the wide range of bioanalysis applications, due to it has easy and fast production which based on the chemical synthesis methods, exist narrow size distribution in the solution, have efficient surface modification by thiols or some bioligands [57, 58]. Most of all, AuNPs surface have great bio-compatibility which can be easily conjugated with specific biomolecules and keeps the biochemical activity for the tagged molecules [59, 60]. Therefore, these approaches have provided great platform for such biosensing [61, 62], drug delivery [63], catalyst [64], heat source [65] applications and also using for the signal amplification while taking AuNPs as the labels in the optical and electrical measurement (**Figure 2.8**).
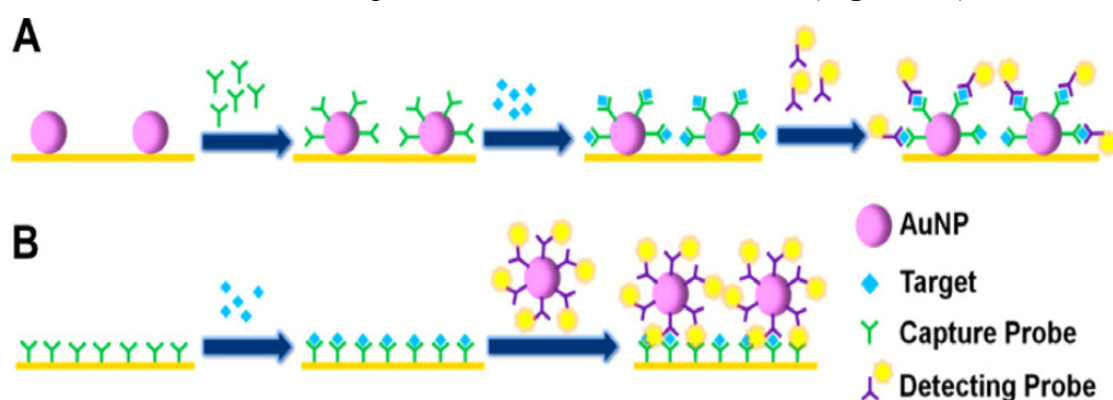
Figure 2.8 Typical signal amplification strategies (A) based on AuNPs serving as the carriers, (B) the AuNPs serving as detection probe. [66]

2.3.2 Gold nanoparticle synthesis in aqueous-phase

In the conventional method for synthesizing uniform particle size of AuNPs colloids is usually based on the bottom-up approach that using the chemical synthesis technique in either aqueous or organic phase. However, the most common way for preparing stable AuNPs in the aqueous phases was reported by Turkevich et al. in 1951 [67]. Herein demonstrated the AuNPs with diameters in the range of 10-20 nm can be easily produced in the solution by rapid stirring of the boiled chloroauric acid ($HAuCl_4$) solution with the reducing agent such as sodium citrate ($Na_3C_6H_5O_7$). The Au^{3+} ions are then reduced to the neutral gold atoms and gradually form to sub-nanometer particles, which the rest of gold atoms are absorbed on the existing particles during the reduction process (**Figure 2.9**).

In addition, variety of reducing agents has been widely developed for synthesizing AuNPs such as sodium borohydride ($NaBH_4$), alkaline tetrakis (hydropxymethyl) phosphonium chloride (THPC) and even by using the nature material of Aloevera plant extract [68]. Based on the chemical synthesis approach, the most important things for producing uniform size distribution of AuNPs in the solution that needs to have vigorous stirring during the AuNPs reduction process in the bulk system [69].
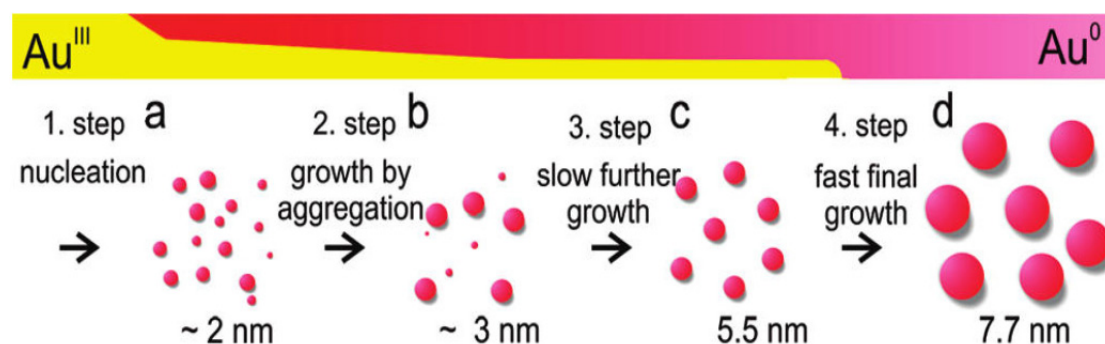
Figure 2.9 The schematic illustration of AuNPs formation process by using chemical synthesis in the aqueous phase. [70]

Having the fine production of AuNPs colloids is considered to provide high sensing performance which using for AuNPs-based colorimetric detection. The key factor to control synthesis nanoparticles with good dispersity in solution have been study for its stabilization or aggregation ability, which depends on the potential of interparticle attractive and repulsive forces (**Figure 2.10**). In the typical electrostatic stabilization approach, particles surface was charged with counter ions in the medium, which form the repulsive electric double layer as stabilizer for against van der Waals attractive forces between the interparticles. However, this stabilization method usually suffers from the disadvantage of highly sensitive to the bulk ionic strength, which leads to decrease in the electrostatic repulsion ability while putting in the environment of high salt concentrations (50 mM of NaCl) [71-73].

Another reports of steric stabilization approach is based on provide a polymeric barrier that prevents AuNPs in the solution from being too close, which have potential for controlling the attractive force between interparticles. In this approach, the thicker of the polymer layers and higher graft densities [74] is considered to provide more effective capability for steric stabilization of AuNPs colloids. Several researchers therefore report that synthesis with thiol-functionalized AuNPs in the aqueous [75] and using thiols containing of different length poly(ethylene oxide) chains [76, 77] or carboxylate modification [78, 79]. Furthermore, poly (N-viny-2-pyrrolidone) (PVP) [80, 81] is the most used of polymer molecule for stabilizing synthesis AuNPs in the water solution. Besides, electrosteric stabilization which provided by surface modified of high density DNA biomolecules (negative charged) is the most effective method for stabilizing AuNPs even present at the high salt concentrations environment [82, 83]. Therefore, based on using chemical grafting or physical adsorption of small molecules or polymers on the AuNPs surface shows great potential for producing stable AuNPs colloids, which particles exhibit better dispersity in the aqueous phase.

However, the development of capable producing monodisperse nanoparticles and that have the ability to controlled AuNPs size and shape is essential for providing high performance bioanalysis. Thus, many research reported for producing monodisperse of AuNPs colloids based on control over the AuNPs growth by using one-phase approach [84, 85], confined the interparticle space with graft micelles [86], reduction with presents various ligands and capping agents [87], digestive ripening of thiol for AuNPs [88]. These approaches present the simple method to achieve control of synthesis AuNPs size and distribution by using weak ligands for decreasing the reducing ability. Most of all, the ability for synthesize AuNPs of uniform size and better dispersity relies on the initial seed-mediate condition, which provides sufficient time for separating the preparation of each particles size [89, 90]. Furthermore, several synthetic methods have also developed the simple methods for preparing AuNPs with different shape and size [91]. Based on utilizing the specific optical properties of AuNPs that is highly related to the size variation, this approach shows great potential for providing wide range of biosensing applications.

(A) Electrostatic stabilization **(B)** Steric stabilization **(C)** Electrosteric stabilization
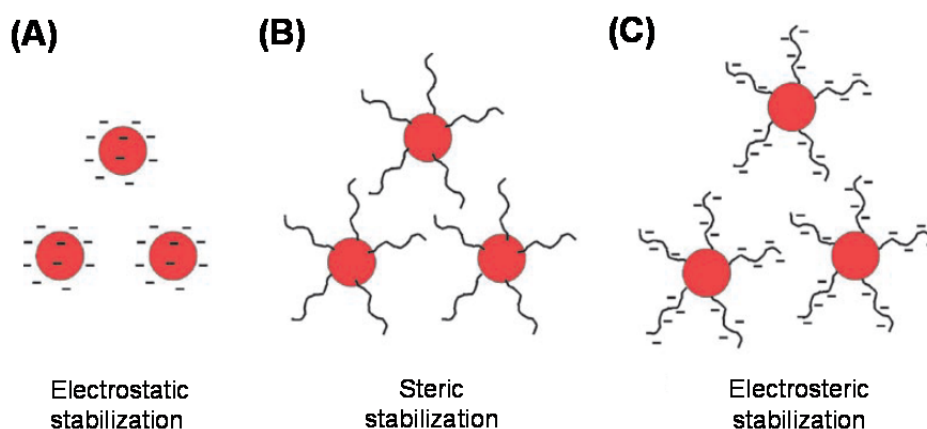
Figure 2.10 Schematic illustrates AuNPs colloid stabilized by using (A) small charged of molecules on the particles surface (electrostatic stabilization), (B) surface grafted of polymers (steric stabilization) and (C) surface grafted by the charged of DNA or polymers (electro-steric stabilization). [92]

2.3.3 Gold nanoparticle synthesis in organic-phase

The AuNPs synthesis in non-polar organic phase has been early reported by Brust *et al.* [93] that brought a new technology for the preparation of nanoparticles. In the two-phase synthesize AuNPs approach, thiol ligands plays the key molecules for stabilizing nanoparticles in the solvent, due to that have strong binding strength on gold surface based on the chemical properties of Au and S (**Figure 2.11**). In this organic phased AuNPs synthesis method, chloroaurate ions ($AuCl_4^-$) were initially transferred to toluene by using tetraoctylammonium bromide (TOAB) as the phase transfer reagent. The mondisperse of AuNPs with diameter between 1.5 ~ 5.2 nm were reduced by using the sodium borohydride ($NaBH_4$), which nanoparticle surface was uniform capped with dodecanethiol ($C_{12}H_{25}SH$) molecules. The two-phase synthesize AuNPs process can be described as eq. (5) (6) [93].

$$AuCl_4^-{}_{(aq)} + N\,(C_8H_{17})_4^+\,(C_6H_5Me) \rightarrow N\,(C_8H_{17})_4^+\,AuCl_4^-\,(C_6H_5Me) \qquad (5)$$

$$m\,AuCl_4^-\,(C_6H_5Me) + n\,C_{12}H_{25}SH(C_6H_5Me) + 3m\,e^- \rightarrow 4m\,Cl^-{}_{(aq)} + [Au_m(CH_{25}SH)_n]$$

$$(C_6H_5Me) \qquad (6)$$
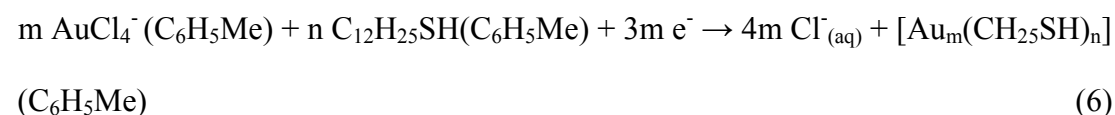
The conditions for well control the synthesis AuNPs size is determine by the gold/thiol ratio (ξ). Based on this approach that AuNPs can be achieved to the smallest diameter of 16 ± 2 Å when the ratio was as lowered below than 1:1 [94].
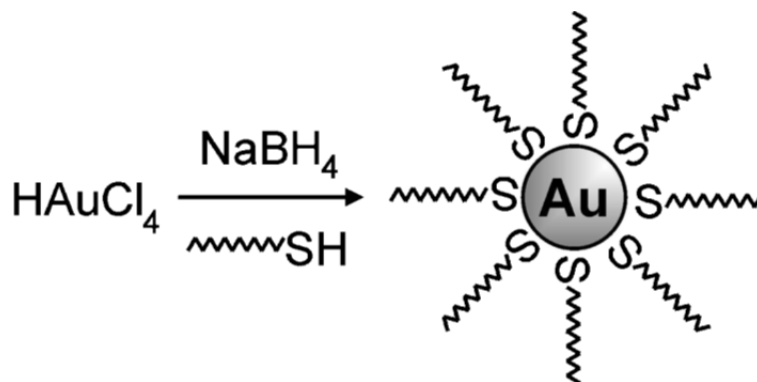
Figure 2.11 Schematic illustrates the formation of AuNPs coated with thiol molecules by reduction Au^{III} ions in the toluene solvent. [95]

Besides, the surfactant stabilized of AuNPs in the organic phase exhibit many advantages such as having high degree of control the particle size and monodispersity [96], easily prepared for high concentrations AuNPs, have the ability to store as powder and re-dissolved in different organic solvents without occur aggregation. In the typical approach for AuNPs prepared in the organic phase usually provide better application of catalytic process and have tunable of surface properties based on the organic functional groups [97, 98]. The formation of self-assembled monolayers (SAMs) can be well controlled by varying the space between interparticles via capping with different length of alkanethiols [99]. Therefore, the synthesis of uniform size and monodisperse AuNPs in the organic phase is considered to provide high sensing performance of using fine AuNPs colloids, which enhance the capability of applying to the catalyst and biochemical applications.

2.3.4 Gold nanoparticles phase transfer

Except directly synthesis stable AuNPs in the water or organic phase, many studies have developed the simple method for moving such nanoparticles across into different phase solutions. The first reported AuNPs to achieve phase transferred from water to an organic solvent of butyl acetate, was by using the co-polymer of methyl methacrylate and glycidyl methacrylate as form the comb stabilizer [100]. In addition, the most effective phase transfer approach was reported by the Au-Ru system that using an alkylamine or alkanethiol as the coating molecules [101]. Due to surface modify of molecules have hydrophobic properties that is capable for AuNPs go through phase transfer between the two-phase interface (**Fig. 2.12 (A)**). Furthermore, since AuNPs transferred from one phase to another which the size distributions were still remain the same in different solution phase. The color exhibits small difference

and observed with shift in the UV-Vis absorption spectra, which these phenomenon were mainly caused by the changes in refractive index of medium (water: 1.33 to toluene: 1.47) after the particles phase transferred (**Figure 2.12 (B)**).

Although many studies have developed the simple methods for phase transfer of AuNPs from aqueous to organic media, such applications for the biosample detection rely on analyzing in the aqueous environment. Thus, several researches reported new way for phase transfer of AuNPs from organic to aqueous phase, which based on covalent capping of irreversible amphiphilic molecules on the particle surface. However, these approaches usually required for precipitation steps or by using the solvent exchange process to achieve the efficient phase transfer. The AuNPs have been stabilized with strong attached ligand in the solution that is not benefit using for the wide range of biosensing applications.

In contrast, the organic compound of 4-dimethyl-aminopyridine (DMAP) has been widely reported to be the most efficient and rapid one-step approach for providing AuNPs across the interphase boundary (organic to aqueous). This approach is essentially different to the typical phase transfer method, which based on covalently bond of thiol-stabilized nanoparticles in the aqueous (**Figure 2.13**). Moreover, based on using DMAP molecules for efficient transferred nanoparticles in the aqueous exhibit higher stability and without causing aggregation after stored for long period of six months [102]. In this regards, the non-covalent bonding of DMAP-stabilized AuNPs considered to achieve better performance while using for homogenous catalysis and wide range applications.
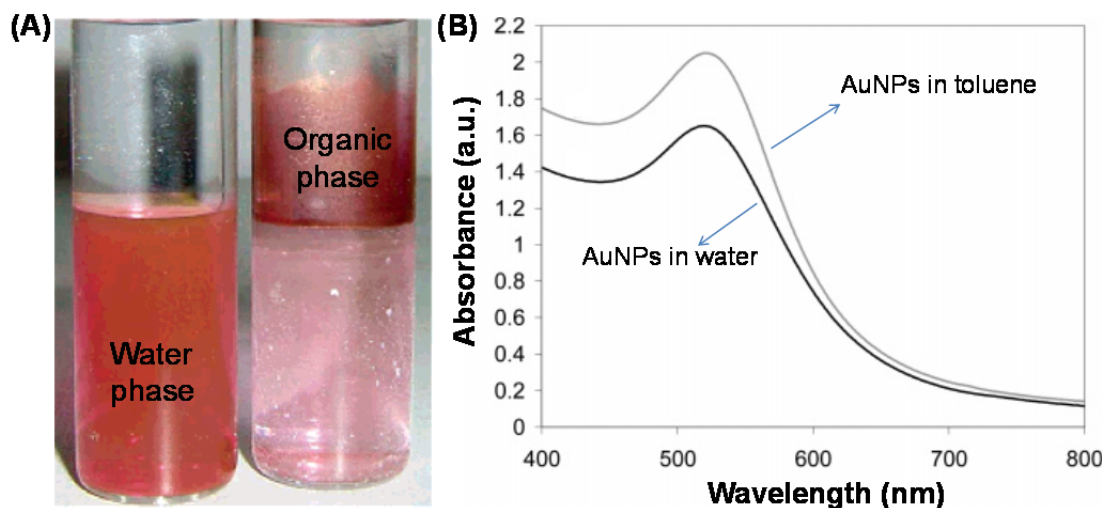
Figure 2.12 (A) Photograph shows the color changes of AuNPs phase transferred from water (bottom of left bottle) into the organic solvent (top of right bottle). [103] (B) UV-Vis spectra shows AuNPs have same absorption band at wavelength 520 nm which the difference of absorbance intensity is caused by the different refractive index of medium. [104]
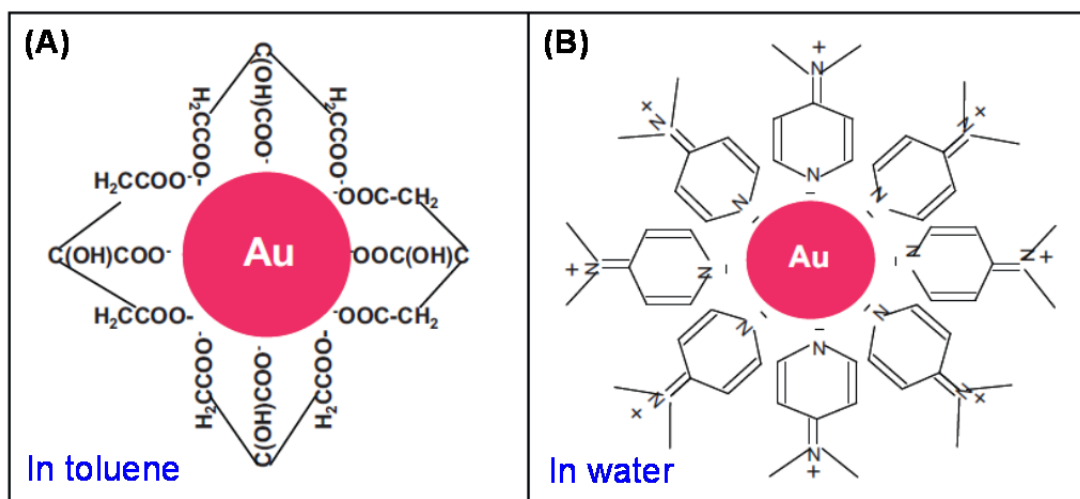
Figure 2.13 Schematic presents the phase transfer of AuNPs from toluene to water, which the particle surface have been charged with different chemical structure of (A) citrate molecules and (B) DMAP stabilizer with positive charged. [105]

2.3.5 Gold nanoparticle synthesis in microfluidic systems

The preparation of aqueous-based AuNP was most achieved by using the chemical synthesis approach, which generally have reacting with two or more reactants in the solution. However, based on using the conventional mixing process in the vessel system always caused to several disadvantages such as reaction environment was not able to achieve homogeneous mixing, and the nucleation for AuNPs growth processes cannot be efficient separated. Since the typical particles reduction process was reacting in a large difference of local environment conditions, which is not capable for well controlling the AuNPs synthesis manner. Therefore, the development for providing better performance of synthesis method is essential to achieve monodispersity of AuNPs with desired size and shape.

However, microfluidic system shows great potential to provide rapid and homogeneous sample mixing in the "micro-reactor", which offers many advantages such as allow conducting chemical reaction in the continuous flow, using smaller amount of reactants, have the rapid and efficient mixing within a short time in compared to the typical reactors [106]. Thus, microfluidic reactor is considered to provide the ideal platform for producing well control of AuNPs synthesis shape and size. Due to the chemical reaction by using laminar flow along with long microchannel scale that the sample mixing was mainly caused by the diffusion at the interface layer, which the microfluidic reactor exhibit high surface-to-volume ratio enable for enhance heat and mass transfer. The efficient mixing in microfluidic system also shows great potential to well control of temperature and concentration gradients for the chemical reaction, which enhance the capability for separating each nucleation process independently. Therefore, based on using microfluidic microreactor is benefit for synthesizing monodisperse AuNPs in the solution.

Microfluidic reactors usually divided into two types of approach: continuous flow microreactors and segmented flow microreactors. Due to the continuous microreactors have ability for continuously varied with sample mixture condition, which can be well controlled of adding different reagents along the reaction channel [107]. Hence, these kinds of microreactors provide the precise condition for individual sample reaction that leads to synthesize uniform AuNPs in the solution (**Figure 2.14**). In addition, decreasing the microchannel scale and increasing the running time of the parallel simple mixing enable for reducing the sample reaction volume and shorten the efficient chemical reaction time. However, the continuous flow is not suitable for providing high degree and flexible fluid manipulation. Due to the fluid flow have always affects by the microchannel surface properties and the actuating system stability. Therefore, it is essential for developing better performance of microfluidic reactors to achieve wide range of applications.
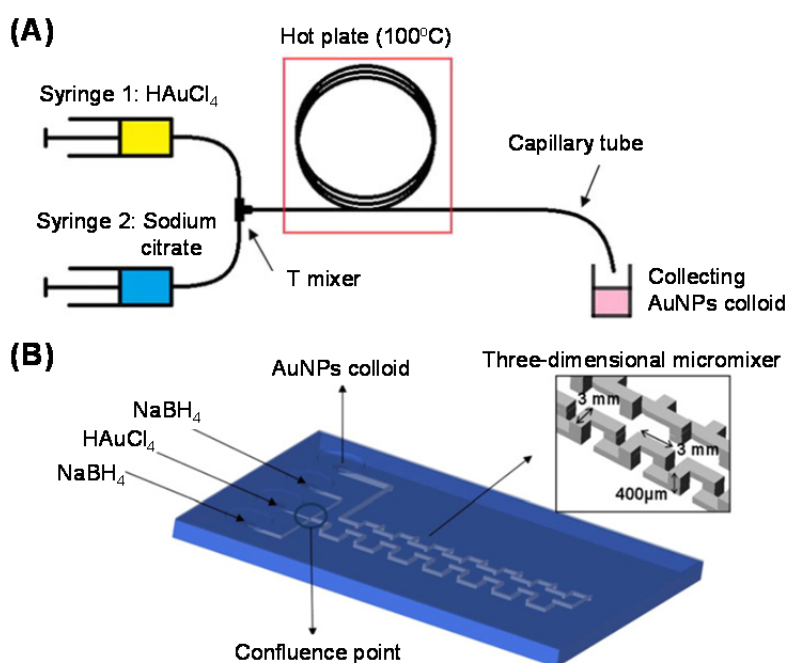
Figure 2.14 Schematic illustration of using microfluidic device for AuNPs synthesis, which Au atom reduction by (A) sodium citrate in $100^{o}C$ temperature, [108] (B) mixing in the three dimensional micromixer with $NaBH_4$ reagent. [109]

Comparing to the single phase microfluidic system, multiphase microfluidic has made the significant advantages including large interfacial area, efficient mixing and faster mass transfer. Based on well controlling for the chemical reaction within droplets or the segment flow is benefit for synthesizing monodisperse of AuNPs. Due to the segmented flow microreactors exhibit the narrow residence time distribution (RTD) [110, 111], which the gas-liquid segment flow have induce recirculation inside the slugs and enhance the capability to achieve rapid mixing for AuNPs synthesis reaction. Furthermore, the nucleation process of nanoparticles growth can be well controlled by initially reaction inside the segment slug, which the slug microreactor have provided homogeneous and fast sample mixing under operating with high flow rates. In addition, due to the segmented flow have encapsulated the whole simple mixing and reaction inside the slugs, which prevents the synthesis AuNPs from blocking or contamination of microchannel [112]. Therefore, the wetting properties of the internal channel wall have great influence to the carrier liquid and able for controlling the segment flow performance. In this regards, based on well develop and control of the segmented flow have great potential for producing highly uniform size distribution of AuNPs that in compared to synthesizing in the continuous flow or other approaches of large system (**Figure 2.15**).
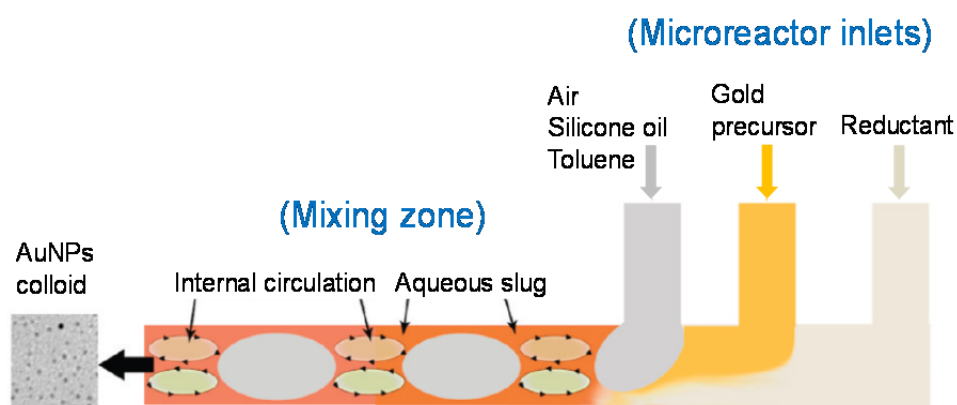
Figure 2.15 Schematic presents typical segment flow for AuNPs synthesis by using microfluidic reactor. The aqueous slugs have divided by gas or organic solution. [113]

2.3.6 Gold nanoparticles for colorimetric detection

In the past few years, the development of AuNPs-based colorimetric detection that relies on the surface plasmon resonance (SPR) has lead this nanotechnology attractively creating simple and versatile platform in the biosensing applications. The advantage of utilizing this approach based on observing of the colloids color changes, which is causing by the interparticle plasmon coupling during the AuNPs aggregation (red to purple) or redispersion from the particle aggregate (purple to red) [114]. Since the first DNA sensor was developed by Mirkin in 1997 [115], AuNPs-based colorimetric detection approach have been increasingly developed for analyzing variety of targets such as proteins [116, 117], nucleic acids [118, 119], metal ions [120, 121], cells [122, 123] and small molecules [124, 125]. Therefore, it was soon become the alternative approach to the conventional detection methods and provided great potential for many applications such as clinical diagnostics, environmental contaminant analysis and drug discovery.

The basic working principle of AuNPs for colorimetric detection is rely on the exist of electrons coherent oscillation on the particle surface, which also called the localized surface plasmon resonance (LSPR) that have induced by the incident electromagnetic field [126]. When applying for the visible light to AuNPs colloids, the specific resonant wavelength caused the free-electrons on the metal surface to oscillate. Due to the wavelength of incident light is much larger than the nanoparticles size that creates the resonance conditions (**Figure 2.16**). When the wave front of light passed through AuNPs, the electron density is polarized at one side and with the specific resonance frequency to occur oscillation. Therefore, this surface electron resonance will causing the specific wavelength absorption and changed in the particles scattering spectroscopy, which the phenomena is found with highly related to

the particles size, shape and the dielectric constants of the medium [127].
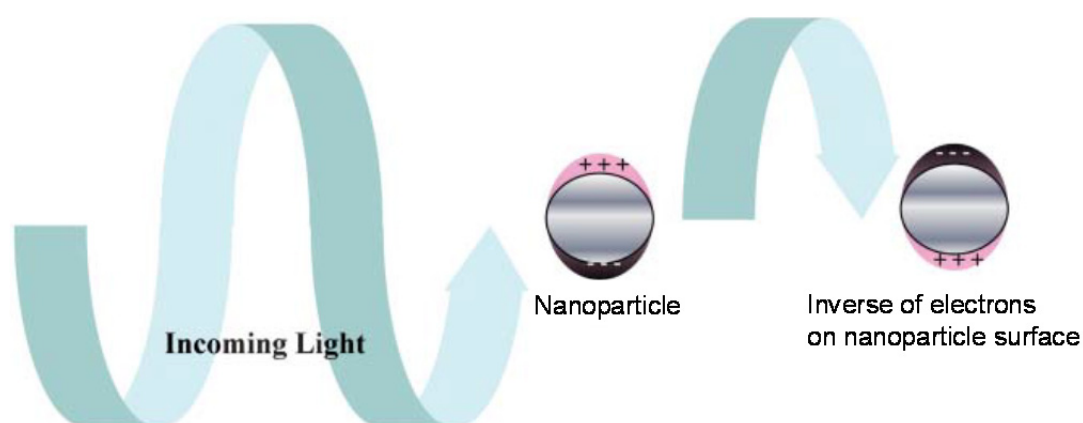
Figure 2.16 Schematic illustrates AuNPs surface plasmon resonance induced by the interaction of electron in the conduction band with visible light. [127]

Generally, AuNPs of diameter in 13 nm have the specific absorption band at ~520 nm of the visible light spectrum, which is considered as absorb with the green light in the visible light range. Thus, the observe color for AuNPs colloids is normally appears to the ruby red color. Due to the nanoparticles have changes of its shape or increase with size diameter that the surface geometry variation would leading to the shift in electric field density of the particles surface. In this condition, those surface electrons will alter its oscillation frequency and causing the different absorption condition with changing to the optical properties. Based on the unique optical properties of AuNPs, which the particles aggregation have causing the interparticle plasmon coupling. When taking the aggregated AuNPs colloids for the absorbance measurement, which the equipment is analysis as observing with larger particle size. Therefore, this physical phenomenon changes so cause the red-shift and broadening the absorption band in the UV-Vis spectra. In this regards, the predictable color changes of the AuNPs aggregation or redispersion in the solution have provided the attractive platform to be using as the colorimetric detection (**Figure 2.17**).
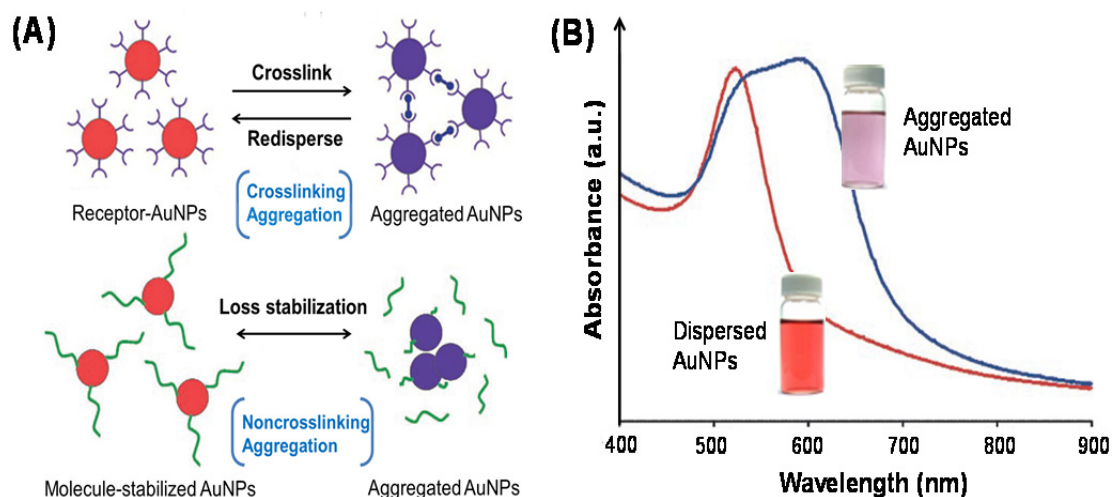
Figure 2.17 (A) Schematic illustrates AuNPs aggregation that caused by crosslinking or noncrosslinking approach. (B) UV-Vis spectra show the AuNPs absorption band which detected from the particles dispersed and aggregated in the solution.

2.3.7 Core etching technique for gold cluster formation

Among the wide range applications that based on utilizing the advantages of AnNPs, to prepare for the quantum clusters (QCs) or called sub-nanoclusters have been increasingly developed in recent years. The QCs usually composed with very few atoms which the core size only in the sub-nanometer regime. Due to such smaller size of metallic material exhibits discrete electronic energy levels, which shows entirely different properties from the nanoparticle. Most of all, the QCs have great photoluminescence properties which easily for changing their emission wavelength from ultra-violet (UV) to near-infrared (NIR) range based on changing the number of core atoms. Therefore, this approach shows great promising for providing ultra-bright, biocompatible and light-emitting sources in the wide range of imaging and detection applications.

However, several researches reported the novel approach for preparing gold QCs by the core etching of AuNPs. Since the first Au cluster etching approach was

reported by Schaaff and Whetten in 1999 [128], which the absorbed monolayer such as alkane thiol (-SR) on the cluster surface have ability for removing Au atoms from the outermost surface layer. Thus, the reaction of Au core etching approach leads to obvious variation in the UV-Vis absorption spectra, which caused the blue shift of the AuNPs specific absorption band. It was significant indicated the particles size have transformed into the smaller dimension. In this regards, the simple method for producing Au clusters by core etching of synthesized AuNPs was treated with excess amounts of molecules such as thiols [129], triphenylphosphine (PPh$_3$) [130] and glutathione (GSH) (**Figure 2.18**). However, in the approach of using thiol as etching molecule, the key factor for controlling cluster size is depend on well control of increased Au:SR ratio. Based on this core etching method is considered to provided new approach for well preparing of metallic cluster in the biosensing detection.
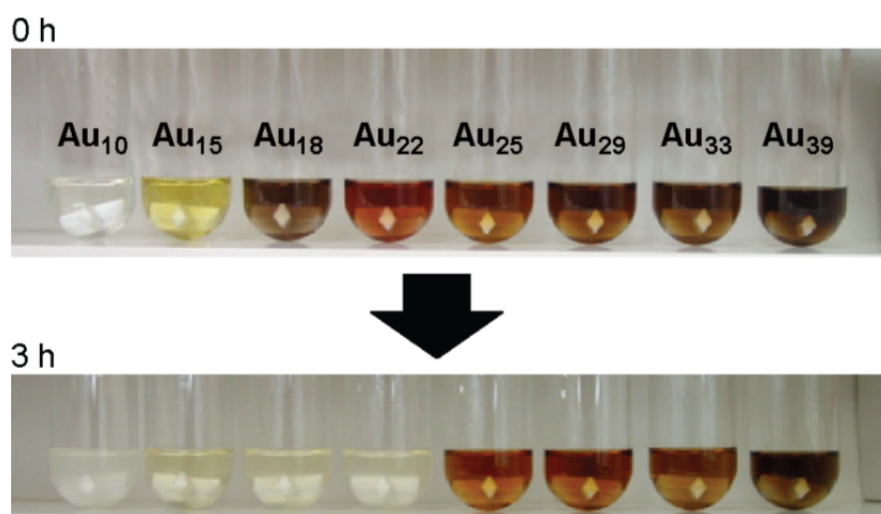
Figure 2.18 Photos show the obvious color changes of Au cluster solution by using core etching technique of GSH molecules. [131]

2.3.8 Gold nanoparticles for dopamine detection

Dopamine (DA), which has a chemical structure of 4-(2-aminoethyl) benzene-1, 2-diol is intensively involved in the normal functions of daily life, including movement, feeding and neurocognition [132]. Moreover, a number of neurological disorders such as Parkinson's disease and schizophrenia [133] are highly correlated to DA concentration. Thus many researchers have focused on developing analytical methods with a high sensitivity and good selectivity for detecting DA in human fluids. A number of established methods for detecting DA have been reported including electrochemical (EC) analyses [134-137], high performance liquid chromatography (HPLC) [138, 139], chemiluminescence detection [140-142], and mass spectrometry approaches [143]. Although these kinds of methods can provided highly specific and sensitive detection of DA, they all have some drawbacks which require sophisticated equipment and time consuming analytical process.

Furthermore, the voltammetric detection of DA in brain tissue is often complicated by the presence of ascorbic acid (AA), which produces an oxidation peak that may interfere with that of DA. While using a standard electrode configuration for electrochemical detection of DA, it is difficult for real quantification analysis of DA with this approach [144]. Recent reports indicate that Nafion and some polymer layers have the ability to eliminate the interference of AA while detecting DA [145, 146]. In addition, the EC electrodes may be subjected to the fouling effect due to the accumulation of oxidized products on the electrodes [147]. In order to overcome this effect, several methods have been proposed to solve these problems by using surface modified electrodes [148, 149]. However, these processes rely on time consuming sample pre-concentration processes prior to the EC measurement. Therefore, it is beneficial to develop a simple, low cost yet high performance method for detecting DA with low interference effects.

However, since AuNPs exhibits unique electrical and optical properties which have been widely investigated and applied in molecular catalysis and biosensors over the last few decades. Typically, synthesized AuNPs with a size of 13 nm exhibit a specific absorption band around 520 nm while dispersed in liquid media. When the AuNPs tend to aggregate, the increased particle size will caused a red shift in the absorption spectrum which is easy to observe and analyze. Therefore, most of the reported AuNPs based biosensors adopt this colorimetric assay as the detection principle. In order to conquer the difficulties of the previous proposed methods used for the detection of DA, many studies have been proposed based on the cross-linking of AuNP aggregation for providing a sensitive detection of DA. The lowest limit of detection (LOD) of DA from the proposed literature which observed the aggregation of AuNPs was reported to be 0.36 μM [150] (**Figure 2.19**).
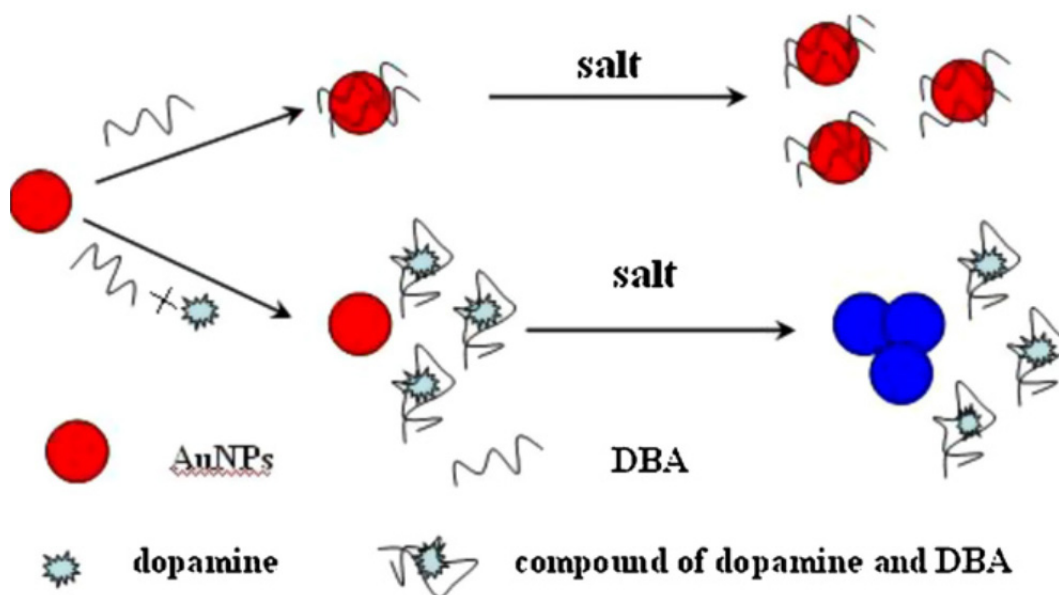
Figure 2.19 Schematic illustrate the mechanism of the colorimetric detection of DA utilizing DBA and unmodified AuNPs. [150]

2.4 Detection in microfluidic systems

2.4.1 Optical detection in microfluidic systems

Optical detection technique has been widely developed in the microfluidic system for using in broad range of applications e.g. analytical chemistry, medical analysis, clinical diagnostic and food technology. Due to the detection method exhibits noninvasive nature, easily integrating with microchip, have rapid response and high sensitivity for getting detection signals [151]. Thus, several miniature optical components have been developed for integrating on the microchip such as coupling optical fibers, design with waveguide or micro-lenses in channel. In these detection approaches which detection light source usually provides by using light emitting diodes (LEDs) or laser diodes. Most of detection method based on detecting absorbance or fluorescence signal of the analytes. However, using the absorbance detection in microfluidic system mainly suffer from getting relative low sensitivity, due to microchip exhibit small optical path length and insufficient analytes for the analysis. Therefore, it is essential developing high performance optical detection in microfluidic system to provide better chemical analysis applications.

2.4.2 Optical fiber-based detection in microfluidic systems

In many developed of optical detection approaches, optical fibers have been mostly demonstrated used for integrating on the microfluidic chip. Due to the optical-fiber has relative simple and flexible ability to connect with analytical instruments. When using the typical optical fiber-based detection method to provide sample absorbance measurement in microfluidic system, which works by transmitting the light through one optical fiber to the analytes. The changes of absorbed light intensity by reacting with analytes is then detected through the other or same fiber to the analyze instrument [152]. However, due to the applying light source usually

designed for perpendicular passing through microchannel. The micrometer size of channel depth shows great influence for the detection sensitivity that is caused by the limited of smaller optical path length. Therefore, many research reported to increase optical path length or design focus micro-lenses in the detection channel for solving low detection sensitivity problems (**Figure 2.20**). In this regards, using optical fibers to integrate in the microfluidic system can provide rapid and sensitive biosensing and enhance the analyze performance in wide range of applications.

Besides, the absorbance measurement based on detecting in the microdevice has ensured to use with very low sample volume (nanoliter to picoliter). Various development of optical detection approach by using microfluidic system exhibit many advantages for providing better platform in the bioanalysis. However, it is difficult to provide rapid kinetic measurement in the conventional microfluidic system. Due to the system is not capable to offer efficient and fast sample mixing with nanoliter range. Thus, several researches reported the millisecond of kinetics measurement can be achieved by using the droplet-based microfluidic system by detection from the changes of sample fluorescent signal. In this regards, to develop for the rapid optical detection in the microfluidic system shows great potential for providing high performance detection using in the bioanalysis.
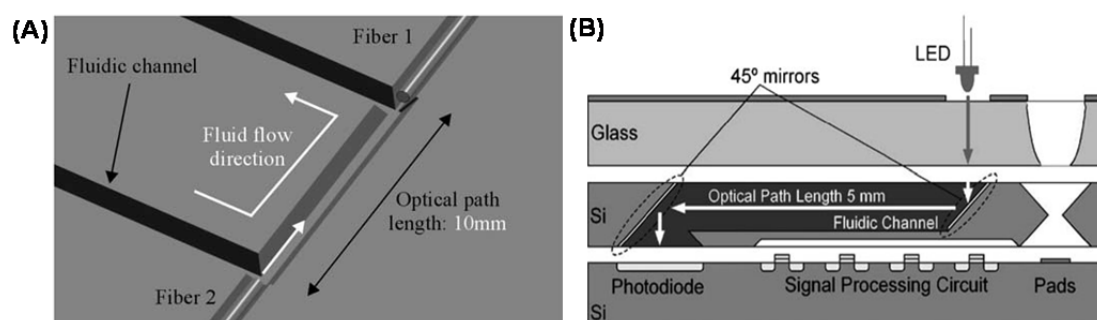
Figure 2.20 The typical optical detection sensor of using microchip for enhance detection sensitivity by (A) increasing the optical path length [153] and (B) design with parallel mirrors in the channel. [154].

Chapter 3 Working principle and theory

3.1 Chip design for liquid-solvent separation

The working principle of proposed liquid-liquid phase separation approach is based on creating large capillary force by using the segmented flow system. The design comb channel of liquid phase separator provides a sufficient force for separating immiscible liquids of low surface tension. The main fluid channel and smaller side channels are designed with the depth in 25 μm and 50 μm, respectively. Besides, the developed channel width of W_1, W_2 and Ws are 280 μm, 350 μm and 70 μm, respectively (**Figure 3.1 (A)**). During the liquid phase separation process, toluene was initially formed into droplets (white) by surrounding with water (blue) at the T-junction channel of the chip. When toluene droplets come to the expansion channel, flow velocity shows decrease in the main fluidic channel which due to hydrodynamics forces and surface tension dominates the droplets movement. Therefore, the first generated toluene droplet was forced to slowly flowing at the main channel and fusion with next droplet. Finally, the formation of continuous toluene flow was benefit to achieve efficient collecting in the downstream.

Furthermore, design different depth of microchannels is capable to create large difference in capillary force, which using for separating immiscible liquids by extracting water to go through smaller size of microchannels. By using the segmented microfluidic system, the generated of toluene droplets exhibits lower surface tension that is difficult to deform and force into the smaller channel. In the opposite, water solution was taking as the carrier flow which is easily passing through the small of comb-like channels at the bottom substrate (**Figure 3.1 (B)**). Therefore, low surface tension liquids of water/toluene are capable to achieve efficient separation by using the proposed separator.
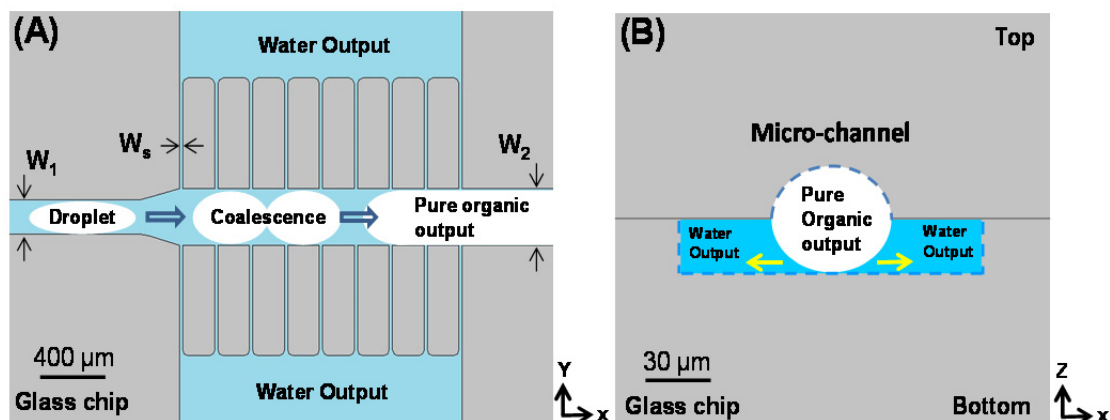
Figure 3.1 Schematic illustration shows the working principle of (A) the design phase separator on the glass chip which by creates large separation force to separate toluene and water phases. (B) The cross-section view for water phase extraction.

3.2 The working principle of using DMAP-AuNPs for DA detection

Figure 3.2 presents the brief mechanism of the developed AuNP core etching technique for DA detection. The fundamentals of the developed method are functionalized DMAP-AuNPs with ligand exchange and phase transfer (toluene to water). Before the colorimetric detection of the DA base on the AuNP core etching process, the AuNPs were first synthesized in a solvent of toluene and then extracted into an aqueous solution by utilizing DMAP molecules. Several studies reported that DMAP molecules can be spontaneously attach onto the AuNP surface due to the positive charge of pyridine nitrogen. The DMAP-stabilized AuNPs then transfer into the water phase, which is caused by the DMAP molecule moving across the water-toluene phase boundary and physisorbing onto the AuNP surface. The addition of DA into the aqueous AuNP solution causes the core etching effect of AuNPs such that the size of AuNPs decreases. The corresponding chemical schematics and the size variation for the AuNPs at different stages are labeled in the scheme below.
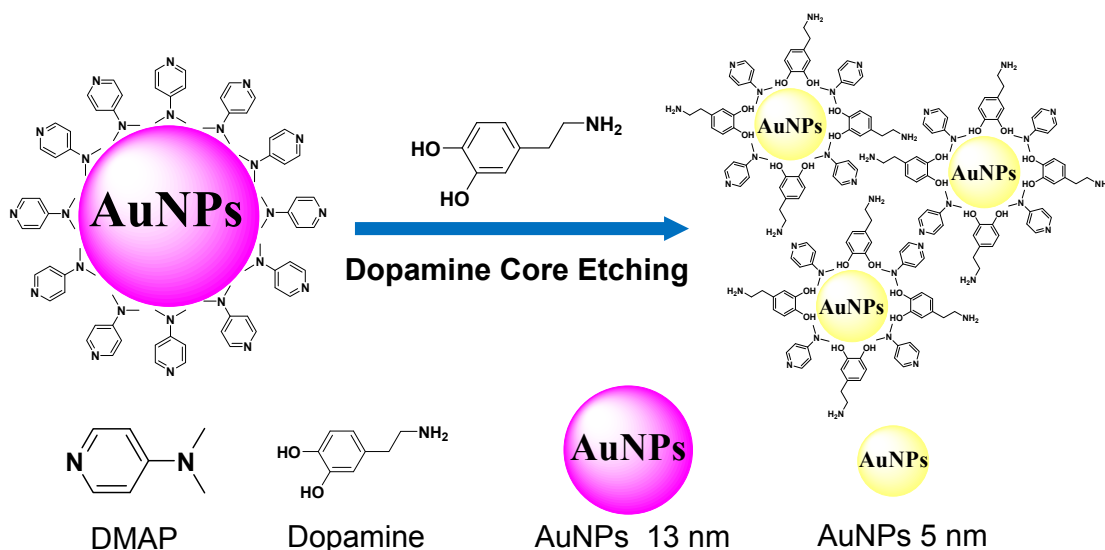
Figure 3.2 Schematic illustrates the developed DA detection method, which based on the core etching effect of DMAP-AuNPs.

3.3 The design of optical detection sensor by using microfluidic chip

The final design of optical detection sensor by using the microfluidic chip is shown in **Figure 3.3**. The developed of optical detection approach composed by continuously generate sample droplets by using a multiphase microfluidic system. When droplets have passing through the optical detection channel that was rapidly detecting for the sample absorption spectrum. Providing a stable segmented flow system in the microchip, toluene used as the carrier fluid for generating droplets at the T-junction channel. In addition, two multi-mode optical-fibers have first etched by immersing in BOE solution to reduce buffer layer diameter. The optical detection sensor finally composed by assembling the etched optical-fibers into the channel.

Therefore, the working principle of this optical detection sensor was presents by transmitting light source through one optical-fiber to the analytes and detecting for the amount of absorption light from the other optical-fiber. When sample droplets have filled up into the optical detection channel, it is rapidly measuring for the absorption

spectrum by using a UV-Vis spectrometer. Most important, the absorbance measurement by using the microdevice only requires sample volume of 50 nL, which exhibits lower sample consumption in comparing to the conventional cuvette system. By using the developed of optical detection approach in the microfluidic chip that is capable to provide rapid and sensitive absorbance detection for wide range of biosensing applications.
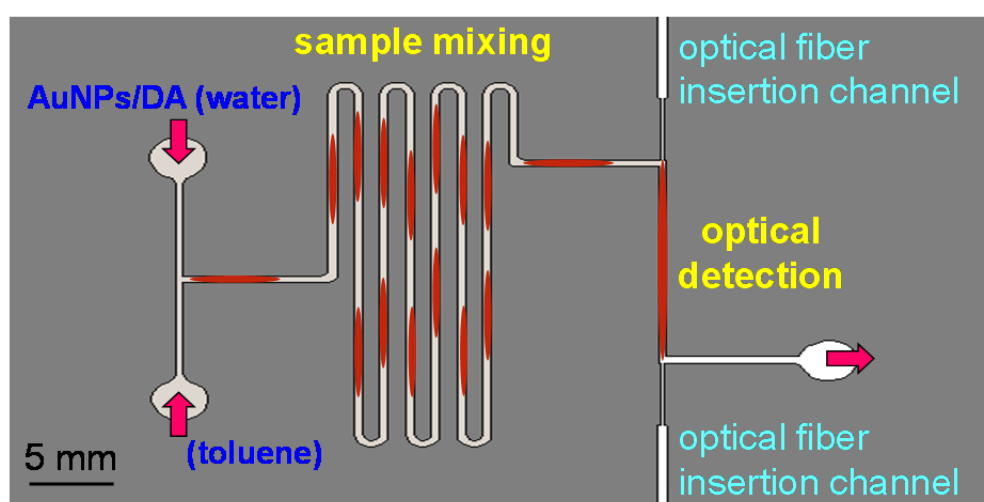
Figure 3.3 Schematic illustrates the developed optical detection sensor by assembling optical fibers on the microfluidic chip.

3.4 Absorbance detection theory

Optical absorption detection is one of the most commonly used detection method in the microfluidic system. However, the development for the microfluidic absorption sensors may suffer from the problems of relatively low sensitivity of the signal, due to the small microchannel dimensions. Besides, the thickness of the microdevice is normally larger than the optical path length, which inducing the significant losses for coupling the incident light to the detector. Therefore, to develop high performance of detection method and design with the structures in microdevice for increasing the optical path-length is beneficial for providing sensitive of absorbance measurement.

The basic working principle of absorbance detection is based on the Beer-Lambert law, which the absorbance can be describes as eq. (7) [155].

$$A = -\log_{10}\left(I_1/I_0\right) = \varepsilon cl \qquad (7)$$

where I_1, I_0 present for the transmitted light and incident light, respectively. The ε ($M^{-1}cm^{-1}$) indicates the extinction coefficient, c (M) is the concentration of analytes and l (cm) is the optical path length. The equation clearly indicates absorbance A is proportional to the analytes concentration and the absorption path length. However, due to the optical detection by using the microfluidic system usually exhibits small sample volume, which is difficult to provide high concentration of analytes for enhance the absorbance detection.

Thus, the best way to solve insufficient optical detection problem of using microfluidic chip usually considered by creating the increased of optical detection path length. However, in typical approach which using the conventional cuvette-based spectrophotometer for absorbance measurement, that the standard optical path length was design into 10 mm. Utilizing MEMS fabrication approach is easily to produce the design channel length for enhance the optical detection ability by using the glass-based microfluidic chip. In this regards, the final work of the study have successfully developed a sensitive optical detection sensor by assembling the optical fibers onto the microfluidic chip. Moreover, based on using the segmented flow system shows great potential to provide fast and uniform sample mixing which is also benefits to achieve rapid and high sensitivity absorbance measurement by using the microdevice.

However, light scattering occurs in microchannel usually affects the optical detection sensitivity which also leading to the serious intensity attenuation. **Figure 3.4** shows light intensity changes by measured from the different distance between light

emitted position and the detector by using microdevice. Due to glass-based microchannel usually leads to the strong light scattering and optical fiber provides an expansion band of emitted light source. Therefore, light intensity exhibits decreasing by the increasing of measured distance between light source and detector. In this regards, when using microdevice for absorbance measurement that usually suffer from the insufficient of light source intensity. However, based on using the commercial spectrometer that is easily to increase the integration time for enhancing light intensity to the absorbance detection. Furthermore, the proposed optical detection channel was design of a reduced channel width, which is benefit for enhancing light transmission in the 10 mm of microchannel. Therefore, this developed microfluidic chip shows great potential to provide high sensitive absorbance detection and achieve fast chemical reaction by using the segmented microfluidic system.
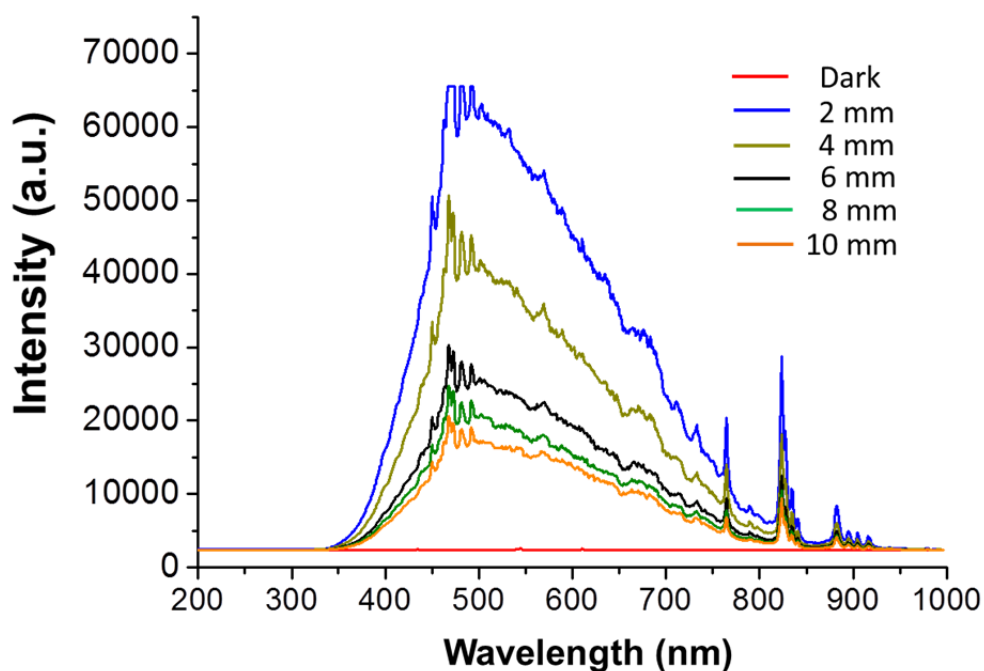
Figure 3.4 Light intensity changes of measured from different distance between light emitted position and the detector by using the microdevice.

Chapter 4 Materials and methods

4.1 Experiment of AuNPs synthesis by using microfluidic chip

4.1.1 Reagents and apparatus

This section describes the experiment preparation for design of liquid-liquid phase separator and using for fine AuNPs synthesis in the organic solvent. Toluene (99.97%) was purchase from Sigma Aldrich® and water solution added with blue ink (Parker Quink) was used for clear observation of two immiscible liquid in the microchannel. The input flow of toluene and water phase were each filled in 5 mL syringe (Terumo®) and controlled by the syringe pump (780200, KD Scientific, USA). A camera Nikon D5100 (Nikon, Tokyo, Japan) was mounted on the Nikon SMZ-800 stereomicroscope for recording the fluidic phenomenon at the T-junction, mixing section and the phase separator area. In additional, deionized (DI) and distilled water used throughout AuNPs synthesis experiment by using microdevice and batch process. Hydrogen tetrachloroaurate ($HAuCl_4 \cdot 3H_2O$) (99.99%) and tetra-n-octylammonium bromide (TOAB) (98%) were purchased from Alfa Aesar® and sodium borohydride ($NaBH_4$) was supplied by Acros®. All experiment solutions were fresh prepared within 1 h at the ambient temperature ($25 \pm 2^{o}C$) prior to the experimental procedure. The stock solutions of 1 M of gold salt ($HAuCl_4$), was prepared by immersed with 1 mL of DI water.

Analyzing for size distribution of AuNPs which have synthesized by two different approaches, nanoparticles were characterized by using a transmission electron microscopy (TEM JEM-3010 JEOL Corp., USA). The sample preparation for TEM characterization was prepared by dropping 5 μL of AuNPs colloidal solution on the carbon-coated copper grid and then dried at $100^{o}C$ for 24 h. The absorbance detection of AuNPs colloids was measuring form a commercial UV-Vis

spectrophotometer (SP-880, Metertech, Taiwan). The size distribution of synthesizing AuNPs in the toluene was evaluated by calculating of 300 particles from the TEM images by using Image J software.

4.1.2 Microfluidic chip fabrication

The study of liquid-liquid phase separator is fabricated by using the micro electro mechanical system (MEMS) lithography etching process on a commercial microscope glass slides ($76 \times 25 \times 1$ mm^3, Marienfeld, Germany). **Figure 4.1** presents the simplified fabrication process of the developed microdevice. The glass slides were first cleaned in a boiling Piranha solution (sulfuric acid (%):hydrogen peroxide (%) = 3:1) for 10 min, a thin layer of hexamethyldisilazane (HMDS, J. T. Baker, USA) was coated as adhesive primer for stable the thick layer of positive photoresist (PR) (AZ4620, Clariant Corp., USA) as the etching mask. The designed pattern on the glass was then fabricated by using the standard lithography process. The channel structures produce by immersed in a BOE etchant (6:1, J. T. Baker, USA) with ultrasonic agitated for 25 min, which to form the etched of channel depth for 25 μm. The PR etching mask was then removed by immersing in a diluted KOH solution (KOH:H$_2$O = 1:3, at 50°C) for few seconds. The fluidic via holes were then drilled on the upper substrate for the solution input. Note the top and bottom of glass substrates have same design channel structure for creating a depth of 50 μm main flowing channel, which the smaller size of comb channel was only fabricated on the bottom glass substrate. Finally, the two substrates were carefully pre-aligned and thermally bonded by putting in a sintering oven at 660°C for 15 min.
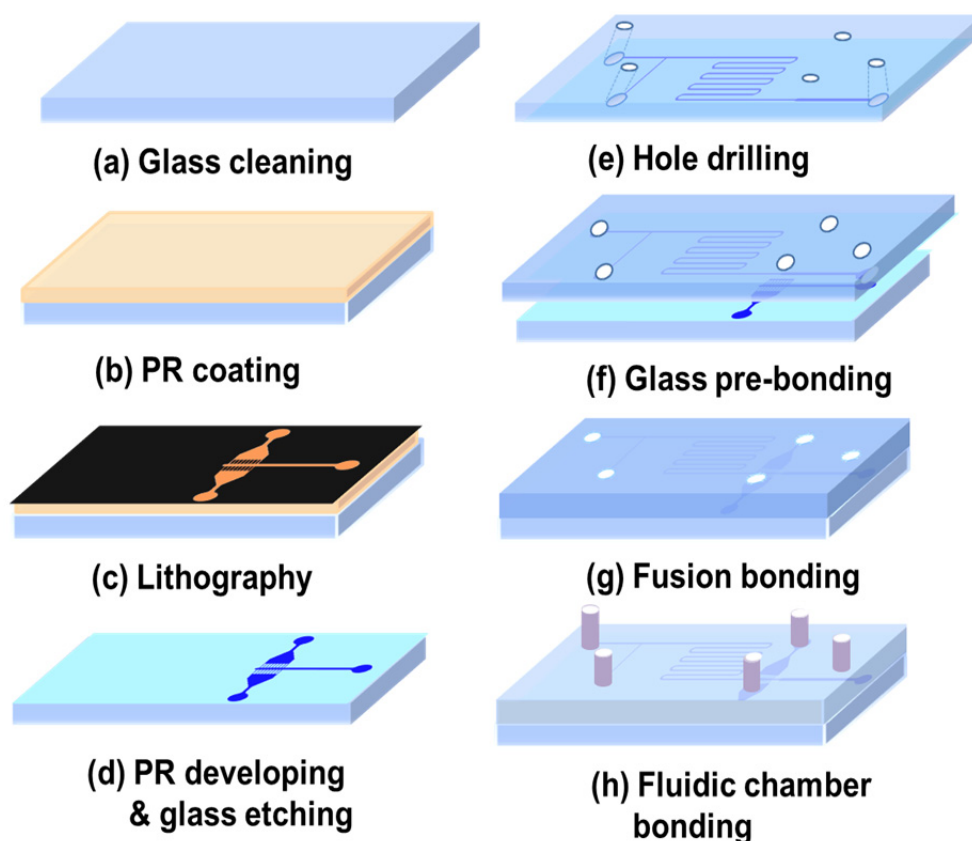
Figure 4.1 Schematic illustrates the microfluidic chip fabrication process of the design liquid-solvent separator.

4.1.3 AuNPs synthesis using typical vessel system

Based on using the typical two-phase AuNPs synthesis approach that was reported by Brust *et al.,* the precursors was prepared by extracting a 1 M (1.0 mL) aqueous gold-salt solution in the centrifugal tube and added with 30.0 mL toluene. The gold-salt in the toluene solvent has been dissolved with a 20 mM tetraoctylammonium bromide (TOAB). Due to the immiscible solution of water and toluene which gold salt ions have been transferred into the top of toluene layer and showed the color in brown. The reduction agent of 0.4 M (10 mL) $NaBH_4$ solution was then added into the toluene bath and rapid stirring for 5 minutes. Therefore, the reduction of AuNPs colloids with size of 13-20 nm was successfully produced and observing ruby red color in the toluene layer after whole synthesis process.

4.1.4 AuNPs synthesis using the microfluidic chip

Using the developed microdevice to synthesize AuNPs in the toluene, this approach is capable for providing uniform and rapid chemical reaction in the segmented flow system. The microfluidic channel was designed with two inlets for solution input and provides a rapid mixing along with the long mixing channel. In the AuNPs synthesis process by using the microdevice, one syringe filled with gold-salt of toluene solvent was injecting into T-junction channel using as the separation phase. Another inlet was injected by 0.4 M NaBH$_4$ solutions which using as the continuous flow. The separation and continuous flow rate was operating in the range from 5-20 µL/min for stably generating droplet from the T-junction. Finally, the uniform size distribution of AuNPs was synthesized in the segmented flow and purely collected at the downstream. Therefore, the developed liquid phase separator was efficiently separating low surface tension of toluene from water solution which using for AuNPs synthesis also prevents it from unnecessary reduction reaction.

4.2 The preparation of DMAP-AuNPs for DA detection

4.2.1 Reagents and apparatus

The details of preparation functionalized DMAP-AuNPs for DA detection is describes in below. The performance of developed AuNPs probes to detect DA was test by using off-chip system, deionized and distilled water using throughout. 4-(Dimethylamino) pyridine (DMAP) were purchased from Alfa Aesar$^{®}$ and sodium borohydride (NaBH$_4$) was supplied by Acros$^{®}$. Dopamine hydrochloride (DA), catechol (CA), ascorbic acid (AA), homovanillic acid (HVA), glutathione (GSH) and phosphate-buffered saline (PBS, 0.01 M, pH 7.4) were purchased from Sigma-Aldrich$^{®}$. All experimental solutions were freshly prepared within 1 h in the

ambient temperature ($25 \pm 2^{\circ}C$) prior to the experimental procedure. The stock solutions of 1 M of gold salt ($HAuCl_4$), and 1 M of DA were both prepared by mixing with 1 mL of DI water.

The mixture process of the DA biosample with the proposed AuNP solution was performed by using the vortex mixer (VM-2000, Digisystem, Taiwan) which vibrated for 3 mins. UV-visible absorption spectrum was analyzed by recording a 3 mL plastic cuvette of the AuNP solution in a commercial UV-Vis spectrophotometer (SP-880, Metertech, Taiwan). The sizes of AuNPs were characterized by transmission electron microscopy (TEM JEM-3010 JEOL Corp., USA). The sample for TEM characterization was prepared by dropping 5 μL of colloidal AuNP solution on a carbon-coated copper grid and then dried at $100^{\circ}C$ for 24 h. Dynamic light scattering (DLS, N5 submicrometer particle size analyzer, Beckman Coulter Inc., USA) was used to measure the size distribution of AuNPs at different stages.

An electrochemical analyzer (Model 611C, CH Instruments, Inc., USA) used to confirm the proposed detection mechanism for DA bonding to the AuNP surface. A standard three electrode electrochemical detection system composed of a platinum (Pt) counter electrode, a gold (Au) working electrode and a chlorination of silver (Ag/AgCl) reference electrode. All electrodes were 200 nm in height and with 1 mm in width. Spacing between working electrode and counter/reference electrodes was 1 mm. DA sample was first prepared in PBS buffer solution for (200 μL, 100 mM) and extracted 40 μL for cyclic voltammetry (CV) measurement, which setting the potential scanned for ±0.6 V with scan rate of 0.1 V/s. Then, added with 20 μL and 100 μL of DMAP-AuNPs colloid to the DA sample and extract for CV measurement again.

4.2.2 Preparation of the DMAP-AuNPs probes

In the preparation of DA colorimetric detection probe which was used by extracting from the toluene-based AuNPs to aqueous phase. The AuNPs synthesis in toluene, 20.0 µL of 1 M aqueous gold-salt and 980.0 µL of DI water were combined in a centrifuge tube, and then added into 30.0 mL toluene dissolved with 20 mM of tetraoctylammonium bromide (TOAB). Since the water and toluene are immiscible to each other, an aqueous solution will be located at the bottom while the toluene solvent will stay at the top. The aqueous gold-salt and toluene beaker was first stirred for 5 min. As the salt ions transferred to the toluene phase, the color of the toluene layer changed from yellow to brown. The brown toluene phase was then extracted to another beaker. Second, the reduction agent of a 0.4 M NaBH$_4$ solution (5 mL) was then added into the toluene bath and stirred for 10 min. At this moment, the reduction of AuNPs to 13 nm in size immediately occurred and the ruby red toluene layer was apparent after the whole reduction reaction. The toluene layer of the AuNPs was then moved to another beaker in preparation for the extraction of DMAP-capped AuNPs.

The procedure for extracting the synthesized AuNPs back into the water phase from the toluene phase can be referred to in work reported by Gittins and Caruso [102]. An amount of 1.0 mL of prepared toluene with TOAB-AuNPs was added along with 1.0 mL of 0.3 M 4-dimethyl-aminopyridine (DMAP) solution for AuNP extraction. The hydrophilic DMAP molecules were replaced by the hydrophobic TOAB molecules on the AuNP surface such that DMAP-AuNPs moved into the water phase. The color of the water phase gradually changed to ruby red and the toluene layer became colorless. Finally, the synthesized DMAP-stabilized gold nanoparticles (DMAP-AuNPs with extinction coefficient at 13 nm diameter is 2.7×10^8 (m^{-1}cm^{-1}), 28 nM) in the water phase were then prepared for the colorimetric detection of DA.

51

4.2.3 Colorimetric detection of DA biosample

The proposed DMAP-AuNPs for colorimetric measurement of a DA biosample were realized by following steps. First, the stock DA solution above was diluted with DI water into different concentrations ($1 \sim 10^{-9}$ M) and then 0.5 mL was added into the prepared 1.0 mL DMAP-AuNPs solution. Then a mixture of the two solutions reacted for 3 min at room temperature. In order to prove the proposed method as a colorimetric detection for a DA biosample, the absorption spectrum of the reacted solutions was then recorded from a 1 cm path-length plastic cuvette shown in **Figure 4.2**, which measured over the wavelength range of 330 to 800 nm. The analyzed DA concentration can also be quantified by the absorption ratio (A_{415}/A_{520}). Moreover, the TEM images and DLS analysis provides further observation of AuNP morphology variation and distribution.
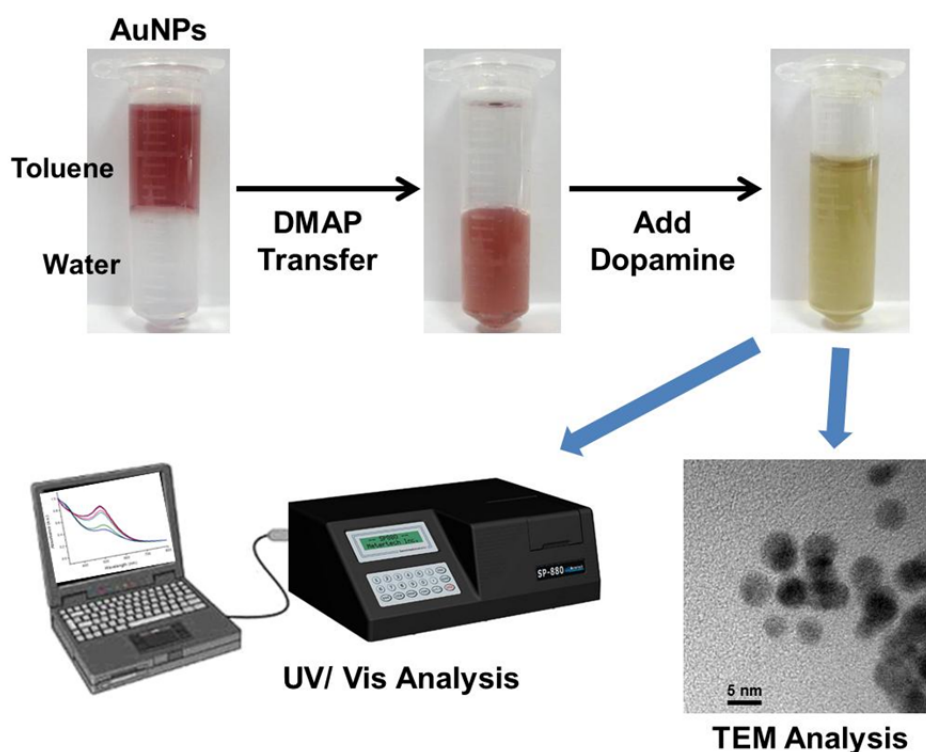
Figure 4.2 A simplified experimental process for the detection of DA by DMAP-AuNPs in aqueous solution.

4.3 Optical detection sensor using microfluidic chip

4.3.1 Reagent and apparatus

The development of optical detection sensor by using microfluidic chip, toluene solvent (99.97%) purchased from Sigma Aldrich® used as a continuous phase for producing AuNPs water droplet in the multi-phase microfluidic system. The injection of toluene and water solution has each filled in a 5 mL syringe (Terumo®) and controlled for the injecting flow rate by using the syringe pump (780200, KD Scientific, USA). DI water was used throughout the experiments for AuNPs synthesis and the application for DA detection, which provide the rapid optical detection by using the microdevice. The previous chapter describes the preparation of AuNPs for DA detection, which this novel biosample detection method was also taking to evaluate the proposed optical detection sensor by using the microdevice.

The developed optical detection sensor was capable providing rapid and continuous absorbance measurement by using microfluidic chip, which composed of assembling etched of multimode optical fiber (50/125 μm, Corning, USA) into detection channel. One of the fibers used for transmitting light source to the analytes and the other takes for detecting sample absorption spectrum by analyzing from a UV-Vis spectrometer (QE65000, Ocean Optic, USA). A 120 W xenon lamp (HMX-4, Nikon, Japan) used as light source for absorbance measurement by using the microdevice, which light introduce to the optical fibers was achieved by coupling to fiber coupler. Evaluating the ability of light transmission within optical detection channel, Rhodamine B solution has diluted to filled into the channel for observing light transmission properties. A camera (D5100, Nikon, Japan) used for observe AuNPs droplets deforming process into the optical detection channel.

4.3.2 Optical fibers assembling on the microdevice

The two multimode optical fibers have initially pretreated before integrating into the microdevice, which stripped their protective plastic layers and then immersed in 6:1 BOE solution (J. D. Baker, USA) for 3.5 h reducing total diameter to achieve 55 μm. **Figure 4.3** shows SEM image of different optical fiber diameter which treated with and without etching process. Further, it also shows optical fiber surface remain keep in smoothness throughout the etching process. The etched multimode optical fibers were inserted into design of fiber insertion channel, which used by "fiber insertion guide" technique [156]. The upper substrate was cut into slightly smaller than the bottom substrate before bonding of two glass plates. After fusion bonding of two glass substrates, the expose of etched channel at the bottom substrate serves as the "guiding channel" for inserting the etched optical fiber. This assembling technique benefits for the optical fiber insertion into micrometer channel without needs for using delicate alignment apparatus. However, there should be carefully handling with the insertion of etched optical fibers to prevent from occurring damage during the optical fiber insertion process. Finally, optical fiber has been fixed in the position with using UV-sensitive glues (2050 A, Tex year, Taiwan).
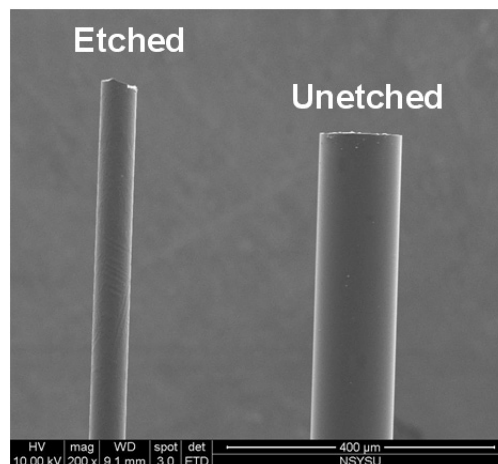
Figure 4.3 SEM image shows the optical fiber with and without etching by immersing in the BOE solution.

4.3.3 Microfluidic chip fabrication

Figure 4.4 (A) presents a schematic illustration of the fabrication process for producing the proposed microdevice on the soda-line glass substrates (76 × 25 × 1 mm^3, Marienfeld, Germany). Note the details of glass-based chip fabrication procedures have been described in the chapter **4.1.2**. Hence, this chip fabrication process mainly focused the method for producing optical fiber insertion channel on the microdevice. Initially, a thin layer of positive photoresist (AZ4620, Clariant Corp., USA) was uniform coated on the glass substrate to use as the mask material for wet etching process. The glass substrate were then etched in a 6:1 BOE solution (J.D. Baker, USA) with added 10% of hydrochloric acid (37%), which capable fabricating a high aspect ratio microchannel of depth in 30 μm. Based on using isotropic etching of glass substrates that was easily produce a micro-weir structure between the design of detection channel and fiber insertion channel, which the structure is benefit to fix optical fiber at the precise position in microchannel.

The photoresist-etching mask on the glass was then removed by immersing into a diluted KOH solution for few seconds. The glass substrates were drilled with fluid inlet/outlet holes via using the diamond-coated drill bits. The two plates with same etched microstructure were then aligned under a microscope (Nikon SMZ-800, Japan) and prebonded by using UV-sensitive glues. Finally, the fabricated of sealed of elliptic microchannel was achieved by thermally bonded the two glass substrates in a sintering oven at 660$^\mathrm{o}$C for 15 min. Note the fabrication process capable producing the proper channel depth for sample flow and optical fibers insertion by using of one design mask, which the depth of sealed microchannel was approximate 60 μm for inserting the etched optical fiber (**Fig 4.4 (B)**).
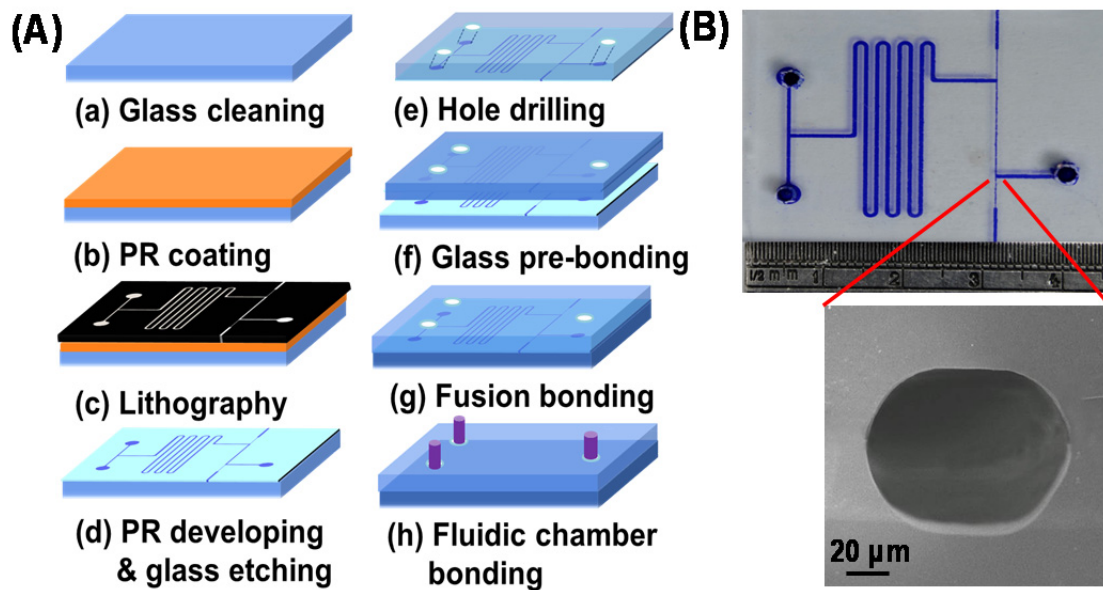
Figure 4.4 (A) Schematic illustrates for the simplified fabrication process of the proposed optical detection microdevice. (B) The photo shows fabricated of microchip and SEM image presents high aspect ratio of optical fiber integration channel.

Chapter 5 Results and discussion

5.1 Liquid-solvent separation for synthesizing AuNPs in toluene

This section describes the details of proposed method for achieving liquid-liquid phase separation and utilizing for fine AuNPs synthesizing in the organic solvent. However, the main idea of developing high efficient liquid phase separator considered to provide better collection and achieved uniform synthesized AuNPs in the toluene. The proposed liquid phase separator prevents AuNPs from the additional contact with reducing agent. Many studies reported creating large capillary force by design different diameter of comb-like microchannel was able to achieve efficient liquid phase separation, which also rely on well tuning of flow breakthrough pressure by using the segmented flow system. This study successfully developed a glass-based microfluidic chip, which design the optimize combination of narrow comb channels, and different depth in the main fluid and separation channels. The microdevice was capable providing high separation efficiency for separating low surface tension liquid. However, due to segmented flow exhibit many advantages of providing uniform chemical reaction for AuNPs reduction. AuNPs synthesized by using microdevice shows narrow size distribution in comparing to synthesize in the conventional vessel-based system. Therefore, the proposed microdevice was benefit producing rapid and uniform chemical reaction for AuNPs synthesis and achieved high efficient of liquid-liquid phase separation.

In the typical liquid-liquid extraction approach by using the microfluidic system, the complete operation procedure usually includes liquid phase contact, sample mixing and the separation. Therefore, results show in **Figure 5.1** presents the photo images of fluidic pattern that generated by the T-junction, mixing section and phase separator. The continuous generating segmented flow (toluene slugs in a water stream)

was stably produced toluene droplets from the T-junction and the developed mixing section provides a uniform and faster mass transfer of chemical reaction by using the multiphase segmented flow system. The proposed liquid-liquid phase separation was successfully achieved by using the phase separator on the microdevice shown in **Figure 5.1 (C)**, which indicates such low surface tension of toluene can be efficiently separated from water solution and have been continuous flow out of the downstream. **Figure 5.1 (D)** shows the fabricated of glass-based microdevice, which presents the complete flow operation process by using the proposed microdevice providing efficient liquid-liquid phase separation.
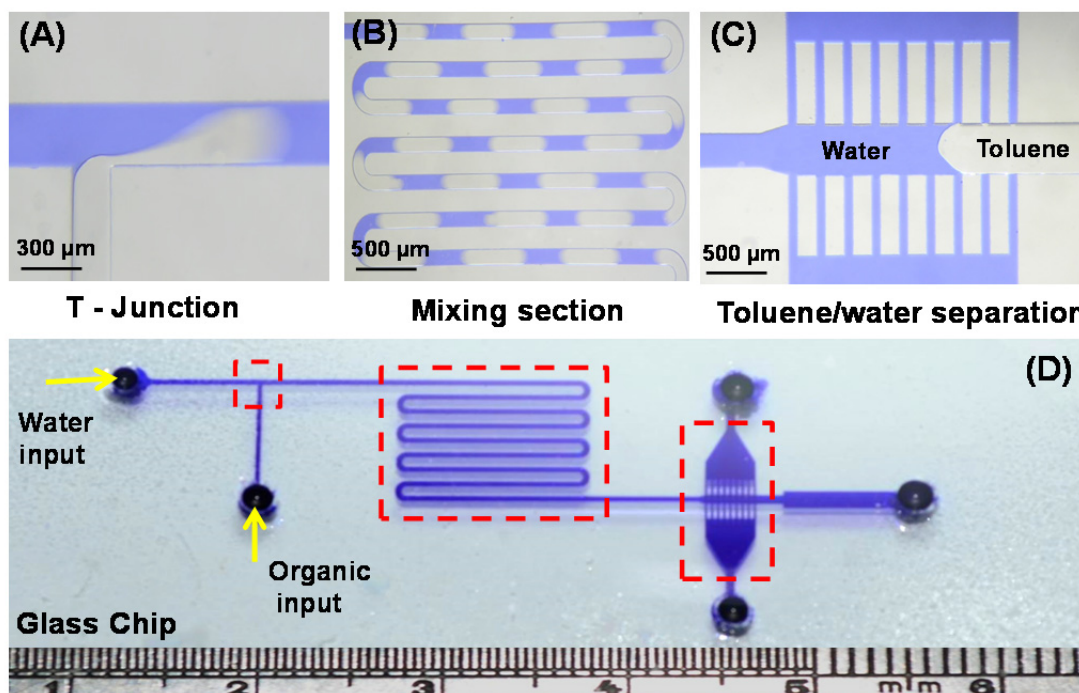
Figure 5.1 The photo shows developed microdevice composed of (A) droplet formation at T-junction channel, (B) the stable segmented flow for sample mixing, (C) toluene and water phase separation by using comb-like capillary. (D) The schematic illustration of flow operation system by using the design glass chip.

The details for using the proposed micordevice to achieve phase separation were described by the interfacial of hydrodynamic forces and liquid surface tension. **Figure 5.2** shows the sequence photos that indicate the continuous separating two immiscible liquid phases captured from the recorded video. Once the toluene droplet flow to the separation channel, the average water flow velocity is decrease via the low flow resistance of channel expansion. Thus, the initial generated toluene droplet was keep in the middle of combs channels (**Figure 5.2 (A)**). Due to the next droplet exist the accelerate foreword movement, the interfaces of two droplets are going to deform and occurred merging into a large droplet (**Figure 5.2 (B)**). Furthermore, since the toluene droplet exhibits the large surface energy while force moving into a narrower channel, which the surface tension will keep the droplet from deformation. Alternatively, the water is easily going through the parallel comb channel at the bottom of the microdevice. In this regards, results indicated that the toluene droplet was successfully merging together and extracted out of the water phase by the design of narrowed separation channel (**Figure 5.2 (D-F)**).
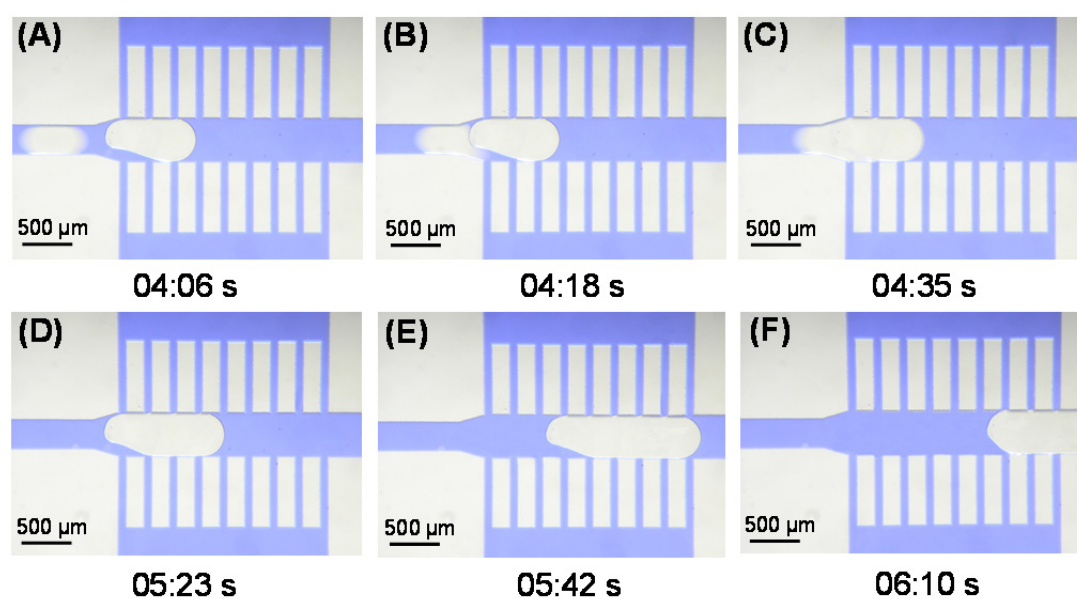
Figure 5.2 The sequence images show the toluene-water separating process within the designed liquid-liquid phase separator.

The optimize operation condition for the proposed microdevice to achieve efficient phase separation is mainly depend on several critical parameters such as liquid-liquid interfacial tension, channel geometry and the operation breakthrough pressure. **Figure 5.3** shows the calculated phase separation efficiency versus the flow rate ratio of the toluene phase and water phase. Note the water flow rate was fixed at 20 µL/min, and different toluene droplet size (600 µm, 840 µm, 1120 µm, 1400 µm) was generated by setting toluene flow rate at 4 µL/min, 8 µL/min, 12 µL/min, 16 µL/min, respectively. When using the capillary force to achieve efficiently liquid phase separation that the approach depends on well control of liquid surface tension to be larger than the droplet breakthrough pressure. Results indicated the increased of toluene droplet diameter was benefit to get higher separation efficiency (92%) for separating liquid-solvent by using the capillary force.
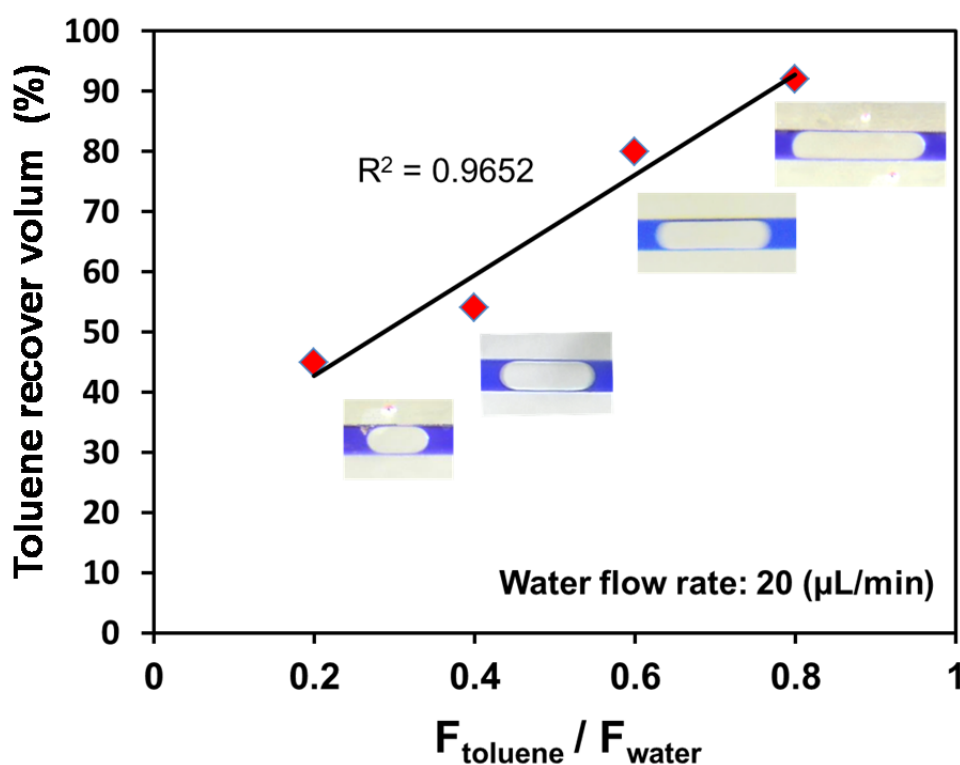
Figure 5.3 The calculated of toluene recover rate versus the flow rate ratio of the developed multi-phase microfluidic system.

Figure 5.4 presents the normalized of absorbance spectra for comparing synthesized AuNPs by using microdevice and conventional vessel system. Results indicated the exhibits of narrower absorption band at 516 nm for AuNPs synthesized by using the microdevice in comparing to AuNPs (@ 522 nm) synthesized in the vessel system. In addition, TEM images also presents the mean diameter were 8.35 nm and 12.61 nm for the AuNPs synthesized by using microdevice and the typical vessel, respectively (**Figure 5.5**). When further characterize the distribution of AuNPs synthesis by using different approaches. Results clearly present the histogram of counting 300 particles by analyzing from the observed TEM images. Results indicated that the AuNPs synthesized in the microdevice (64%) exhibited smaller size and a narrower size distribution ((particles of mean diameter/total particles) × 100%) in comparing to the AuNPs synthesized in vessel (58%). This study successfully developed a novel liquid-liquid phase separator for synthesizing AuNPs with narrower size distribution in the toluene. The uniform size of AuNPs in toluene shows great potential for using to the colorimetric detection.
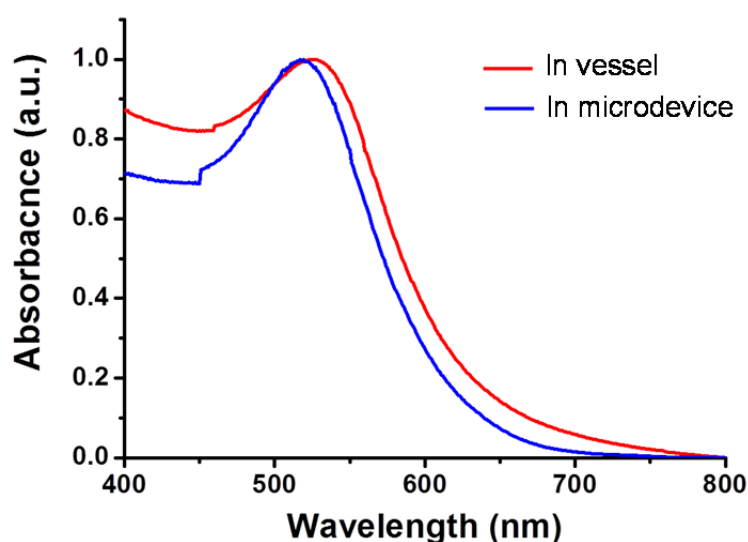
Figure 5.4 The normalized of absorbance spectra show AuNPs synthesized by using the microdevice and conventional vessel system. Note the absorption band of synthesis in microdevice exhibits narrower band width comparing to use the vessel.
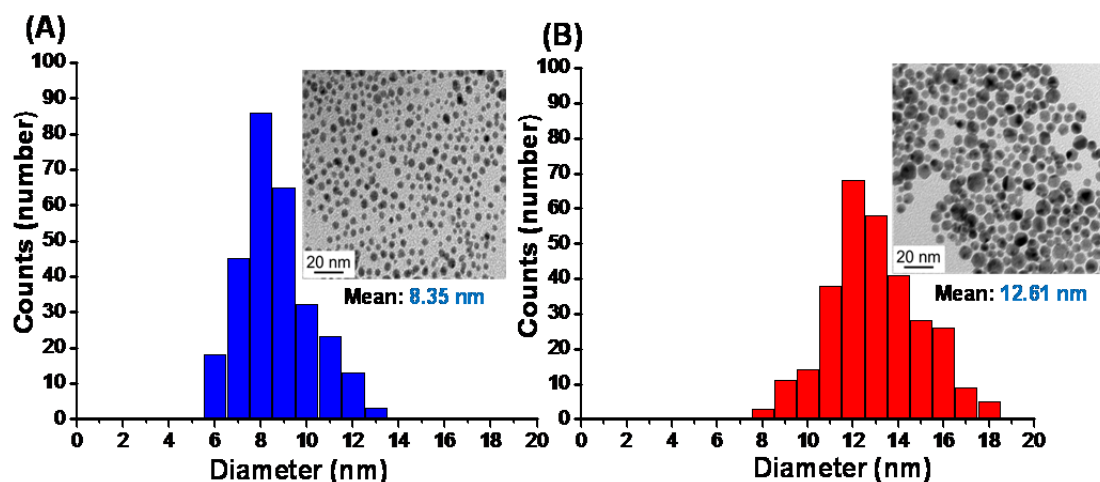
Figure 5.5 Size distribution histograms and TEM images show the synthesized AuNPs by using different approach in (A) the microdevice and (B) the vessel system. Note the particles exhibits the narrower size distribution and smaller mean diameter by synthesizing AuNPs in the microfluidic system.

5.2 Core etching of DMAP-AuNPs for colorimetric DA detection

This section describes the successful development of an alternative colorimetric approach which using a novel core-etching process on the synthesized of DMAP-AuNPs. The original synthesized AuNPs in the toluene was phase transferred into the aqueous phase by ligand exchange of the DMAP molecular. The original diameter of AuNPs is then separated into the smaller sizes right after addition of DA solution and easily observed the changes from the solution colors. Furthermore, results shows that the developed method appear to have no significant problem with detecting DA presence of typical interference in the solution. Following gives the details of the developed AuNPs etching protocol for DA detection, which provides a novel and versatile approach for rapid biosensing applications.

In typical colorimetric measurements for the detection of DA by the citrate reduction of AuNPs, the addition of DA into the AuNP colloid will induce aggregation. For the proposed method of core etching of the AuNPs, however, shows that DA tends

to split the original synthesized DMAP-AuNPs into smaller ones. Scheme 1 simply illustrates the mechanism of the proposed method for colorimetric detection of DA. Results from this series of experiments also prove that DA molecule will have a similar chemical reaction as the thiol molecules that cause the removal of the Au atoms from the outer surface layer and form the smaller AuNPs size. The observable color and size changes of the AuNPs provide a simple and sensitive detection of a DA biosample in aqueous solution.

The synthesized AuNP colloid was first stabilized by the DMAP molecule repulsion that prevents AuNPs from aggregating. The addition of DA into the colloid produces an immediate change in the color. To analyze the sensitivity of the proposed DMAP-AuNPs to detect a DA biosample, 0.5 mL of DA with different concentrations $(1\sim10^{-9}$ M) is each added into 1.0 mL of DMAP-AuNPs colloid. **Figure 5.6 (A)** shows the color of the AuNPs colloid has changed from the original ruby red to green after the mixture. According to the typical AuNP colorimetric detection method, this addition of DA would cause a color change from red to blue due to the fact that AuNPs tend to be conjugated by the addition of DA. Our results show greater colorimetric variations using the proposed DMAP-AuNPs, which can therefore provide a novel and sensitive measurement of DA biosample compared to the typical AuNP aggregation phenomenon. Furthermore, the change in DA concentration from $1\sim10^{-4}$ M was easily observed by the naked eye. To confirm the accuracy of the proposed detection method for DA, a series of UV-Vis spectra were then recorded for the different experimental concentrations.

Figure 5.6 (B) shows the series normalized absorption spectra for detecting different concentrations of DA using the synthesized AuNP colloids. Note that the spectrum was normalized with maximum absorbance as 1 at 330 nm wavelength and minimum absorbance as 0 at 800 nm wavelength, respectively. In the plotted series of

recorded wavelengths, the absorption band has an obvious blue shift from 520 nm to 415 nm caused by the increased DA concentration. Under a low concentration of the added DA (from 10^{-4} to 10^{-9} M) to the AuNP colloid, there is only one absorption peak at 520 nm. However, the spectrum variation shows a decrease of the absorbance intensity at 520 nm and an increase at shorter wavelengths for this DA concentration range. This result simply demonstrates that the original DMAP-AuNPs size of 13 nm have decreased by the addition of DA. Once the DA concentration reaches about 10^{-3} M, a new absorption peak appears at about 415 nm. This observed phenomenon also indicates the distribution of the original AuNP colloid of 13 nm has been transformed into the smaller-sized ones. Furthermore, it can be noted that the spectrum has no specific absorption peak when the concentration of DA reaches 1 M. These results indicate that all the original DMAP-AuNPs have been etched by the DA molecule and have changed into smaller sizes. When the AuNPs are smaller than 5 nm, there will be insignificant plasma resonance to be monitored by the UV-Vis spectrophotometer. These results indicate that the DA concentration is highly correlated to the core etching ability of the AuNPs and can be easily monitored by the absorption spectrum.
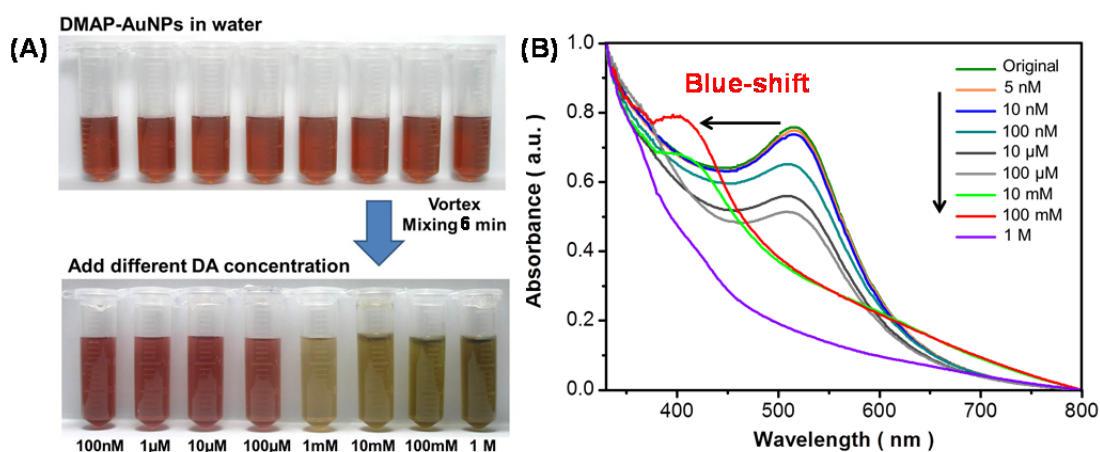
Figure 5.6 (A) Photographs showing the color change of DMAP-AuNPs reacted with various DA concentration solutions. (B) The normalized absorption spectra of AuNPs in different DA concentrations (incubation time: 20 min at room temperature).

To provide further confirmation of the change in AuNP morphology, both TEM and DLS were utilized for a detailed analysis. **Figure 5.7 (A)** presents the morphology of DMAP-AuNPs transferred into the water phase from toluene. It clearly shows the original DMAP-AuNPs with the uniform average size around 13 nm. Once the 10^{-1} M DA is added into the DMAP-AuNP colloid, the relatively smaller particle size is obtained, as shown in **Figure 5.7 (B)**. Results confirmed that the proposed DMAP-AuNPs have been core etched by the DA molecule and split into smaller AuNPs. Furthermore, DLS analysis clearly indicates the average diameter of the AuNPs tend to decrease after the addition of DA (**Figure 5.7 (C~D)**). The measured AuNP mean diameter has changed from the original size of 12.5 nm into 5.2 nm. The above results provide proof that the DA molecule plays an important role in the core etching of the DMAP-AuNPs. The proposed method can therefore provide a novel and simple method for detection of a DA biosample.
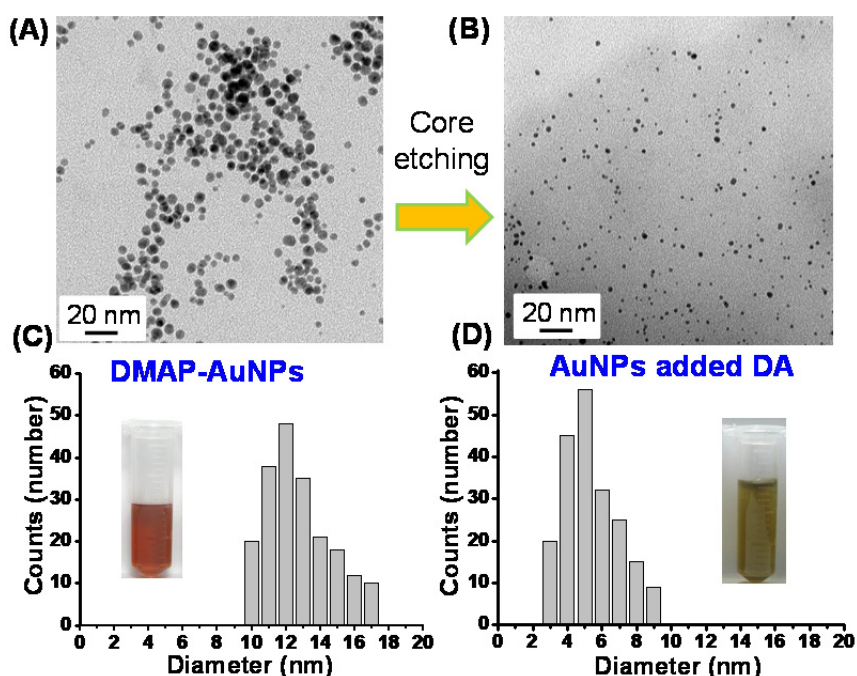
Figure 5.7 TEM images of (a) DMAP stabilized AuNPs in water, and (B) after the addition of 10^{-1} M DA, causing decrease of AuNP size. Histogram show the size distribution of (C) DMAP-AuNPs and (D) after addition of DA to the AuNPs colloids.

To demonstrate utility of the chemical reaction used in the proposed method to detect DA, **Figure 5.8** shows the cyclic voltammogram responses of 200 μL (1×10^{-1} M) DA in PBS buffer solution (red CV curve) and then extracted from the addition of 20 μL and 100 μL DMAP-AuNPs colloids (blue and green CV curve). Due to DA binds to the gold surface that induce the original DA concentration in the solution decreased, resulting in the decreasing DA oxide and redox currents. This result suggests that DA can be ligand-exchanged for the DMAP molecule and strongly bonded to the AuNP surface. As existing DA molecules in the solution tend to occupy the exposed AuNP surface, core etching of the AuNPs will occur and to split the original DMAP-AuNPs into the smaller size. The above experimental results all indicate that the proposed colorimetric detection method is a novel and sensitive detection of DA by the core etching process of DMAP-AuNPs.

With this approach, the change in DA concentration can be easily monitored by the naked eye, and is capable of detecting a nano-molar of DA concentration by the spectrophotometer. As shown in **Figure 5.9**, the absorption ratio (A_{415}/A_{520}) will increase as DA concentration increases. The linear equation could be fitted as $A_{415}/A_{520} = 0.0011$ (x) (DA, nM) + 0.915 ($R^2 = 0.9969$) with the detected DA concentration in the range of ($10 \sim 10^2$ nM), which shows the proposed detection method has good sensitivity. For measuring a wide range of DA concentrations ($10 \sim 10^5$ nM), the trend line equation could be fitted as $A_{415}/A_{520} = 0.0263 \log$ (c) (DA, nM) + 0.8693 ($R^2 = 0.9822$). Most of all, DA concentration in the human urine are 50-100 mcg/mL that the proposed method was capable for measuring such level and achieved the detection limit of DA concentration as low as 5 nM. Comparing to the other proposed colorimetric methods, this study shows a great sensitivity for the detection of DA. The method presented in this research provides an alternative approach for developing new nanoparticle-based biosensors.
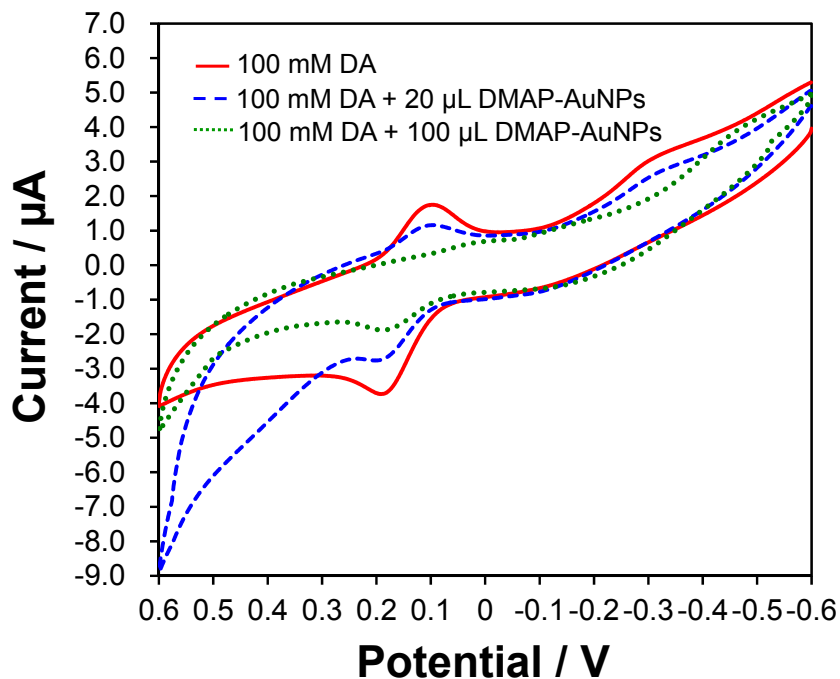
Figure 5.8 Cyclic voltammogram responses of detecting 200 µL (1×10^{-1} M) DA and DA sample after added 20 µL and 100 µL of DMAP-AuNPs solutions. Results show that the concentration of DA has been reduced by the AuNPs.
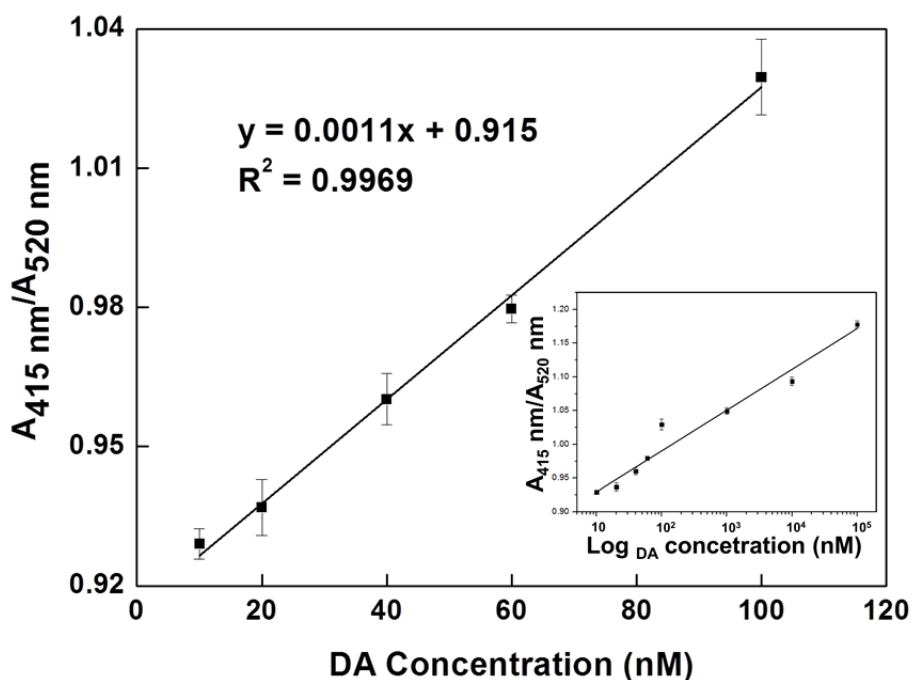
Figure 5.9 Calculated absorption ratio value A_{415}/A_{520} of added versus different DA concentration and with correlation coefficients of 0.9969.

The selectivity for detecting DA in the presence of other interferents such as ascorbic acid (AA), homovanillic acid (HVA), catechol (CA) and an important interferent of glutathione (GSH) was also experimentally investigated (n = 5). Pure interferents and DA mixed with interferents were analyzed using the AuNP colloids. The selectivity of the developed method for detecting various samples were evaluated using a defined parameter of the absorption ratio index (ARI) which was defined as $(A_{415}/A_{520})_{Sample}/(A_{415}/A_{520})_{Blank}$. Therefore, the ARI for the dummy test (blank) should be 1. **Figure 5.10** presents the histogram of detecting various samples. Quite clearly, the developed method is insensitive to the interferents of AA, HVA, CA and GSH as the ARI for detecting these pure samples was close to 1. Alternatively, the ARI values for detecting pure DA and DA added with various interferents appear to have similar ARIs, indicating the existing interferents did not affect the detecting results. This result further confirms that the developed core-etching technique exhibits a good selectivity for detecting DA.
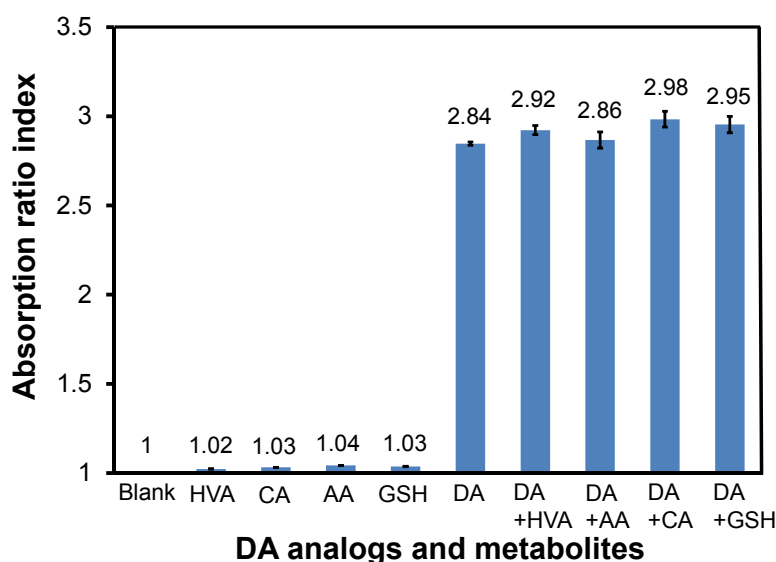
Figure 5.10 Measured absorption ratio index versus various samples including dopamine and some typical interferents of DA. The experiment used 1 mL (28 nM) AuNP colloids added to 0.5 mL (10 mM) of sample solutions. The ARI was measured after 3 min of vortex mixing at room temperature.

5.3 DA detection in microfluidic chip

Optical detection method is attractive to provide sensitive biosensing by using microfluidic system in recent years. These detection approaches mainly based on using optical fibers as transmission light source and signals, which the fibers also provide relative simple process to assemble on the microfluidic chip and easily connect to the commercial analytical instruments. However, absorbance measurement is the most straightforward and popular analyzing method for bioanalysis, which the absorption spectra are highly related to the sample concentration and provides specific identity information. Therefore, this study successfully developed a novel optical detection sensor by assembling the etched of optical fibers on microfluidic chip and shows great potential to achieve rapid on-line absorbance measurement. Furthermore, droplet-based microfluidic systems have well developed for using the chemical and biological applications that exhibit many advantages by enhance and accelerate such chemical reaction within the slugs. Most of the all, when using droplets as the microreactor that only requires sample volume in the range from picoliters to nanoliters and exhibits high-throughput fabrication ability. In this regards, this study utilizing a segmented microfluidic system as microreactor to achieve uniform sample mixing and applying to the bioanalysis. Due to the previous chapter described a novel colorimetric probe for DA detection, which has been proved by using off-chip system. This section illustrates the approach of using optical detection microdevice to achieve on-line absorbance measurement and applied for AuNPs detecting DA.

In order to solve the typical disadvantages by using optical detection in microfluidic systems, many study reported via integrated simple components for increasing detection sensitivity. However, based on the absorbance detection theory, that absorption intensity highly related to analytes concentration and optical path

length. The dimension of optical detection channel is the key point to affect sensing performance by using the optical detection in the microfluidic systems. Therefore, the study developed an optical detection microdevice for rapid absorbance measurement which by detecting analytes in a longer optical detection channel. Most of all, absorbance detection in the microdevice only requires an ultra-low sample consumption. Segmented microfluidic system provides many advantages to achieve rapid mixing and prevents sample from causing dispersion during the fluidic transportation. It is considered to provide many advantages for taking chemical and biomedical reaction inside the droplets. However, droplet formation in the multiphase microfluidic systems usually achieved by injecting the disperse phase and continuous phase from T-junctions microchannel and generated at the crossing section. This process creates large shear force and interfacial tension between the immiscible liquids that generating uniform droplets in the continuous flow.

The developed optical detection sensor is composed by initially formed sample (AuNPs) droplets and detecting for the absorption spectrum in the optical detection channel. The chaotic advection inside droplets system provides great ability to achieve rapid and uniform sample mixing. By using the microdevice is considered to provide faster chemical reaction in the long of mixing channels and successive measuring sample absorption spectrum. In addition, the above chapter presents novel technique for providing high performance DA detection. The detection method is simply based on using core etching of DMAP-AuNPs as the colorimetric detection probes. In this regards, the final of this works successfully developed a novel optical detection sensor to provide rapid and sensitive absorbance measurement. Moreover, microdevice also has the ability using for kinetic measurement of DA core etching reaction process. Therefore, the proposed microdevice exhibits a great platform for optical detection and benefit using to the biosensing applications.

The absorbance measurement in the microfluidic system was simply achieved by assembling two etched optical fibers into the microchannel. One fiber used for transmitting light source and the other used for measuring absorption intensity. Results show the optical fibers assembled in the microchannel have been fixed at the position between the optical detection channel and optical fiber insertion channel. Note the etched optical fibers must carefully insert in the center of channel while using for the absorbance measurement. In addition, sample solution was initially formed droplets at T-junction by using the multiphase microfluidic system. Later, sample droplets have sequence filled into optical detection channel for the measurement. The fabricated input and output channels have 2 times wider than the optical detection channel, which is benefit to be well controlled droplets flow into the detection channel. Therefore, the small dimension of optical detection channel provided ultra-low sample consumption to achieve sensitive absorbance measurement, which the detection channel have designed for a length of 10 mm.

Besides, the developed microdevice has been evaluated for light transmission capability by using the design optical detection channel, which observed light emitted performance by exciting from the fluorescence solution. **Figure 5.11** shows light source successfully coupled into the optical fiber and emitted from the right side channel. The incident light beam exhibits strong intensity and uniform passed through the microchannel (10 mm). Notes the etched of optical fiber still has smooth surface for light emission and the arc of microchannel also prevents light beam from occurring expansion. Results indicated the incident light was capable transmitted through the long optical detection channel. Although there have small decrease of light intensity to the detector, the absorbance measurement for sample analysis showed no influence by using the microdevice. Therefore, the developed optical detection sensor shows great potential for providing sensitive biosensing applications.
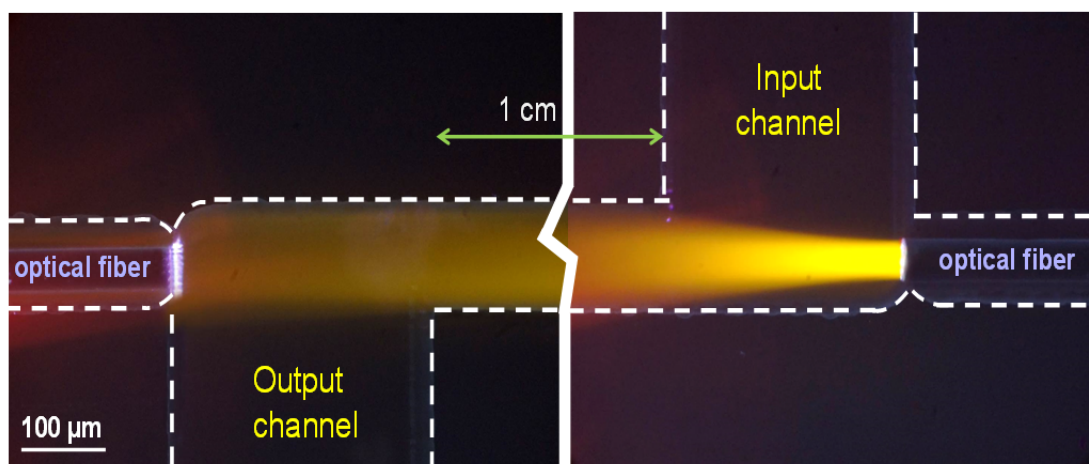
Figure 5.11 Photo shows the developed optical detection sensor by assembling etched optical fibers on microfluidic chip, which left side indicates the optical detection and right side was coupling light source for using absorbance measurement.

However, this study developed a novel optical detection approach for measuring sample absorbance by using the droplet-based microfluidic system. **Figure 5.12** shows the sequence images to clearly illustrate sample droplets deformation process, which rely on the hydrodynamic pressure to force droplets continuously extruding into the optical detection channel. Results indicated the initial generated sample droplets were easily forced into a narrow of optical detection channel, which the droplets were driven by the large of continuous flow pressure. Therefore, such small of microfluidic channel provides great advantages for decreasing sample consumption in the applications of biochemical analysis. Furthermore, this approach successfully designed a longer optical path length of optical detection channel which also exhibits narrow channel width. In this regards, when measuring for the sample absorbance by using the microdevice that only requires 50 nL of sample volume for bioanalysis. Therefore, the proposed optical detection channel provided novel and ultra-low sample consumption for better applying to the optical detection in microfluidic systems.
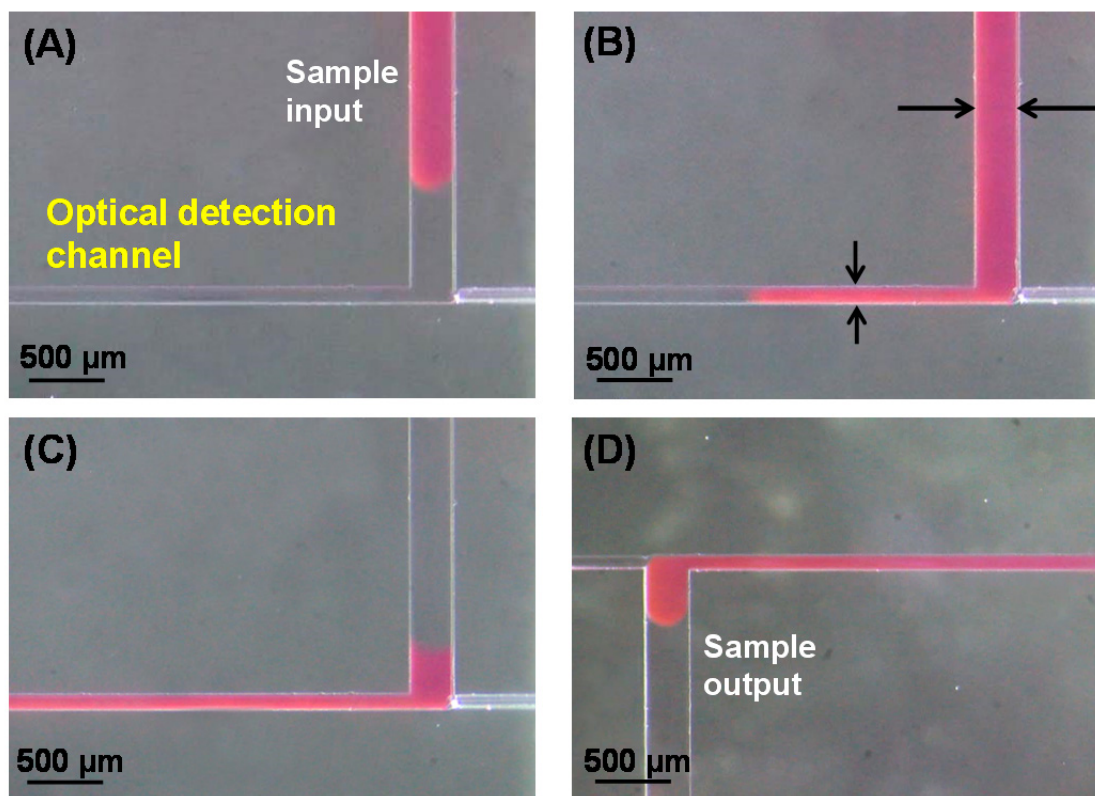
Figure 5.12 The sequence images show sample droplet filled into a narrow optical detection channel, which provides lower sample consumption for absorbance measurement by using the microdevice.

Comparing the detection performance of sample absorbance measurement by using the typical cuvette and microfluidic systems, the synthesized toluene-based AuNPs was using as sample solution for evaluate the detection capability of different approaches. **Figure 5.13** shows the comparison of measuring AuNPs absorption spectra via detecting AuNPs colloids by using the cuvette system and microdevice. Due to the typical absorbance measurement by using the cuvette system was analyzed from a UV-Vis spectrophotometer, that AuNP solution has to be measuring in a 3 mL of plastic cuvette. Although result shows clear spectrum of AuNPs specific absorption band at 520 nm, these approach mainly suffer from the disadvantages of using large sample volume which is not benefit for providing low cost biosensing.

However, when using the proposed microdevice for absorbance measurement that only requires for 50 nL of sample volume by detecting in the small of optical detection channel. Thus, microdevice shows great potential to provide simple and low cost detection method to achieve sensitive biosensing. Furthermore, this study developed a droplet-based microfluidic system to provide fast and uniform sample mixing to analyze for the chemical reaction. Using the developed optical detection sensor, that the synthesized aqueous-based AuNPs was initially formed into droplets in a two-phase microfluidic system by setting flow velocity in the range from 5-25 μL/min. When droplets sequence filled into the optical detection channel, sensor was capable providing rapid absorbance measurement. Results indicated taking the absorbance detection in the microdevice exhibits good compatibility with the conventional spectrophotometer, which indicates the developed optical detection method has the potential to create a novel and simple approach for the biochemical analysis. Most of all, low sample consumption and rapid analysis by using the microdevice provided great advantages for using the biosensing applications.
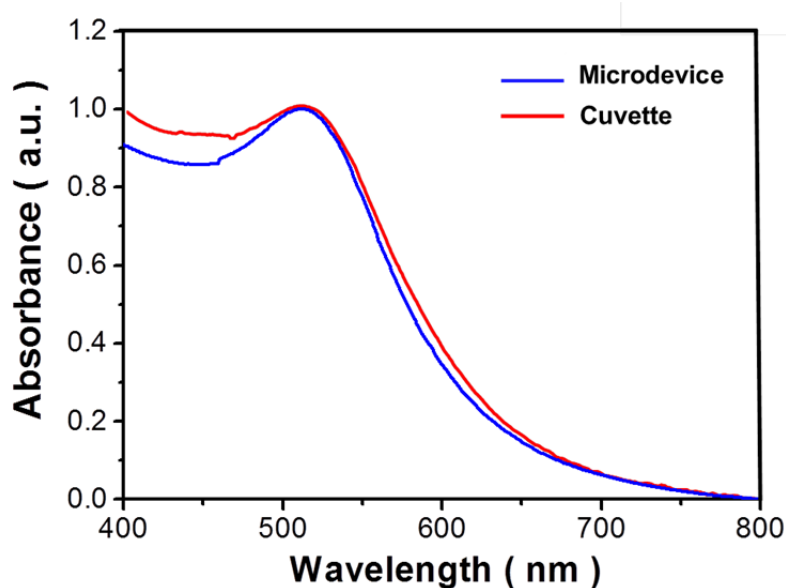
Figure 5.13 The normalized of absorption spectra from detecting AuNPs colloids by using the conventional cuvette system and comparing to the microdevice.

Due to the proposed optical detection method shows capability for providing rapid absorbance measurement in the microfluidic system. The stability of the optical detection sensor was also test by detecting for AuNPs droplet absorbance in the microdevice, which the operating flow rate was setting in the range of 5-25 μL/min. However, due to AuNPs exhibits the specific absorption band at 520 nm wavelength, **Figure 5.14 (A)** shows the detected absorbance variation by recording from AuNPs droplet cycle that have passing through the optical detection channel with the setting flow rate in 5 μL/min. Results indicates when the AuNPs droplet have been stably produced in the multi-phase microfluidic system and filled up into the optical detection channel, the sensor has rapidly and stably measuring for the absorbance variation via recorded with time series. Besides, each of the pulse signals represents the optical detection process for measuring AuNPs droplet absorbance in the detection channel. Note the absorbance intensity of sample was depending on the stable line in the pulse signals. The space between each measured signal indicates that was by detecting to toluene solution, which shows no absorption signal at the wavelengths 520 nm. Moreover, in the pulse signal of measured from AuNPs droplet that two sharp peaks representing of the droplet edges, which the light scattering caused the increasing of absorbance intensity. Therefore, the proposed optical detection sensor exhibits a rapid and stable absorbance measurement by using the microfluidic system.

In addition, **Figure 5.14 (B)** presents the measured AuNPs droplet absorbance by detecting from the microdevice with operating flow rate in the range of 5-25 μL/min. Results indicated that the proposed detection method was capable for providing rapid absorbance measurement by using a high flow rate microfluidic system. However, while the operating flow rate was above the 20 μL/min, the measured absorbance intensity only shows few increased for the detection of AuNPs droplet in the microdevice. Results indicated the proposed optical detection sensor was confirmed to

achieve a rapid and stable detection for absorbance measurement in the microfluidic system with operating in the high flow rate.
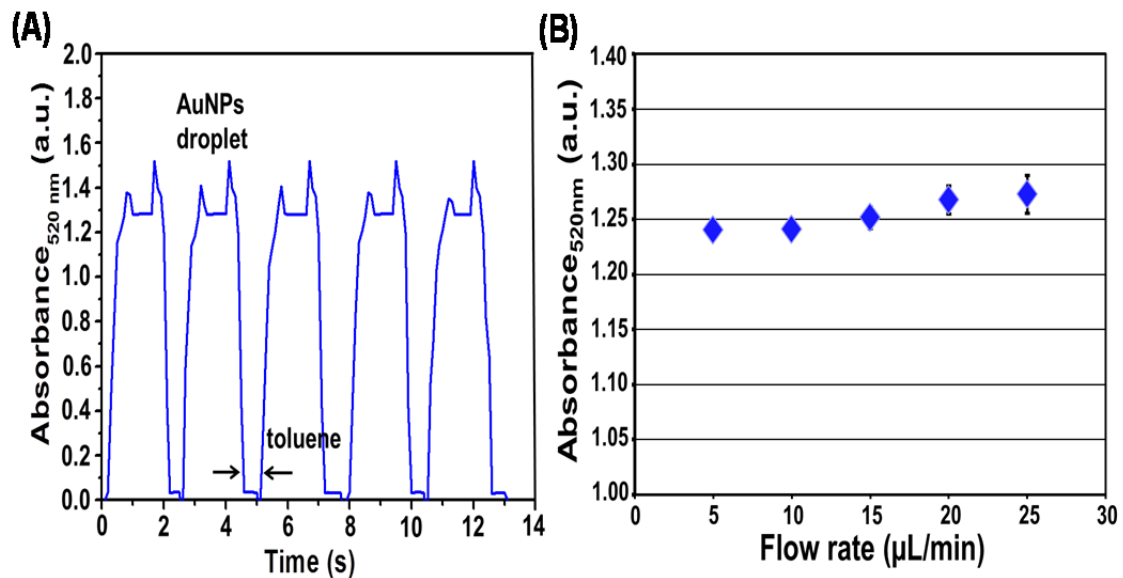
Figure 5.14 Calculated of absorbance A_{520} versus (A) cycling detection of AuNPs droplet with time series, and (B) detected of AuNPs by operating different flow rate.

The advantage of using microfluidic system for chemical analysis usually provides fast and uniform mixing process, which the microdevice also exhibit small sample consumption. Furthermore, when using the microdevice for detecting such biosamples within a sealed of microchannel. It is capable prevents the samples to suffer the unnecessary contamination, which usually caused by the pretreatment process. Thus, the development of microfluidic chip by using optical detection shows great potential to provide better platform for the biochemical analysis. Due to the proposed optical detection sensor was confirmed providing rapid absorbance measurement, which also exhibits good stability for the optical detection by using the microdevice. In this regards, the ability for providing rapid analysis by using the microdevice was evaluated from continuously monitoring droplet absorbance, which the sample droplets have added to different DA concentrations with DMAP-AuNPs

colloids. Note the different core etching conditions that caused by the addition of varied DA concentration, have rapidly measured by using the microdevice at setting the flow rate in 5 μL/min.

Figure 5.15 (A) shows the measured absorbance of wavelength 520 nm versus detecting AuNPs droplets that has been mixed with different DA concentration in the range of 20-100 nM. However, due to the proposed DA detection technique was relied on DA molecular causing DMAP-AuNPs of core etching process in the solution, which the particles was transformed into the smaller-sized one. Hence, analyzing this DA detection approach by using the microdevice, which the original AuNPs specific absorption spectra (A_{520}) exhibited a decreasing intensity by the addition increased DA concentrations. Results indicated the analytical performance by using the optical detection sensor shows great ability to achieve rapid and continuous absorbance measurement. Therefore, the microdevice provides on-site detection for the biochemical analysis by using the microfluidic system.

Furthermore, previous section reported such developed DA detection approach shown a sensitive detection by using the synthesized DMAP-AuNPs in the off-chip system. **Figure 5.15 (B)** presents the developed optical detection sensor also capable for providing sensitive biochemical analysis by using the microfluidic system. Most of all, the successive absorbance measurement by using the microdevice was capable for detecting different variation of DA concentration. Results indicated the measured absorbance (A_{520}) intensity showed obvious decreased which caused by the increase of DA concentrations. The linear equation could be fitted as A_{520} = -0.0034 (x) (DA, nM) + 1.278 (R^2 = 0.9963) with the detected DA concentration in the range of 20-100 nM, which shows the proposed optical detection sensor has good sensitivity for the sample absorbance detection by using the microfluidic system. Therefore, in comparing to the typically absorbance measurement by using the cuvette system, this

approach shows great improvement of providing sensitive chemical analysis. Besides, the microdevice even provides the successive optical detection which benefit to achieve rapid biosensing applications.
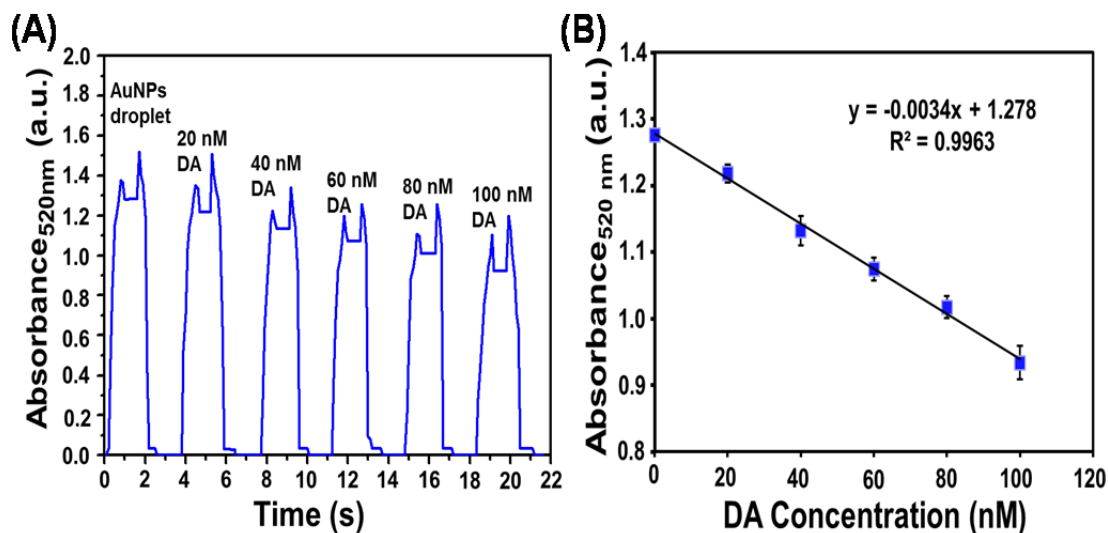
Figure 5.15 Calculated of absorbance A_{520} versus (A) detected the AuNPs added with different DA concentration (20-100 nM), and (B) presents the sensor exhibits a linear correlation coefficient of 0.9963 for different DA concentration measurement.

In addition, the fast kinetic measurement is essential for understanding biological and chemical reaction, such as the RNA with protein folding, protein-protein interaction and enzymatic mechanism. The typical kinetic detection methods was by initially mixing with two or more reactant solutions in the chamber, and then monitoring for the sample reaction response by stopped or quenched the flow at the detection position. However, using the conventional instrument for kinetic measurement usually consumed large volume of samples, which was not beneficial to achieve low cost of bioanalysis applications. In this regards, several researches reported that droplet-based microfluidic system was capable for providing kinetics measurement within milliseconds. These approaches exhibit good ability for rapid sample mixing and without causing dispersion in the microfluidic system. Therefore,

to monitor sample kinetic response by using droplet microfluidic systems shows great potential providing high sensitivity bioanalysis.

The previous results confirmed that proposed microdevice was capable for providing rapid and sensitive absorbance measurement by using droplet microfluidic system. The developed optical detection sensor even shows great advantage of costing low sample consumption for the high performance bioanalysis. Besides, in order to evaluate the capability of using droplet microfluidic system for providing rapid kinetic measurement. The reaction kinetic of DA molecular core etching DMAP-AuNPs was analyzed by monitoring the sample absorption responses within the droplets. In the proposed kinetic measurement approach, DMAP-AuNPs colloids was initially mixing of 10 mM DA solution and then continuously recording the measured absorption signals by using the optical detection sensor. However, due to the DA core etching AuNPs technique caused the particles size transformed into the smaller one, which leads to AuNPs specific absorption band blue shift to the wavelength 415 nm. Thus, the test of using microdevice for providing rapid kinetic measurement was proved by recording absorbance A_{415} in the droplet microfluidic system at the setting of 5 μL/min flow rate. In this regards, the proposed approach is considered to provide simple and sensitive optical detection for monitoring biochemical kinetic reactions.

Figure 5.16 (A) shows the rapid kinetic measurement of monitoring DA molecular core etching DMAP-AuNPs reactions by using the proposed microdevice. Note each of histograms describes the normalized of calculating from 30 droplets/min by using the segment flow system, which exhibits the measured absorption A_{415} intensity changes versus 20 minutes saturation time. Due to the proposed core etching approach have leads to the blue shift of AuNPs absorption spectrum. Results show the kinetic measurement of AuNPs absorption (A_{415}) intensity exhibit clear increasing by

the longer reaction time by adding into the DA solution. Therefore, microdevice exhibits great capability for providing rapid kinetic measurement by analyzing from the absorbance variation. However, utilizing the typical spectrometer for absorbance measurement is not capable to achieve sequence analysis. The developed approach shows many advantages to provide rapid and high sensitive bioanalysis by using the microfluidic system. Furthermore, results indicated the final reactions of DA molecules core etching process only required 8 minutes of saturation time. Therefore, the proposed optical detection approach successfully provided rapid absorbance measurement and also can be used for kinetic measurement by detecting with the droplet microfluidic system.

The segmented flow system exhibits many advantages to achieve fast sample mixture and uniform mass transferred which benefit providing high performance bioanalysis. **Figure 5.16 (B)** shows the normalized signals of kinetic measurement of DA core etching AuNPs reactions, which the comparison of measuring by using the typical cuvette and the microdevice. Due to the segmented microfluidic systems was known for producing chaotic flow inside the droplet. The proposed microdevice shows great capability for providing uniform sample mixing. However, the emulation for the capability of achieving fast yet uniform sample mixing by using the segmented microfluidic system. The microdevice was analyzed with AuNPs core etching reaction by detecting in different process of using the typical spectrophotometer and the developed optical detection sensor. Results indicated the microdevice provided rapid kinetic measurement, which shows the DA core etching approach exhibits a faster saturation response by the sample mixed within the segmented microfluidic system. In comparing to measuring chemical reaction process by using the same optical detection path length (10 mm) of cuvette system, microdevice exhibits the better capability for providing continuous observation. Therefore, this proposed microdevice

shows great potential to achieve on-situ yet high performance detection that benefit using for the biosensing applications.
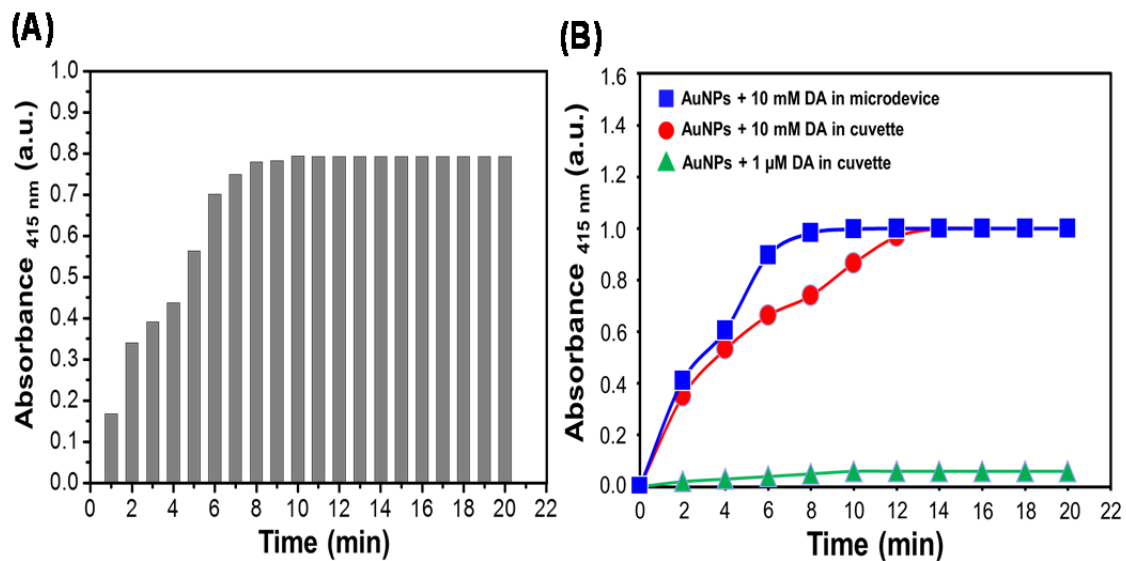
Figure 5.16 (A) Histograms shows the calculated of 600 droplets from recorded A_{415} intensity changes, which measured 20 minutes by using the microdevice. (B) The comparison of kinetic measurement for DA core etching reaction by using the microdevice and cuvette. Note the microdevice exhibits faster reaction response.

Chapter 6 Conclusions and Future works

6.1 Conclusions

This research successfully developed a novel liquid-liquid phase separator for efficiently separating the immiscible liquids, which created large separation ability by using capillary force and liquid surface tension. Results show the proposed microdevice exhibits 92% separation efficiency for separating low surface tension of water/toluene. Moreover, the larger size of generated segmented droplet is benefit to achieve higher efficiency of liquid phase separation. The proposed microdevice exhibited stable chemical reaction for AuNPs synthesized in the toluene solvent, which generated better monodispersity and smaller particles size in comparing to the conventional vessel system. Note the segmented flow system provided a simple method for sample extraction by using microfluidic chip, which also benefits to achieve rapid and uniform chemical reaction of biosensing and nanoparticle synthesis applications.

Besides, the developed novel core etching technique exhibited high performance analysis for detecting DA neurotransmitter which by using synthesized aqueous-based DMAP-AuNPs. The binding of DMAP molecules on AuNPs surface was initially confirmed by using cyclic voltammetry detection. The addition of DA molecules induced core etching effect of DMAP-AuNPs that causes AuNPs size reduced and results in blue shift of the absorption spectra. Results indicated the DA detection method achieved a low detection limit of 5 nM, and exhibits good selectivity to the DA molecules while presents in some common interferents. The developed assay also presented wide DA concentration detecting range of $10 \sim 10^5$ nM, and has good linear correlation coefficients of 0.9969 in the range of $10 \sim 10^2$ nM. These results demonstrated DMAP-AuNPs appropriate as a simple and sensitive detector of DA

biosample in aqueous solution, and the proposed core etching technique provided novel and high sensitivity detection for the future rapid biosensing applications.

Furthermore, the developed optical-fiber-based detection sensor by using the microfluidic chip successfully provided rapid and sensitive absorbance measurement. The performance of the developed optical detection sensor was evaluated by the absorbance measurement of analyzing AuNPs detecting DA by using the droplet-based microfluidic system. The etched of multimode optical fibers have carefully assembled on the glass microchip for measuring AuNPs absorption spectrum. Utilizing MEMS fabrication technique was easily to create the length of 10 mm detection channel on the substrate, which enhanced the sensitivity of optical detection by using the microdevice. Note the absorbance detection of using the proposed microdevice required vary low sample consumption in comparing to analysis in the conventional cuvette. Results indicated the optical detection sensor capable to measure with AuNPs absorbance by using the segmented flow system at the operating flow rate in the range from 5-25 µL/min. The kinetic measurement of DA molecules core etching AuNPs reaction also exhibits faster response by using the droplet-based microfluidic system.

Therefore, this research successfully developed novel and versatile microfluidic chip to achieve liquid-liquid phase separation, uniform size AuNPs synthesis, rapid and sensitive biosensing. The developed of core etching technique provided new approach of using AuNPs as the colorimetric probes. The optical detection microdevice exhibits lower sample consumption which benefit for using in the wide range of bioanalysis applications. These approaches showed great potential in the development of nanotechnology and microfluidic system.

6.2 Future works

In this study, we mainly utilized the segmented microfluidic system to provide fast mass transfer and uniform chemical reaction, which benefit using for the nanoparticles synthesis and biosensing applications. The developed microdevice provided a simple approach to achieve efficient liquid-liquid phase separation for using in the wide range sample extraction applications. The optical detection sensor also shows many advantages of providing rapid and sensitive biosensing for the biomedical analysis.

However, the future trends suggest that the development of multi-detection sensor is capable for enhancing biochemical detection and shorten the time consuming which shows great potential to provide fast clinical diagnostic. For enhancing the developed optical detection sensor by using the microfluidic chip, the future works is considered to design with multi-detection channel by assembling several optical fibers onto the chip. In this regards, different biosamples can be rapidly mixed by using the segmented flow, and then detecting for multi samples at the same time. Besides, by using the multiphase microfluidic system was capable for synthesizing uniform AuNPs in the toluene. However, it is difficult for accurately controlling the synthesized AuNPs shape and size by using the microfluidic system. Therefore, to achieve better AuNPs synthesis with controllable size distribution by using the segmented flow system, it is considered have well studying for the synthesis process with multiphase droplet parameter such as reducing agent concentration inside the droplet, sample mixing rate and contacting time, the relation of liquid droplet size between the AuNPs size distribution. Utilizing the novel technique of segmented flow system is benefit for developing better platform of using to the new field for nanotechnology and bioanalysis.

Reference

[1]   V. Srinivasan, V. K. Pamula, and R. B. Fair, "Droplet-based microfluidic lab-on-a-chip for glucose detection," *Analytica Chimica Acta,* vol. 507, pp. 145-150, 2004.

[2]   A. Manz, N. Graber, and H. á. Widmer, "Miniaturized total chemical analysis systems: a novel concept for chemical sensing," *Sensors and Actuators B: Chemical,* vol. 1, pp. 244-248, 1990.

[3]   H. Song, M. R. Bringer, J. D. Tice, C. J. Gerdts, and R. F. Ismagilov, "Experimental test of scaling of mixing by chaotic advection in droplets moving through microfluidic channels," *Applied Physics Letters,* vol. 83, pp. 4664-4666, 2003.

[4]   A. D. Stroock, S. K. Dertinger, A. Ajdari, I. Mezić, H. A. Stone, and G. M. Whitesides, "Chaotic mixer for microchannels," *Science,* vol. 295, pp. 647-651, 2002.

[5]   P. Mary, V. Studer, and P. Tabeling, "Microfluidic droplet-based liquid-liquid extraction," *Analytical Chemistry,* vol. 80, pp. 2680-2687, 2008.

[6]   J. Tang, X. B. Zhang, W. F. Cai, and F. M. Wang, "Liquid-liquid extraction based on droplet flow in a vertical microchannel," *Experimental Thermal and Fluid Science,* vol. 49, pp. 185-192, 2013.

[7]   D. Y. Liu, G. T. Liang, X. X. Lei, B. Chen, W. Wang, and X. M. Zhou, "Highly efficient capillary polymerase chain reaction using an oscillation droplet microreactor," *Analytica Chimica Acta,* vol. 718, pp. 58-63, 2012.

[8]   H. Song, J. D. Tice, and R. F. Ismagilov, "A microfluidic system for controlling reaction networks in time," *Angewandte Chemie,* vol. 115, pp. 792-796, 2003.

[9]   S. Y. Teh, R. Lin, L. H. Hung, and A. P. Lee, "Droplet microfluidics," *Lab on a Chip,* vol. 8, pp. 198-220, 2008.

[10]   I. Kobayashi, K. Uemura, and M. Nakajima, "Formulation of monodisperse emulsions using submicron-channel arrays," *Colloids and Surfaces A: Physicochemical and Engineering Aspects,* vol. 296, pp. 285-289, 2007.

[11]   M. T. Guo, A. Rotem, J. A. Heyman, and D. A. Weitz, "Droplet microfluidics for high-throughput biological assays," *Lab on a Chip,* vol. 12, pp. 2146-2155, 2012.

[12]   L. Mazutis, J. C. Baret, P. Treacy, Y. Skhiri, A. F. Araghi, M. Ryckelynck, V. Taly, and A. D. Griffiths, "Multi-step microfluidic droplet processing: kinetic analysis of an in vitro translated enzyme," *Lab on a Chip,* vol. 9, pp. 2902-2908, 2009.

[13] Z. Han, W. Li, Y. Huang, and B. Zheng, "Measuring rapid enzymatic kinetics by electrochemical method in droplet-based microfluidic devices with pneumatic valves," *Analytical Chemistry,* vol. 81, pp. 5840-5845, 2009.

[14] A. Huebner, D. Bratton, G. Whyte, M. Yang, C. Abell, and F. Hollfelder, "Static microdroplet arrays: a microfluidic device for droplet trapping, incubation and release for enzymatic and cell-based assays," *Lab on a Chip,* vol. 9, pp. 692-698, 2009.

[15] Y. Schaerli and F. Hollfelder, "The potential of microfluidic water-in-oil droplets in experimental biology," *Molecular Biosystems,* vol. 5, pp. 1392-1404, 2009.

[16] D. C. Yin, H. M. Lu, L. Q. Geng, Z. H. Shi, H. M. Luo, H. S. Li, Y. J. Ye, W. H. Guo, P. Shang, and N. I. Wakayama, "Growing and dissolving protein crystals in a levitated and containerless droplet," *Journal of Crystal Growth,* vol. 310, pp. 1206-1212, 2008.

[17] B. Zheng, L. S. Roach, and R. F. Ismagilov, "Screening of protein crystallization conditions on a microfluidic chip using nanoliter-size droplets," *Journal of the American Chemical Society,* vol. 125, pp. 11170-11171, 2003.

[18] I. Shestopalov, J. D. Tice, and R. F. Ismagilov, "Multi-step synthesis of nanoparticles performed on millisecond time scale in a microfluidic droplet-based system," *Lab on a Chip,* vol. 4, pp. 316-321, 2004.

[19] D. Koziej, C. Floryan, R. A. Sperling, A. J. Ehrlicher, D. Issadore, R. Westervelt, and D. A. Weitz, "Microwave dielectric heating of non-aqueous droplets in a microfluidic device for nanoparticle synthesis," *Nanoscale,* vol. 5, pp. 5468-5475, 2013.

[20] A. Utada, E. Lorenceau, D. Link, P. Kaplan, H. Stone, and D. Weitz, "Monodisperse double emulsions generated from a microcapillary device," *Science,* vol. 308, pp. 537-541, 2005.

[21] J. D. Tice, A. D. Lyon, and R. F. Ismagilov, "Effects of viscosity on droplet formation and mixing in microfluidic channels," *Analytica Chimica Acta,* vol. 507, pp. 73-77, 2004.

[22] J. Xu, G. Luo, S. Li, and G. Chen, "Shear force induced monodisperse droplet formation in a microfluidic device by controlling wetting properties," *Lab on a Chip,* vol. 6, pp. 131-136, 2006.

[23] T. Thorsen, R. W. Roberts, F. H. Arnold, and S. R. Quake, "Dynamic pattern formation in a vesicle-generating microfluidic device," *Physical Review Letters,* vol. 86, p. 4163, 2001.

[24] S. L. Anna, N. Bontoux, and H. A. Stone, "Formation of dispersions using "flow focusing" in microchannels," *Applied Physics Letters,* vol. 82, pp.

364-366, 2003.

[25]   R. Dreyfus, P. Tabeling, and H. Willaime, "Ordered and disordered patterns in two-phase flows in microchannels," *Physical Review Letters,* vol. 90, pp. 144505-144505, 2003.

[26]   C. N. Baroud, F. Gallaire, and R. Dangla, "Dynamics of microfluidic droplets," *Lab on a Chip,* vol. 10, pp. 2032-2045, 2010.

[27]   A. Guenther, M. Kreutzer, and K. Jensen, "Multiphase Transport Phenomena in Microfluidic Systems," *Langmuir,* vol. 21, pp. 1547-1555, 2005.

[28]   O. K. Castell, C. J. Allender, and D. A. Barrow, "Continuous molecular enrichment in microfluidic systems," *Lab on a Chip,* vol. 8, pp. 1031-1033, 2008.

[29]   C. J. Gerdts, V. Tereshko, M. K. Yadav, I. Dementieva, F. Collart, A. Joachimiak, R. C. Stevens, P. Kuhn, A. Kossiakoff, and R. F. Ismagilov, "Time - Controlled Microfluidic Seeding in nL - Volume Droplets To Separate Nucleation and Growth Stages of Protein Crystallization," *Angewandte Chemie International Edition,* vol. 45, pp. 8156-8160, 2006.

[30]   M. J. Fuerstman, P. Garstecki, and G. M. Whitesides, "Coding/decoding and reversibility of droplet trains in microfluidic networks," *Science,* vol. 315, pp. 828-832, 2007.

[31]   H. Song, D. L. Chen, and R. F. Ismagilov, "Reactions in droplets in microfluidic channels," *Angewandte Chemie International Edition,* vol. 45, pp. 7336-7356, 2006.

[32]   M. N. Kashid, I. Gerlach, S. Goetz, J. Franzke, J. Acker, F. Platte, D. Agar, and S. Turek, "Internal circulation within the liquid slugs of a liquid-liquid slug-flow capillary microreactor," *Industrial & Engineering Chemistry Research,* vol. 44, pp. 5003-5010, 2005.

[33]   M. Mendorf and D. W. Agar, "Scale-up of Capillary Extraction Equipment," *Chemie Ingenieur Technik,* vol. 83, pp. 1120-1124, 2011.

[34]   M. N. Kashid, D. W. Agar, and S. Turek, "CFD modelling of mass transfer with and without chemical reaction in the liquid–liquid slug flow microreactor," *Chemical Engineering Science,* vol. 62, pp. 5102-5109, 2007.

[35]   A. Salim, M. Fourar, J. Pironon, and J. Sausse, "Oil–water two-phase flow in microchannels: Flow patterns and pressure drop measurements," *The Canadian Journal of Chemical Engineering,* vol. 86, pp. 978-988, 2008.

[36]   P. Kuban, J. Berg, and P. K. Dasgupta, "Vertically stratified flows in microchannels. Computational simulations and applications to solvent extraction and ion exchange," *Analytical Chemistry,* vol. 75, pp. 3549-3556, 2003.

[37] N. Assmann and P. R. von Rohr, "Extraction in microreactors: intensification by adding an inert gas phase," *Chemical Engineering and Processing: Process Intensification,* vol. 50, pp. 822-827, 2011.

[38] P. Uhlmann, F. Varnik, P. Truman, G. Zikos, J. Moulin, P. Müller-Buschbaum, and M. Stamm, "Microfluidic emulsion separation—simultaneous separation and sensing by multilayer nanofilm structures," *Journal of Physics: Condensed Matter,* vol. 23, p. 184123, 2011.

[39] S. Aljbour, H. Yamada, and T. Tagawa, "Sequential reaction-separation in a microchannel reactor for liquid–liquid phase transfer catalysis," *Topics in Catalysis,* vol. 53, pp. 694-699, 2010.

[40] T. Maruyama, H. Matsushita, J. I. Uchida, F. Kubota, N. Kamiya, and M. Goto, "Liquid membrane operations in a microfluidic device for selective separation of metal ions," *Analytical Chemistry,* vol. 76, pp. 4495-4500, 2004.

[41] J. G. Kralj, H. R. Sahoo, and K. F. Jensen, "Integrated continuous microfluidic liquid–liquid extraction," *Lab on a Chip,* vol. 7, pp. 256-263, 2007.

[42] D. M. Fries, T. Voitl, and P. R. von Rohr, "Liquid extraction of vanillin in rectangular microreactors," *Chemical Engineering & Technology,* vol. 31, pp. 1182-1187, 2008.

[43] A. Günther, M. Jhunjhunwala, M. Thalmann, M. A. Schmidt, and K. F. Jensen, "Micromixing of miscible liquids in segmented gas-liquid flow," *Langmuir,* vol. 21, pp. 1547-1555, 2005.

[44] M. T. Kreutzer, A. Günther, and K. F. Jensen, "Sample dispersion for segmented flow in microchannels with rectangular cross section," *Analytical Chemistry,* vol. 80, pp. 1558-1567, 2008.

[45] W. Gaakeer, M. de Croon, J. van der Schaaf, and J. Schouten, "Liquid–liquid slug flow separation in a slit shaped micro device," *Chemical Engineering Journal,* vol. 207, pp. 440-444, 2012.

[46] J. H. Tsai and L. Lin, "Active microfluidic mixer and gas bubble filter driven by thermal bubble micropump," *Sensors and Actuators A: Physical,* vol. 97, pp. 665-671, 2002.

[47] O. K. Castell, C. J. Allender, and D. A. Barrow, "Liquid–liquid phase separation: characterisation of a novel device capable of separating particle carrying multiphase flows," *Lab on a Chip,* vol. 9, pp. 388-396, 2009.

[48] D. Angelescu, B. Mercier, D. Siess, and R. Schroeder, "Microfluidic capillary separation and real-time spectroscopic analysis of specific components from multiphase mixtures," *Analytical Chemistry,* vol. 82, pp. 2412-2420, 2010.

[49] K. L. Kelly, E. Coronado, L. L. Zhao, and G. C. Schatz, "The optical properties of metal nanoparticles: the influence of size, shape, and dielectric

environment," *The Journal of Physical Chemistry B,* vol. 107, pp. 668-677, 2003.

[50] J. F. Li, Y. F. Huang, Y. Ding, Z. L. Yang, S. B. Li, X. S. Zhou, F. R. Fan, W. Zhang, Z. Y. Zhou, and B. Ren, "Shell-isolated nanoparticle-enhanced Raman spectroscopy," *Nature,* vol. 464, pp. 392-395, 2010.

[51] X. Qian, X. H. Peng, D. O. Ansari, Q. Yin Goen, G. Z. Chen, D. M. Shin, L. Yang, A. N. Young, M. D. Wang, and S. Nie, "In vivo tumor targeting and spectroscopic detection with surface-enhanced Raman nanoparticle tags," *Nature Biotechnology,* vol. 26, pp. 83-90, 2008.

[52] J. Wang, "Nanoparticle‐Based Electrochemical Bioassays of Proteins," *Electroanalysis,* vol. 19, pp. 769-776, 2007.

[53] N. J. Wittenberg and C. L. Haynes, "Using nanoparticles to push the limits of detection," *Wiley Interdisciplinary Reviews: Nanomedicine and Nanobiotechnology,* vol. 1, pp. 237-254, 2009.

[54] E. Katz and I. Willner, "Integrated nanoparticle–biomolecule hybrid systems: synthesis, properties, and applications," *Angewandte Chemie International Edition,* vol. 43, pp. 6042-6108, 2004.

[55] N. L. Rosi and C. A. Mirkin, "Nanostructures in biodiagnostics," *Chemical Reviews,* vol. 105, pp. 1547-1562, 2005.

[56] M. Faraday, "The Bakerian lecture: experimental relations of gold (and other metals) to light," *Philosophical Transactions of the Royal Society of London,* pp. 145-181, 1857.

[57] N. L. Rosi, D. A. Giljohann, C. S. Thaxton, A. K. Lytton-Jean, M. S. Han, and C. A. Mirkin, "Oligonucleotide-modified gold nanoparticles for intracellular gene regulation," *Science,* vol. 312, pp. 1027-1030, 2006.

[58] M. D. Malinsky, K. L. Kelly, G. C. Schatz, and R. P. Van Duyne, "Chain length dependence and sensing capabilities of the localized surface plasmon resonance of silver nanoparticles chemically modified with alkanethiol self-assembled monolayers," *Journal of the American Chemical Society,* vol. 123, pp. 1471-1482, 2001.

[59] B. Tang, L. Cao, K. Xu, L. Zhuo, J. Ge, Q. Li, and L. Yu, "A new nanobiosensor for glucose with high sensitivity and selectivity in serum based on fluorescence resonance energy transfer (FRET) between CdTe quantum dots and Au nanoparticles," *Chemistry-a European Journal,* vol. 14, pp. 3637-3644, 2008.

[60] N. T. K. Thanh and Z. Rosenzweig, "Development of an aggregation-based immunoassay for anti-protein A using gold nanoparticles," *Analytical Chemistry,* vol. 74, pp. 1624-1628, 2002.

[61] S. Zeng, K. T. Yong, I. Roy, X. Q. Dinh, X. Yu, and F. Luan, "A review on functionalized gold nanoparticles for biosensing applications," *Plasmonics,* vol. 6, pp. 491-506, 2011.

[62] Y. Li, H. J. Schluesener, and S. Xu, "Gold nanoparticle-based biosensors," *Gold Bulletin,* vol. 43, pp. 29-41, 2010.

[63] P. Ghosh, G. Han, M. De, C. K. Kim, and V. M. Rotello, "Gold nanoparticles in delivery applications," *Advanced Drug Delivery Reviews,* vol. 60, pp. 1307-1315, 2008.

[64] T. Mitsudome, A. Noujima, T. Mizugaki, K. Jitsukawa, and K. Kaneda, "Efficient aerobic oxidation of alcohols using a hydrotalcite-supported gold nanoparticle catalyst," *Advanced Synthesis & Catalysis,* vol. 351, pp. 1890-1896, 2009.

[65] D. Pissuwan, S. M. Valenzuela, and M. B. Cortie, "Therapeutic possibilities of plasmonically heated gold nanoparticles," *Trends in Biotechnology,* vol. 24, pp. 62-67, 2006.

[66] X. Cao, Y. Ye, and S. Liu, "Gold nanoparticle-based signal amplification for biosensing," *Analytical Biochemistry,* vol. 417, pp. 1-16, 2011.

[67] P. CooperáStevenson, "A study of the nucleation and growth processes in the synthesis of colloidal gold," *Discussions of the Faraday Society,* vol. 11, pp. 55-75, 1951.

[68] S. P. Chandran, M. Chaudhary, R. Pasricha, A. Ahmad, and M. Sastry, "Synthesis of gold nanotriangles and silver nanoparticles using Aloevera plant extract," *Biotechnology Progress,* vol. 22, pp. 577-583, 2006.

[69] J. Kimling, M. Maier, B. Okenve, V. Kotaidis, H. Ballot, and A. Plech, "Turkevich method for gold nanoparticle synthesis revisited," *The Journal of Physical Chemistry B,* vol. 110, pp. 15700-15707, 2006.

[70] J. Polte, R. Erler, A. F. Thunemann, S. Sokolov, T. T. Ahner, K. Rademann, F. Emmerling, and R. Kraehnert, "Nucleation and growth of gold nanoparticles studied via in situ small angle X-ray scattering at millisecond time resolution," *ACS Nano,* vol. 4, pp. 1076-1082, 2010.

[71] C. De Vasconcelos, M. Pereira, and J. Fonseca, "Polyelectrolytes in solution and the stabilization of colloids," *Journal of Dispersion Science and Technology,* vol. 26, pp. 59-70, 2005.

[72] J. Liu and E. Luijten, "Stabilization of colloidal suspensions by means of highly charged nanoparticles," *Physical Review Letters,* vol. 93, p. 247802, 2004.

[73] W. R. Glomm, "Functionalized gold nanoparticles for applications in bionanotechnology," *Journal of Dispersion Science and Technology,* vol. 26,

pp. 389-414, 2005.

[74]   M. K. Corbierre, N. S. Cameron, and R. B. Lennox, "Polymer-stabilized gold nanoparticles with high grafting densities," *Langmuir,* vol. 20, pp. 2867-2873, 2004.

[75]   K.-S. Kim, D. Demberelnyamba, and H. Lee, "Size-selective synthesis of gold and platinum nanoparticles using novel thiol-functionalized ionic liquids," *Langmuir,* vol. 20, pp. 556-560, 2004.

[76]   E. E. Foos, A. W. Snow, M. E. Twigg, and M. G. Ancona, "Thiol-terminated di-, tri-, and tetraethylene oxide functionalized gold nanoparticles: a water-soluble, charge-neutral cluster," *Chemistry of Materials,* vol. 14, pp. 2401-2408, 2002.

[77]   A. G. Kanaras, F. S. Kamounah, K. Schaumburg, C. J. Kiely, and M. Brust, "Thioalkylated tetraethylene glycol: a new ligand for water soluble monolayer protected gold clusters," *Chemical Communications,* pp. 2294-2295, 2002.

[78]   S. Chen and K. Kimura, "Synthesis and characterization of carboxylate-modified gold nanoparticle powders dispersible in water," *Langmuir,* vol. 15, pp. 1075-1082, 1999.

[79]   H. Yao, O. Momozawa, T. Hamatani, and K. Kimura, "Stepwise size-selective extraction of carboxylate-modified gold nanoparticles from an aqueous suspension into toluene with tetraoctylammonium cations," *Chemistry of Materials,* vol. 13, pp. 4692-4697, 2001.

[80]   H. Tsunoyama and T. Tsukuda, "Magic numbers of gold clusters stabilized by PVP," *Journal of the American Chemical Society,* vol. 131, pp. 18216-18217, 2009.

[81]   P. Alexandridis, "Gold nanoparticle synthesis, morphology control, and stabilization facilitated by functional polymers," *Chemical Engineering & Technology,* vol. 34, pp. 15-28, 2011.

[82]   D. A. Giljohann, D. S. Seferos, P. C. Patel, J. E. Millstone, N. L. Rosi, and C. A. Mirkin, "Oligonucleotide loading determines cellular uptake of DNA-modified gold nanoparticles," *Nano Letters,* vol. 7, pp. 3818-3821, 2007.

[83]   A. K. Lytton Jean and C. A. Mirkin, "A thermodynamic investigation into the binding properties of DNA functionalized gold nanoparticle probes and molecular fluorophore probes," *Journal of the American Chemical Society,* vol. 127, pp. 12754-12755, 2005.

[84]   N. Zheng, J. Fan, and G. D. Stucky, "One-step one-phase synthesis of monodisperse noble-metallic nanoparticles and their colloidal crystals," *Journal of the American Chemical Society,* vol. 128, pp. 6550-6551, 2006.

[85] E. Oh, K. Susumu, R. Goswami, and H. Mattoussi, "One-phase synthesis of water-soluble gold nanoparticles with control over size and surface functionalities," *Langmuir,* vol. 26, pp. 7604-7613, 2010.

[86] H. Xu, J. Xu, X. Jiang, Z. Zhu, J. Rao, J. Yin, T. Wu, H. Liu, and S. Liu, "Thermosensitive unimolecular micelles surface-decorated with gold nanoparticles of tunable spatial distribution," *Chemistry of Materials,* vol. 19, pp. 2489-2494, 2007.

[87] Z. Wang, B. Tan, I. Hussain, N. Schaeffer, M. F. Wyatt, M. Brust, and A. I. Cooper, "Design of polymeric stabilizers for size-controlled synthesis of monodisperse gold nanoparticles in water," *Langmuir,* vol. 23, pp. 885-895, 2007.

[88] B. Prasad, S. I. Stoeva, C. M. Sorensen, and K. J. Klabunde, "Digestive-ripening agents for gold nanoparticles: alternatives to thiols," *Chemistry of Materials,* vol. 15, pp. 935-942, 2003.

[89] T. K. Sau, A. Pal, N. Jana, Z. Wang, and T. Pal, "Size controlled synthesis of gold nanoparticles using photochemically prepared seed particles," *Journal of Nanoparticle Research,* vol. 3, pp. 257-261, 2001.

[90] L. Lu, H. Wang, Y. Zhou, S. Xi, H. Zhang, J. Hu, and B. Zhao, "Seed-mediated growth of large, monodisperse core–shell gold–silver nanoparticles with Ag-like optical properties," *Chemical Communications,* pp. 144-145, 2002.

[91] M. Grzelczak, J. Pérez-Juste, P. Mulvaney, and L. M. Liz-Marzán, "Shape control in gold nanoparticle synthesis," *Chemical Society Reviews,* vol. 37, pp. 1783-1791, 2008.

[92] W. Zhao, M. A. Brook, and Y. Li, "Design of gold nanoparticle-based colorimetric biosensing assays," *ChemBioChem,* vol. 9, pp. 2363-2371, 2008.

[93] M. Brust, M. Walker, D. Bethell, D. J. Schiffrin, and R. Whyman, "Synthesis of thiol-derivatised gold nanoparticles in a two-phase liquid–liquid system," *Chemical Communications,* pp. 801-802, 1994.

[94] A. Frenkel, S. Nemzer, I. Pister, L. Soussan, T. Harris, Y. Sun, and M. Rafailovich, "Size-controlled synthesis and characterization of thiol-stabilized gold nanoparticles," *The Journal of Chemical Physics,* vol. 123, p. 184701, 2005.

[95] L. Sun, R. M. Crooks, and V. Chechik, "Preparation of polycyclodextrin hollow spheres by templating gold nanoparticles," *Chemical Communications,* pp. 359-360, 2001.

[96] D. V. Leff, P. C. Ohara, J. R. Heath, and W. M. Gelbart, "Thermodynamic control of gold nanocrystal size: experiment and theory," *The Journal of*

Physical Chemistry, vol. 99, pp. 7036-7041, 1995.

[97] A. Kumar, S. Mandal, S. P. Mathew, P. Selvakannan, A. Mandale, R. V. Chaudhari, and M. Sastry, "Benzene-and anthracene-mediated assembly of gold nanoparticles at the liquid-liquid interface," *Langmuir,* vol. 18, pp. 6478-6483, 2002.

[98] A. N. Shipway and I. Willner, "Nanoparticles as structural and functional units in surface-confined architectures," *Chemical Communications,* pp. 2035-2045, 2001.

[99] M. Sastry, "Phase transfer protocols in nanoparticle synthesis," *Current Science,* vol. 85, pp. 1735-1745, 2003.

[100] S. Underwood and P. Mulvaney, "Effect of the solution refractive index on the color of gold colloids," *Langmuir,* vol. 10, pp. 3427-3430, 1994.

[101] J. Yang, J. Y. Lee, and H.-P. Too, "A phase transfer identification of core–shell structures in Au–Ru nanoparticles," *Analytica Chimica Acta,* vol. 537, pp. 279-284, 2005.

[102] D. I. Gittins and F. Caruso, "Spontaneous phase transfer of nanoparticulate metals from organic to aqueous media," *Angewandte Chemie International Edition,* vol. 40, pp. 3001-3004, 2001.

[103] X. Feng, H. Ma, S. Huang, W. Pan, X. Zhang, F. Tian, C. Gao, Y. Cheng, and J. Luo, "Aqueous-organic phase-transfer of highly stable gold, silver, and platinum nanoparticles and new route for fabrication of gold nanofilms at the oil/water interface and on solid supports," *The Journal of Physical Chemistry B,* vol. 110, pp. 12311-12317, 2006.

[104] V. J. Gandubert and R. B. Lennox, "Assessment of 4-(dimethylamino) pyridine as a capping agent for gold nanoparticles," *Langmuir,* vol. 21, pp. 6532-6539, 2005.

[105] S. K. Ghosh, "Spectroscopic evaluation of 4-(dimethylamino) pyridine versus citrate as stabilizing ligand for gold nanoparticles," *Colloids and Surfaces A: Physicochemical and Engineering Aspects,* vol. 371, pp. 98-103, 2010.

[106] A. J. Demello, "Control and detection of chemical reactions in microfluidic systems," *Nature,* vol. 442, pp. 394-402, 2006.

[107] C. H. Chang, B. K. Paul, V. T. Remcho, S. Atre, and J. E. Hutchison, "Synthesis and post-processing of nanomaterials using microreaction technology," *Journal of Nanoparticle Research,* vol. 10, pp. 965-980, 2008.

[108] F. Jamal, G. Jean Sébastien, P. Maël, P. Edmond, and R. Christian, "Gold nanoparticle synthesis in microfluidic systems and immobilisation in microreactors designed for the catalysis of fine organic reactions," *Microsystem Technologies,* vol. 18, pp. 151-158, 2012.

[109] S. Gómez-de Pedro, M. Puyol, and J. Alonso-Chamarro, "Continuous flow synthesis of nanoparticles using ceramic microfluidic devices," *Nanotechnology,* vol. 21, p. 415603, 2010.

[110] J. Yue, R. Boichot, L. Luo, Y. Gonthier, G. Chen, and Q. Yuan, "Flow distribution and mass transfer in a parallel microchannel contactor integrated with constructal distributors," *AlChE Journal,* vol. 56, pp. 298-317, 2010.

[111] J. Köhler and T. Kirner, "Nanoliter segment formation in micro fluid devices for chemical and biological micro serial flow processes in dependence on flow rate and viscosity," *Sensors and Actuators A: Physical,* vol. 119, pp. 19-27, 2005.

[112] S. L. Poe, M. A. Cummings, M. P. Haaf, and D. T. McQuade, "Solving the clogging problem: precipitate-forming reactions in flow," *Angewandte Chemie International Edition,* vol. 45, pp. 1544-1548, 2006.

[113] V. Sebastian Cabeza, S. Kuhn, A. A. Kulkarni, and K. F. Jensen, "Size-controlled flow synthesis of gold nanoparticles using a segmented flow microfluidic platform," *Langmuir,* vol. 28, pp. 7007-7013, 2012.

[114] S. K. Ghosh and T. Pal, "Interparticle coupling effect on the surface plasmon resonance of gold nanoparticles: from theory to applications," *Chemical Reviews,* vol. 107, pp. 4797-4862, 2007.

[115] R. Elghanian, J. J. Storhoff, R. C. Mucic, R. L. Letsinger, and C. A. Mirkin, "Selective colorimetric detection of polynucleotides based on the distance-dependent optical properties of gold nanoparticles," *Science,* vol. 277, pp. 1078-1081, 1997.

[116] Z. Wang, J. Lee, A. R. Cossins, and M. Brust, "Microarray-based detection of protein binding and functionality by gold nanoparticle probes," *Analytical Chemistry,* vol. 77, pp. 5770-5774, 2005.

[117] J. Das, M. A. Aziz, and H. Yang, "A nanocatalyst-based assay for proteins: DNA-free ultrasensitive electrochemical detection using catalytic reduction of p-nitrophenol by gold-nanoparticle labels," *Journal of the American Chemical Society,* vol. 128, pp. 16022-16023, 2006.

[118] C. S. Thaxton, D. G. Georganopoulou, and C. A. Mirkin, "Gold nanoparticle probes for the detection of nucleic acid targets," *Clinica Chimica Acta,* vol. 363, pp. 120-126, 2006.

[119] X. Mao, Y. Ma, A. Zhang, L. Zhang, L. Zeng, and G. Liu, "Disposable nucleic acid biosensors based on gold nanoparticle probes and lateral flow strip," *Analytical Chemistry,* vol. 81, pp. 1660-1668, 2009.

[120] J. S. Lee, M. S. Han, and C. A. Mirkin, "Colorimetric detection of mercuric ion (Hg^{2+}) in aqueous media using DNA-functionalized gold nanoparticles,"

Angewandte Chemie, vol. 119, pp. 4171-4174, 2007.

[121]   J. M. Slocik, J. S. Zabinski, D. M. Phillips, and R. R. Naik, "Colorimetric response of peptide-functionalized gold nanoparticles to metal ions," *Small,* vol. 4, pp. 548-551, 2008.

[122]   C. D. Medley, J. E. Smith, Z. Tang, Y. Wu, S. Bamrungsap, and W. Tan, "Gold nanoparticle-based colorimetric assay for the direct detection of cancerous cells," *Analytical Chemistry,* vol. 80, pp. 1067-1072, 2008.

[123]   B. D. Chithrani, A. A. Ghazani, and W. C. Chan, "Determining the size and shape dependence of gold nanoparticle uptake into mammalian cells," *Nano Letters,* vol. 6, pp. 662-668, 2006.

[124]   H. C. Lee, T. H. Chen, W. L. Tseng, and C. H. Lin, "Novel core etching technique of gold nanoparticles for colorimetric dopamine detection," *Analyst,* vol. 137, pp. 5352-5357, 2012.

[125]   S. Durocher, A. Rezaee, C. Hamm, C. Rangan, S. Mittler, and B. Mutus, "Disulfide-linked, gold nanoparticle based reagent for detecting small molecular weight thiols," *Journal of the American Chemical Society,* vol. 131, pp. 2475-2477, 2009.

[126]   M. C. Daniel and D. Astruc, "Gold nanoparticles: assembly, supramolecular chemistry, quantum-size-related properties, and applications toward biology, catalysis, and nanotechnology," *Chemical Reviews,* vol. 104, pp. 293-346, 2004.

[127]   S. Eustis and M. A. El. Sayed, "Why gold nanoparticles are more precious than pretty gold: noble metal surface plasmon resonance and its enhancement of the radiative and nonradiative properties of nanocrystals of different shapes," *Chemical Society Reviews,* vol. 35, pp. 209-217, 2006.

[128]   T. G. Schaaff and R. L. Whetten, "Controlled etching of Au: SR cluster compounds," *The Journal of Physical Chemistry B,* vol. 103, pp. 9394-9396, 1999.

[129]   H. Qian, M. Zhu, E. Lanni, Y. Zhu, M. E. Bier, and R. Jin, "Conversion of polydisperse Au nanoparticles into monodisperse Au25 nanorods and nanospheres," *The Journal of Physical Chemistry C,* vol. 113, pp. 17599-17603, 2009.

[130]   J. M. Pettibone and J. W. Hudgens, "Gold cluster formation with phosphine ligands: etching as a size-selective synthetic pathway for small clusters?," *ACS Nano,* vol. 5, pp. 2989-3002, 2011.

[131]   Y. Shichibu, Y. Negishi, H. Tsunoyama, M. Kanehara, T. Teranishi, and T. Tsukuda, "Extremely high stability of glutathionate-protected Au_{25} Clusters against core etching," *Small,* vol. 3, pp. 835-839, 2007.

[132] T. Selvaraju and R. Ramaraj, "Simultaneous determination of ascorbic acid, dopamine and serotonin at poly (phenosafranine) modified electrode," *Electrochemistry Communications,* vol. 5, pp. 667-672, 2003.

[133] S. Arreguin, P. Nelson, S. Padway, M. Shirazi, and C. Pierpont, "Dopamine complexes of iron in the etiology and pathogenesis of Parkinson's disease," *Journal of Inorganic Biochemistry,* vol. 103, pp. 87-93, 2009.

[134] C. M. Chen, G. L. Chang, and C. H. Lin, "Performance evaluation of a capillary electrophoresis electrochemical chip integrated with gold nanoelectrode ensemble working and decoupler electrodes," *Journal of Chromatography A,* vol. 1194, pp. 231-236, 2008.

[135] A. Hermans, R. B. Keithley, J. M. Kita, L. A. Sombers, and R. M. Wightman, "Dopamine detection with fast-scan cyclic voltammetry used with analog background subtraction," *Analytical Chemistry,* vol. 80, pp. 4040-4048, 2008.

[136] Y. Sun, J. Fei, J. Hou, Q. Zhang, Y. Liu, and B. Hu, "Simultaneous determination of dopamine and serotonin using a carbon nanotubes-ionic liquid gel modified glassy carbon electrode," *Microchimica Acta,* vol. 165, pp. 373-379, 2009.

[137] Y. R. Kim, S. Bong, Y. J. Kang, Y. Yang, R. K. Mahajan, J. S. Kim, and H. Kim, "Electrochemical detection of dopamine in the presence of ascorbic acid using graphene modified electrodes," *Biosensors and Bioelectronics,* vol. 25, pp. 2366-2369, 2010.

[138] P. Uutela, R. Reinila, K. Harju, P. Piepponen, R. A. Ketola, and R. Kostiainen, "Analysis of intact glucuronides and sulfates of serotonin, dopamine, and their phase I metabolites in rat brain microdialysates by liquid chromatography−tandem mass spectrometry," *Analytical Chemistry,* vol. 81, pp. 8417-8425, 2009.

[139] W. Sun, Y. Duan, Y. Li, T. Zhan, and K. Jiao, "Electrochemistry and Voltammetric Determination of Adenosine with N-Hexylpyridinium Hexafluorophosphate Modified Electrode," *Electroanalysis,* vol. 21, pp. 2667-2673, 2009.

[140] S. J. Clarke, C. Hollmann, F. A. Aldaye, and J. L. Nadeau, "Effect of ligand density on the spectral, physical, and biological characteristics of CdSe/ZnS quantum dots," *Bioconjugate Chemistry,* vol. 19, pp. 562-568, 2008.

[141] Y. Hu, X. Wu, Y. Su, X. Hou, and J. Zhang, "Capillary zone electrophoresis hyphenated with laser-induced fluorescence detection for sensitive determination of noradrenaline and dopamine with 5-(4, 6-dichloro-s-triazin-2-ylamino) fluorescein as fluorescent label," *Microchimica Acta,* vol. 166, pp. 289-294, 2009.

[142] S. Zhao, Y. Huang, M. Shi, R. Liu, and Y. M. Liu, "Chemiluminescence resonance energy transfer-based detection for microchip electrophoresis," *Analytical Chemistry,* vol. 82, pp. 2036-2041, 2010.

[143] M. Moini, C. L. Schultz, and H. Mahmood, "CE/electrospray ionization-MS analysis of underivatized d/l-amino acids and several small neurotransmitters at attomole levels through the use of 18-crown-6-tetracarboxylic acid as a complexation reagent/background electrolyte," *Analytical Chemistry,* vol. 75, pp. 6282-6287, 2003.

[144] N. Jia, Z. Wang, G. Yang, H. Shen, and L. Zhu, "Electrochemical properties of ordered mesoporous carbon and its electroanalytical application for selective determination of dopamine," *Electrochemistry Communications,* vol. 9, pp. 233-238, 2007.

[145] P. Y. Chen, R. Vittal, P. C. Nien, and K. C. Ho, "Enhancing dopamine detection using a glassy carbon electrode modified with MWCNTs, quercetin, and Nafion®," *Biosensors and Bioelectronics,* vol. 24, pp. 3504-3509, 2009.

[146] S. R. Ali, Y. Ma, R. R. Parajuli, Y. Balogun, W. Y. C. Lai, and H. He, "A nonoxidative sensor based on a self-doped polyaniline/carbon nanotube composite for sensitive and selective detection of the neurotransmitter dopamine," *Analytical Chemistry,* vol. 79, pp. 2583-2587, 2007.

[147] A. Liu, I. Honma, and H. Zhou, "Simultaneous voltammetric detection of dopamine and uric acid at their physiological level in the presence of ascorbic acid using poly (acrylic acid)-multiwalled carbon-nanotube composite-covered glassy-carbon electrode," *Biosensors and Bioelectronics,* vol. 23, pp. 74-80, 2007.

[148] N. F. Atta, A. Galal, and R. A. Ahmed, "Poly (3, 4-ethylene-dioxythiophene) electrode for the selective determination of dopamine in presence of sodium dodecyl sulfate," *Bioelectrochemistry,* vol. 80, pp. 132-141, 2011.

[149] B. K. Swamy and B. J. Venton, "Carbon nanotube-modified microelectrodes for simultaneous detection of dopamine and serotonin in vivo," *Analyst,* vol. 132, pp. 876-884, 2007.

[150] Y. Zheng, Y. Wang, and X. Yang, "Aptamer-based colorimetric biosensing of dopamine using unmodified gold nanoparticles," *Sensors and Actuators B: Chemical,* vol. 156, pp. 95-99, 2011.

[151] H. Gai, Y. Li, and E. S. Yeung, "Optical detection systems on microfluidic chips," *Microfluidics*, vol. 304, pp. 171-201, 2011.

[152] M. E. Bosch, A. J. R. Sánchez, F. S. Rojas, and C. B. Ojeda, "Recent development in optical fiber biosensors," *Sensors,* vol. 7, pp. 797-859, 2007.

[153] S. Bargiel, A. Górecka Drzazga, J. A. Dziuban, P. Prokaryn, M. Chudy, A.

Dybko, and Z. Brzózka, "Nanoliter detectors for flow systems," *Sensors and Actuators A: Physical,* vol. 115, pp. 245-251, 2004.

[154] T. Noda, H. Takao, K. Yoshioka, N. Oku, M. Ashiki, K. Sawada, K. Matsumoto, and M. Ishida, "Performance of absorption photometry microchip for blood hemoglobin measurement integrated with processing circuits and Si (110) 45 mirrors," *Sensors and Actuators B: Chemical,* vol. 119, pp. 245-250, 2006.

[155] D. Onoshima, J. Wang, M. Aki, K. Arinaga, N. Kaji, M. Tokeshi, S. Fujita, N. Yokoyama, and Y. Baba, "A deep microfluidic absorbance detection cell replicated from a thickly stacked SU-8 dry film resist mold," *Analytical Methods,* vol. 4, pp. 4368-4372, 2012.

[156] C. H. Lin and G. B. Lee, "Micromachined flow cytometers with embedded etched optic fibers for optical detection," *Journal of Micromechanics and Microengineering,* vol. 13, p. 447, 2003.

Biography

Name: 李和政 (Ho-Cheng Lee)

Date of birth: 1983/11/01

Education:

- ➤ **B. E.** in Mechanical Engineering, Department of Mechanical Engineering, Private Chung Hua University, Hsinchu, Taiwan, (2003~2006).

- ➤ **Master.** in Mechanical Engineering, Institute of Mechanical Engineering, Private Chung Hua University, Hsinchu, Taiwan, (2007~2008).

- ➤ **Ph. D.** in Mechanical Engineering, Institute of Mechanical Engineering, National Sun Yat-sen University, Kaohsiung, Taiwan, (2010~2014).

Publication list

International Journals:

1. **H. C. Lee,** H. H. Hou, R. J. Yang, C. H. Lin and L. M. Fu, "Microflow cytometer incorporating sequential micro-weir structure for three-dimensional focusing," *Microfluidics and Nanofluidics*, Vol. 11, pp. 469-478, 2011. (**SCI, Impact Factor = 3.371**) (Instruments & Instrumentation **5/58**)

2. **H. C. Lee,** T. H. Chen, W. L. Tseng and C. H. Lin, "Novel core etching technique of gold nanoparticles for colorimetric dopamine detection," *Analyst*, Vol. 137, pp. 5352-5357, 2012. (**SCI, Impact Factor = 4.230**) (Chemistry, Analytical **8/73**)

3. **H. C. Lee,** C. Y. Wang and C. H. Lin, "High performance humidity sensors utilizing dopamine biomolecule-coated gold nanoparticles," *Sensors and*

Actuators B: Chemical, Vol. 191, pp.204-210, 2013. (**SCI, Impact Factor = 3.535**) (Chemistry, Analytical **11/75**)

4. C. Y. Wang, **H. C. Lee**, Y. C. Wu and C. H. Lin, "High performance CO sensors utilizing sprayed distributed toluene-based gold nanoparticles," *Applied Mechanics and Materials,* Vol. 479-480, pp.702-707, 2014. (**SCI, Impact Factor = 1.041**).

International Conference:

1. **H. C. Lee**, S. W. Lin and C. H. Lin, "Three-dimensional focusing for microflow cytometer with sequence micro-weir structures" in (6th) Nanao/Micro Engineered and Molecular Systems Conference (IEEE NEMS), 2011, Kaohsiung, Taiwan. **(Oral)**

2. R. C. Lin, S. K. Hsiung, **H. C. Lee** and C. H. Lin, "A microstructure-embedded microfluidic chip for continuous sample separating applications," in SEMBA & BioPro International conference, 2012, Taichung, Taiwan. **(Poster)**

3. **H. C. Lee**, T. H. Chen, W. L. Tseng and C. H. Lin, "Novel core etching technique on synthesized gold nanoparticles for colorimetric detection of dopamine biosample," in (7th) Nanao/Micro Engineered and Molecular Systems Conference (IEEE NEMS), March, 2012, Kyoto, Japan. **(Poster)**

4. C. Y. Wang, **H. C. Lee** and C. H. Lin, "High performance humidity sensors based on dopamine biomolecules coated gold nanoparticles," in (11th) IEEE Sensors, October, 2012, Taipei, Taiwan. **(Poster)**

5. **H. C. Lee**, T. H. Chen, W. L. Tseng and C. H. Lin, "Novel core etching technique on synthesized gold nanoparticles for colorimetric detection of dopamine biosample," in ISMM, June, 2012, Hsinchu, Taiwan. **(Oral)**

6. **H. C. Lee** and C. H. Lin, "Liquid-liquid phase separator for synthesizing gold nanoparticles in toluene," in (9th) Nanao/Micro Engineered and Molecular Systems Conference (IEEE NEMS), 2014, Hawaii, USA. **(Oral)**

7. **H. C. Lee** and C. H. Lin, "Novel droplet-based microfluidic optical detection sensor for gold nanoparticle detecting dopamine," in (18th) μTAS, 2014, San Antonio, USA. **(Poster)**

Conference:

1. **H. C. Lee**, S. W. Lin and C. H. Lin, "Three-dimensional focusing for microflow cytometer with sequence micro-weir structures," in 奈米工程暨微系統技術研討會, Sept, 2010, Kaohsiung, Taiwan. **(Oral)**

2. **H. C. Lee,** T. H. Chen, W. L. Tseng and C. H. Lin, "Novel core etching technique of synthesized gold nanoparticles for colorimetric dopamine detection," in Precision Machinery and Manufacturing Technology (PMMT), May, 2012, Pingtung, Taiwan. **(Oral)**

3. C. Y. Wang, **H. C. Lee** and C. H. Lin, "High performance humidity sensors based on dopamine biomolecules coated gold nanoparticles," in Precision Machinery and Manufacturing Technology (PMMT), May, 2013, Pingtung, Taiwan. **(Oral)**